Transcriptional control of the H-NS antagonists LeuO and RcsB-BglJ in *Escherichia coli*

I n a u g u r a l - D i s s e r t a t i o n

zur

Erlangung des Doktorgrades

der Mathematisch-Naturwissenschaftlichen Fakultät

der Universität zu Köln

vorgelegt von

Thomas Stratmann

geb. in Warstein

Köln, den 23. Februar 2012

Berichterstatter: Prof. Dr. Karin Schnetz

Prof. Dr. Jürgen Dohmen

Tag der mündlichen Prüfung: 17. April 2012

Contents

Zusammenfassung

Das Nukleoid-assoziierte Protein H-NS ist an der Organisation und Kompaktierung des bakteriellen Chromatins beteiligt und fungiert als globaler Repressor. Dabei reprimiert es vornehmlich die Transkription von solchen Genen, die in Zusammenhang mit Stressantwort und Pathogenität bekannt sind. Die Bindung von H-NS an die DNA und die Ausbildung eines Nukleoproteinkomplexes an Promotorregionen führt dabei zur Repression. Der Repression durch H-NS können jedoch genspezifische Transkriptionsfaktoren entgegengewirken, welche die Transkription reprimierter Gene dadurch aktivieren, dass sie mit H-NS um die DNA-Bindestelle konkurrieren oder die Ausbildung des Nukleoproteinkomplexes behindern (H-NS-Antagonisten). Zwei Beispiele für H-NS-Antagonisten sind der LysR-Typ Transkriptionsfaktor LeuO und der FixJ/NarL-Typ heterodimere Transkriptionsfaktor RcsB-BglJ. LeuO ist ein pleiotroper Regulator von Stressanworten und Virulenzfaktoren. RcsB-BglJ aktiviert die Transkription des H-NS-reprimierten bgl- (aryl-β,D-Glukosid) Operons.

In der vorliegenden Arbeit wurden neue Zielgene von RcsB-BglJ in *Escherichia coli* mittels einer Microarray-Analyse identifiziert. Die Ergebnisse dieser Analyse zeigen, dass die meisten Zielgene durch RcsB-BglJ Heterodimere aktiviert werden. Unter den Zielgenen befindet sich neben zahlreichen Gene Membran-assoziierter und unbekannter Funktion auch das Gen *leuO*. Eine detaillierte Analyse der Transkriptionsregulation von *leuO* zeigte, dass die Transkription von *leuO* stark durch RcsB-BglJ aktiviert wird, indem RcsB-BglJ in der Nähe eines neu kartierten Promotors bindet. RcsB-BglJ wirkt der Repression von *leuO* durch H-NS und das H-NS-ähnliche Protein StpA entgegen. Weitere Daten zeigen, dass LeuO seine eigene Expression negativ autoreguliert und die Aktivierung von *leuO* durch RcsB-BglJ hemmt.

Die Regulation des *leuO*-Gens durch RcsB-BglJ sowie die Autoregulation durch LeuO, wie hier gezeigt, und die Aktivierung von *bglJ* durch LeuO, wie zuvor publiziert, deuten auf einen *feedback loop*-Kontrollmechanismus hin, der die Transkription von *bglJ* und *leuO* koppelt. Dieser *loop* könnte für das gegenseitige Anschalten der beiden H-NS-Antagonisten und die Regulation ihrer Zielgene als Antwort auf bestimmte Umweltbedingungen von Bedeutung sein. Screens lieferten mögliche weitere Faktoren, die an der Regulation des *bglJ-leuO feedback loops* beteiligt sein könnten.

Abstract

The bacterial nucleoid-associated protein (NAP) H-NS is involved in the organization and compaction of the bacterial chromatin and acts as a global respressor, mainly of genes that have been acquired by horizontal gene transfer and that are related to stress responses and pathogenicity. Binding of H-NS to the DNA and formation of a nucleoprotein complex at promoter regions leads to repression. This repressor effect of H-NS can be antagonized by gene-specific transcription factors (H-NS antagonists) that activate transcription of H-NS-repressed genes by competing with H-NS for binding or by disturbing formation of the nucleoprotein complex. Two examples of such H-NS antagonists are the LysR-type transcription factor LeuO and the FixJ/NarL-type transcription factor heterodimer RcsB-BglJ. LeuO is a pleiotropic regulator of stress responses and virulence determinants. RcsB-BglJ activates transcription of the H-NS-repressed *bgl* (aryl-β,D-glucoside) operon.

In this work, novel targets of RcsB-BglJ were identified in *Escherichia coli* by microarray analyses. The results suggest that heterodimerization of RcsB and BglJ is essential for regulation. Further, in addition to genes related to unknown or predicted function in the membrane the *leuO* gene was identified as a target gene. Detailed analysis of transcriptional regulation of *leuO* demonstrated that RcsB-BglJ strongly activates transcription of *leuO* by binding proximal to a newly mapped *leuO* promoter. Thus RcsB-BglJ antagonizes repression of *leuO* by H-NS and the H-NS-like protein StpA. Additional data presented here show that LeuO negatively autoregulates its own expression and inhibits activation of *leuO* by RcsB-BglJ.

Regulation of *leuO* by RcsB-BglJ and autoregulation by LeuO, as shown here, as well as activation of *bglJ* by LeuO, as published previously, indicates a feedback control mechanism of two global transcriptional regulators and H-NS antagonists.This feedback regulation may ensure turn on of their expression in response to specific environmental signals. Screens to search for novel regulators or upstream signals were performed by transposon mutagenesis and by using a genomic expression library. These screens indicate that additional factors may be involved in the regulation of this *leuO-bglJ* feedback loop.

1. Introduction

Bacteria face the need to structure their genetic material in a way that makes it compact and storable, but at the same time accessible for replication and for transcription of the encoded genes. Similar to eukaryotic chromatin, there is a bacterial chromatin that consists of DNA and different kinds of nucleoid-associated proteins (NAPs) (Dame, 2005, Dillon & Dorman, 2010). These NAPs usually exert a dual function: by binding to DNA they confer to compaction of the nucleoid and also to regulation of gene expression. Nucleoid-structuring and gene-regulating functions are linked to the structural properties of the NAPs and their binding of DNA target sequences. One of these NAPs is the heat-stable (or histone-like) nucleoid-structuring protein and pleiotropic repressor H-NS. Repression mediated by H-NS is often modulated by specific regulators (H-NS antagonists). In this work the role of LeuO and RcsB-BglJ, two examples of such H-NS antagonists, and the transcriptional regulation of *leuO* was analyzed.

1.1 H-NS is a nucleoid-associated protein and global repressor of transcription

The H-NS protein is highly conserved in Gram-negative bacteria, and functionally and structurally related H-NS-like proteins have been found in many bacterial species. In *Eschericha coli* H-NS is present at approximately 20,000 copies per cell during the exponential growth phase in which the transcriptional activity in the cells is high (Azam & Ishihama, 1999, Ali *et al.*, 1999). Large-scale binding studies have revealed that H-NS is bound to approximately 250 to 375 loci spread throughout the *E. coli* chromosome and that it structures the nucleoid into domains of 11 kb on average (Noom *et al.*, 2007, Grainger *et al.*, 2006, Oshima *et al.*, 2006, Uyar *et al.*, 2009). Despite the distribution of the H-NS-bound sites all over the chromosome, these sites are spatially clustered into two distinct foci within the cell as recently revealed by fluorescent live imaging (Wang *et al.*, 2011).

Besides its role in structuring of the chromosome, H-NS is mainly known as a global repressor affecting the transcription of 5 % of the *E. coli* genes (Hommais *et al.*, 2001, Dorman, 2004). The repressor function of H-NS has been best studied in *E. coli* and *Salmonella* spp. and includes the control of pathogenicity determinants and stress responses, as follows. A well-studied example of the regulation of pathogenicity-relevant

processes is the *Salmonella* pathogenicity island 2 (SPI2), which is required for infection of the *Salmonella* host's gut cells. This SPI2 encodes genes for the secretion of virulence effector proteins into the host cell. Expression of these effectors is tightly repressed by H-NS (Fass & Groisman, 2009, Stoebel *et al.*, 2008). Repression by H-NS of SPI2 and of other virulence genes involved is antagonized and fine-tuned by a complex network of two-component systems (EnvZ/OmpR, PhoPQ, and SpiR/SsrB), additional nucleoid-associated proteins (IHF, Fis), and transcription factors (SlyA) that respond to specific signals in the host environment. In *Escherichia coli*, H-NS represses transcription at the locus of enterocyte effacement (LEE) in enterohemorrhagic strains (EHEC) (Barba *et al.*, 2005, Laaberki *et al.*, 2006). This pathogenicity-relevant locus is required for successful colonization of the host tissue. The H-NS-like protein Ler antagonizes H-NS at this locus. One of many examples of H-NS-repressed stress response systems is regulation of the *proU* (*proVWX*) operon which encodes transporters for osmoprotectants (Owen-Hughes *et al.*, 1992, Lucht *et al.*, 1994). Other classical examples of H-NS-mediated repression of stress response systems are the three acid resistance systems in *E. coli* (glutamate-, arginine-, and lysine-dependent acid resistance) for which H-NS is the master repressor (Krin *et al.*, 2010). H-NS also represses the *rrn* (rRNA-encoding) operons (Schneider *et al.*, 2003). Despite its mainly negative effect on transcription, H-NS positively influences transcription of the flagellar regulator operon *flhDC* and thus motility of the bacteria (Bertin *et al.*, 1994). However, H-NS does not activate transcription of *flhDC* directly but downregulates its repressor HdfR (Ko & Park, 2000). Thus, the absence of H-NS leads to elevated expression of the HdfR repressor, repression of *flhDC* and flagellar genes and decreased motility.

It has further been shown that many of the H-NS-repressed genes have been acquired by horizontal gene transfer (i. e. by phage infection, transformation or conjugation) (Navarre *et al.*, 2007, Navarre *et al.*, 2006, Lucchini *et al.*, 2006). This lead to the conclusion that selective repression (or 'silencing') of such xenogeneic material by H-NS may protect a cell from expression of potentially deleterious genes which may, however, provide advantages under certain environmental conditions (Oshima *et al.*, 2006, Navarre *et al.*, 2006, Lucchini *et al.*, 2006, Navarre *et al.*, 2007, Dorman, 2007).

Repression by H-NS is mediated through binding of H-NS to the DNA and the consecutive formation of an H-NS-DNA complex (nucleoprotein complex). Numerous studies have

addressed the mechanism of DNA binding, site-specific recognition and transcriptional regulation by H-NS as follows. The H-NS protein has a molecular weight of 15.6 kDa and consists of 137 amino acids. Its N-terminal domain mediates dimerization and higher order oligomerization, and the C-terminal domain contains a winged helix-turn-helix motif (wHTH) that mediates DNA binding. N- and C-terminus are flexibly connected by a linker domain which is required for higher order oligomerization of H-NS (Figure 1A) (Rimsky, 2004, Stella *et al.*, 2005). H-NS presumably binds as dimer to a high affinity site on the DNA (the nucleation site) within AT-rich DNA sites (Bouffartigues *et al.*, 2007). Such AT-rich sites are generally associated with horizontally acquired genes and with promoter regions. The structural feature of bent DNA often found at AT-rich sequences has been regarded as basis for binding site recognition by H-NS (Owen-Hughes *et al.*, 1992, Dame *et al.*, 2002). For this initial binding the degenerate consensus DNA motif 'TCGATAAATT' has been proposed (Lang *et al.*, 2007). However, initial binding is probably not based on sequence-specific protein-DNA interactions but rather on an indirect read-out mechanism involving weak interaction of arginine residues in the wHTH DNA binding domain of H-NS with the DNA minor groove at the nucleation site (Gordon *et al.*, 2011, Cordeiro *et al.*, 2011). Binding to the nucleation site then leads to the formation of an extended nucleoprotein complex by higher order oligomerization of H-NS dimers along the AT-rich DNA (defined as 'coating' or 'stiffening', Figure 1B) and by building DNA-H-NS-DNA bridges ('bridging') (Bouffartigues *et al.*, 2007, Lang *et al.*, 2007, Dame *et al.*, 2006). Changes in the intracellular levels of divalent cations such as Mg^{2+} drive switching between bridging and stiffening (Liu *et al.*, 2010). A structural study has revealed that the nucleoprotein complex can be modelled as a superhelical structure that may explain the bridging and stiffening models (Figure 1C) (Arold *et al.*, 2010).

1. Introduction
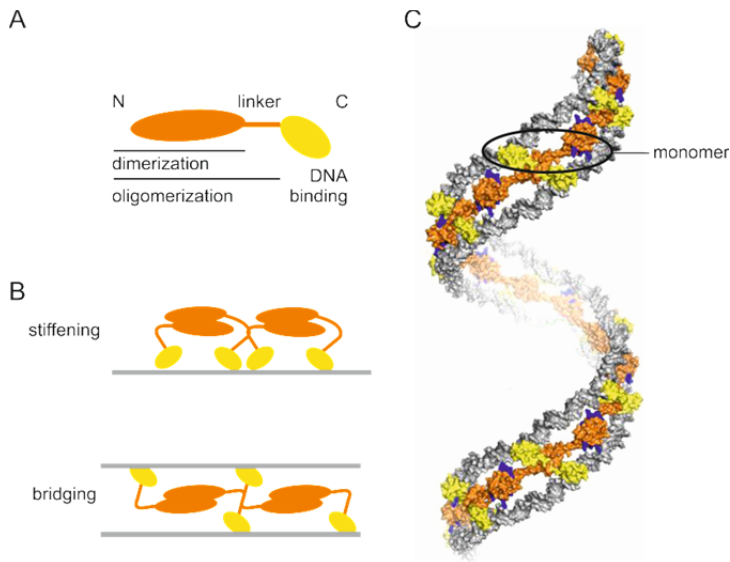
Figure 1: H-NS structure and DNA binding

(A) Schematic model of H-NS monomer consisting of an N-terminal dimerization domain, a linker domain involved in oligoerization (both orange), and a C-terminal DNA binding domain (yellow). (B) Binding of H-NS dimers to DNA (grey line) in stiffening and bridging mode. (C) Model of H-NS superhelix (yellow: putative position of the wHTH domains; orange: oligomer of the H-NS N-terminus; blue: amino acids R15, R19, and K32 involved in DNA binding) accommodating two DNA double helices (grey). Panel C modified from (Arold *et al.*, 2010).

In *E. coli*, the H-NS-like protein StpA can contribute to gene regulation and silencing (Zhang *et al.*, 1996, Wolf *et al.*, 2006, Doyle *et al.*, 2007, Muller *et al.*, 2006). StpA and H-NS are highly similar, showing 58 % sequence identity on the amino acid level and can form heterodimers (Muller *et al.*, 2010). It is believed that StpA, which is more prominent than H-NS in the stationary growth phase and under growth at high temperature, functions as a molecular backup of H-NS (Zhang *et al.*, 1996, Sonden & Uhlin, 1996). However, a genome-wide comparison of H-NS binding sites and StpA binding sites in *hns* and *stpA* mutants has revealed that deletion of *hns* diminishes binding of StpA at many sites with only one third of H-NS binding sites bound by StpA independently of H-NS (Uyar *et al.*, 2009). Binding of H-NS and StpA is similar in that both proteins can coat the DNA (stiffening) and form protein-DNA bridges. Unlike H-NS, StpA is able to form such bridges also under conditions of low magnesium concentration (Lim *et al.*, 2011).

The formation of the H-NS-DNA nucleoprotein complex next to promoters mediates repression of transcription. Repression can be caused by occluding RNA polymerase from the promoter which is masked by the nucleoprotein complex or, as shown in some cases, by trapping bound RNA polymerase at the promoter as demonstrated for *rrn* and *hdeAB* transcription (Dame *et al.*, 2002, Shin *et al.*, 2005, Oshima *et al.*, 2006) (Figure 2B).

Additionally, repression by binding of H-NS within the transcription unit has been demonstrated for some loci, such as the *proU* and *bgl* operons, respectively (Nagarajavel *et al.*, 2007). Repression by H-NS is most commonly relieved by the binding of locus-specific transcriptional regulators which compete with H-NS for binding or restructure the H-NS-nucleoprotein complex (Figure 2D) (Stoebel *et al.*, 2008). Besides, alterations in H-NS activity by basic physiological conditions of the cells such as osmolarity, temperature, and pH (Liu *et al.*, 2010), locus-specific changes of the DNA structure (bending) (Falconi *et al.*, 1998), or enhancement of the transcription rate (Nagarajavel *et al.*, 2007), can relieve H-NS-mediated repression. Two examples of transcriptional regulators that act as H-NS antagonists are the LysR-type transcription factor LeuO and the heterodimeric FixJ/NarL-type transcription factor RcsB-BglJ. The role and regulation of these regulators, LeuO and RcsB-BglJ, was analyzed in this work.
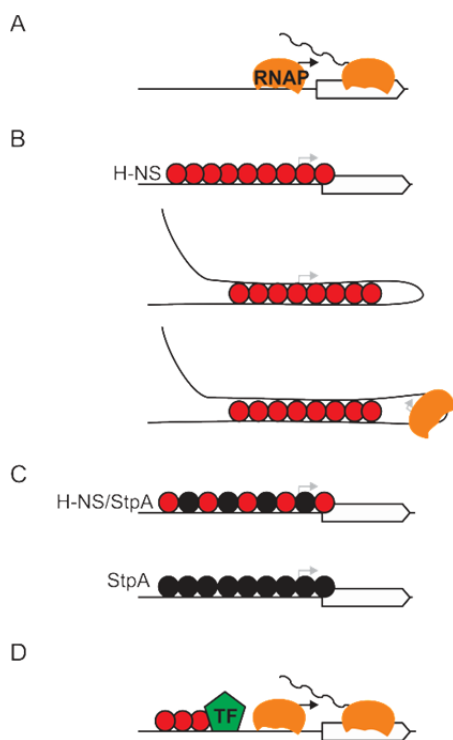
Figure 2: Schematic model of repression by H-NS and StpA.

(A) The RNA polymerase holoenzyme (RNAP) requires access to the promoter to initiate transcription. (B) H-NS represses transcription by initial binding to nucleation sites followed by spreading of nucleoprotein complex of H-NS and DNA. The nucleoprotein complex may spread into a promoter and render the promoter inaccessible for RNAP. Alternatively, RNAP may be trapped bound to a promoter. (C) H-NS can be partially or fully substituted by StpA. (D) Repression by H-NS/StpA can be antagonized by a specific transcription factor (TF). The transcription factor may hinder spreading of the repressing nucleoprotein complex and/or recruit RNA polymerase to the promoter.

1.2 LeuO is a pleiotropic regulator and H-NS antagonist

LeuO is a LysR-type transcription factor and a master regulator of multiple loci including genes related to stress response and pathogenicity of *Enterobacteriaceae*. The LysR family is the most abundant group of transcription factors in prokaryotes (Schell, 1993). Initially, the LysR family was described on the basis of a conserved wHTH motif in their N-terminal DNA binding domain (Henikoff *et al.*, 1988). A typical feature of LysR-type proteins is the composition of a central domain and the C-terminal domain. Though very diverse among LysR-family members, the C-terminal domain usually contains a binding pocket for a small co-effector molecule that binds and alters the regulatory activity of the protein by causing a conformational change of the active tetrameric form of the protein (Maddocks & Oyston, 2008).

LeuO has been studied mostly in *Escherichia coli* and *Salmonella enterica*, but also in other bacteria including *Yersinia enterocolitica*, and *Vibrio cholerae* (Rodriguez-Morales *et al.*, 2006, Moorthy & Watnick, 2005, Lawrenz & Miller, 2007). Among other targets, LeuO acts as a transcriptional activator and H-NS antagonist at the *bgl* operon (Ueguchi *et al.*, 1998), encoding proteins for the uptake and utilization of aryl-β,D-glucosides. LeuO further activates transcription of the H-NS-repressed outer membrane porin genes *ompS1* and *ompS2* in *Salmonella enterica* (Flores-Valdez *et al.*, 2003, Fernandez-Mora *et al.*, 2004, Rodriguez-Morales *et al.*, 2006). LeuO regulates transcription of the *yjjP* gene and activates the divergent *yjjQ-bglJ* operon encoding FixJ/NarL-type transcription factors (Stratmann *et al.*, 2008). At this locus, LeuO binding regions flank the core promoter of the *yjjQ-bglJ* operon and may compete with H-NS for binding. It has further been demonstrated that at least two out of three different LeuO binding sites are required for full activation the *yjjQ-bglJ* promoter, and it has been proposed that synergistic binding to these two sites may restructure the nucleoprotein complex and relieve repression (Stratmann *et al.*, 2008). In addition, LeuO antagonizes H-NS at the CRISPR-associated *cas* operon (Shimada *et al.*, 2009, Hernandez-Lucas *et al.*, 2008, Westra *et al.*, 2010, Medina-Aparicio *et al.*, 2011). The CRISPR-*cas* system encodes a prokaryotic defense system against foreign DNA that enters the cell during bacteriophage infections and plasmid conjugation (Brouns *et al.*, 2008). Although mainly known as an activator, LeuO represses transcription of the acid stress regulator CadC (Shi & Bennett, 1995) and the small RNA *dsrA* (Repoila & Gottesman, 2001). A recent

genome-wide study of LeuO binding revealed that LeuO may regulate many targets involved in structuring the cell surface such as fimbrial genes (Shimada *et al.*, 2011). Moreover, most of the LeuO targets are repressed by H-NS, and thus LeuO emerged as important H-NS antagonist and global regulator as it has been shown that 90 % of LeuO-bound loci also show binding of H-NS (Stoebel *et al.*, 2008, Hernandez-Lucas *et al.*, 2008, Shimada *et al.*, 2009, Shimada *et al.*, 2011).

Remarkably, expression of the *leuO* gene is itself repressed by H-NS under standard laboratory growth conditions (Figure 3) (Klauck *et al.*, 1997, Chen *et al.*, 2001). As LeuO is an H-NS antagonist with pleiotropic function, activation of *leuO* expression should occur in response to specific environmental cues. Indeed, moderately increased expression of *leuO* has been detected upon amino acid starvation and in the stationary growth phase (Fang *et al.*, 2000, Majumder *et al.*, 2001, Shimada *et al.*, 2011). The promoter and regulatory region of *leuO* gene is highly AT-rich (Haughn *et al.*, 1986), typical of H-NS repressed loci (Navarre *et al.*, 2007), and H-NS and LeuO binding sites have been mapped to this region (Chen *et al.*, 2001, Chen *et al.*, 2003, Chen *et al.*, 2005, Chen & Wu, 2005).
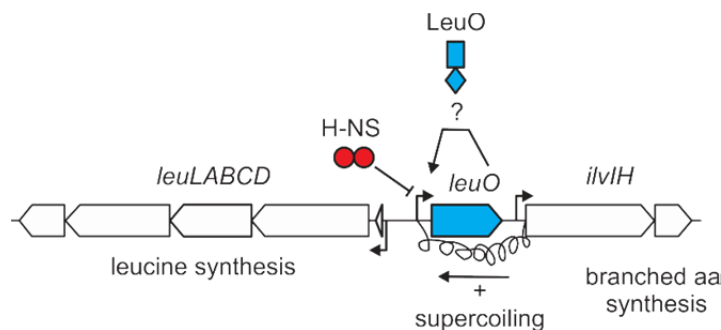
Figure 3: Organization of the *leuO* locus.

Organization of the *leuO* locus of the *E. coli* K-12 chromosome. The *leuO* gene (NC_000913: 84,368 to 85,312) is located between the *leuLABCD* operon encoding genes for leucine snthesis and the *ilvIH* operon involved in synthesis of branched-chain amino acids. Transcription of *leuO* is repressed by H-NS and activated by supercoiling coupled to transcription of the downstream *ilvIH* operon (Wu & Fang, 2003). Postive autoregulation has been suggested (Chen & Wu, 2005).

The *leuO* gene is located inbetween the divergent *leuLABCD (leu)* and the downstream *ilvIH* operons encoding enzymes for branched-chain amino acid synthesis (Figure 3). This *leu-leuO-ilvIH* gene cluster is a paradigm for the role of transcription-induced local changes of DNA supercoiling in promoter regulation. Initially, the *leu-500* promoter mutant of *S.*

enterica serovar Typhimurium that carries a point mutation rendering the promoter of the *leu* operon inactive was found to be repressed in *topA* (topoisomerase I) mutants (Graf & Burns, 1973, Margolin *et al.*, 1985). It was then shown that the mutant *leu-500* promoter is supercoiling-sensitive and responds to transcription-induced local changes of DNA supercoiling as tested with plasmids (Pruss & Drlica, 1985, Richardson *et al.*, 1988, Lilley & Higgins, 1991, Chen *et al.*, 1992, Chen *et al.*, 1994, Tan *et al.*, 1994). Further experiments with plasmids carrying the natural context of the *leu-leuO-ilvIH* gene cluster demonstrated that activation of the *leu-500* promoter (and also the wild-type *leu* promoter) depends on transcription of the divergent *ilvIH* promoter and the *leuO* gene both in *S.* Typhimurium and in *E. coli*. This suggested that topological coupling operates over 1.9 kb in the chromosome (Wu *et al.*, 1995, Fang & Wu, 1998a, Fang & Wu, 1998b). Taken together with the finding that expression of *leuO* and *ilvIH* is elevated in the late stationary phase, these results lead to the proposal of a supercoiling relay mechanism in which activation of *ilvIH* results in activation of *leuO* and finally the *leu* promoter (Fang & Wu, 1998a, Fang & Wu, 1998b, Wu & Fang, 2003). Furthermore, the presence of LeuO binding sites in the *leu-leuO* intergenic region and the capability of LeuO to delimit spreading of an H-NS-DNA nucleoprotein complex was taken as indication that LeuO acts as a positive autoregulator in the natural context (Chen & Wu, 2005). Besides this, activation of H-NS-repressed loci by LeuO is presumably achieved by competition of LeuO with H-NS for DNA binding (De la Cruz *et al.*, 2007, Shimada *et al.*, 2011).

1.3 RcsB-BglJ is an antagonist of H-NS-mediated repression of the *bgl* operon

The heterodimeric transcription factor RcsB-BglJ has been identified as antagonist of H-NS-mediated repression of the *bgl* operon. RcsB and BglJ belong to the FixJ/NarL family characterized by a conserved LuxR-type helix-turn-helix (HTH) motif in the C-terminal DNA binding domain (Gao *et al.*, 2007, Henikoff *et al.*, 1990). RcsB is the response regulator of the Rcs (regulation of capsule synthesis) two-component phosphorelay system (TCS) that senses perturbations of the outer membrane and the peptidoglycan layer (Majdalani & Gottesman, 2005, Farris *et al.*, 2010, Laubacher & Ades, 2008). RcsB is involved in the control of motility, cell division, outer membrane protein expression, capsule synthesis, acid stress response, and the regulatory non-coding RNA RprA (Castanie-Cornet *et al.*, 2010, Huang *et al.*, 2006,

Majdalani & Gottesman, 2005). RcsB is a unique bacterial response regulator in that it acts as homodimer but also as heterodimer with RcsA (regulation of capsule synthesis), GadE (regulation of acid stress response), and BglJ (activation of the *bgl* operon), respectively (Majdalani & Gottesman, 2005, Castanie-Cornet *et al.*, 2010, Venkatesh *et al.*, 2010). These three proteins likewise belong to the FixJ/NarL family of transcription factors (Henikoff *et al.*, 1990, Giel *et al.*, 1996). In *Salmonella* Typhi, interaction of RcsB with TviA was found to control Vi antigen synthesis (Winter *et al.*, 2009). The activity of the RcsB-RcsB homodimer and the RcsB-RcsA heterodimer depends on phosphorylation of RcsB (Majdalani & Gottesman, 2005). However, the RcsB-BglJ heterodimer activates transcription of the only known target locus so far, the *bgl* operon, independently of RcsB phosphorylation (Venkatesh *et al.*, 2010). Since the *rcsB* gene is constitutively expressed, regulation of *bgl* by RcsB-BglJ is controlled by the presence or absence of BglJ. Interestingly, the three genes *rcsA*, *gadE*, and *bglJ*, respectively, encoding the three RcsB heterodimerization partners are all repressed by H-NS (Majdalani & Gottesman, 2005, Stratmann *et al.*, 2008, Sayed & Foster, 2009).

The RcsB heterodimerization partner BglJ is encoded in an operon together with YjjQ, another FixJ/NarL-type transcription factor (Figure 4) (Stratmann *et al.*, 2008). YjjQ has been proposed to be important for pathogenicity of avian pathogenic *E. coli* (APEC) since a Tn5 transposon insertion in the 3' end of *yjjQ* lead to attenuation of virulence of the mutant in an animal infection model (Li *et al.*, 2008). However, this insertion may also affect expression of the downstream-encoded *bglJ* gene. Further transposon insertions mapped to the 3'end of *yjjQ* render expression of the *bglJ* gene constitutive which leads to activation of the only known target of BglJ, the *bgl* operon (Giel *et al.*, 1996, Madhusudan *et al.*, 2005). Transcriptional regulation of the *yjjQ-bglJ* operon has been described (Stratmann *et al.*, 2008). Transcription directed by the *yjjQ-bglJ* promoter is repressed by H-NS which binds to the AT-rich 555-bp intergenic region of *yjjQ* and the divergent *yjjP* gene. Binding sites upstream and downstream of the *yjjQ-bglJ* promoter are required for efficient repression by H-NS. The core promoter region, however, is not bound by H-NS. Interestingly, LeuO was found to antagonize H-NS-mediated repression of the *yjjQ-bglJ* promoter, as described in chapter 1.2.
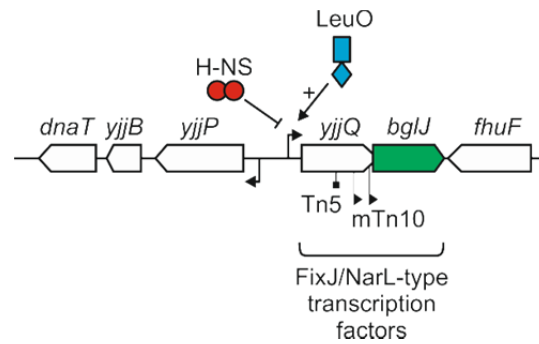
Figure 4: Organization of the *yjjP-yjjQ-bglJ* locus.

Organization of the *yjjP-yjjQ-bglJ* locus located between *yjjB* (encoding a conserved inner membrane protein) and *fhuF* (encoding a ferric iron reductase protein). The *yjjQ-bglJ* operon (NC_000913: 4,601,500 to 4,602,860) encodes FixJ/NarL-type transcription factors. Transcription of the operon is repressed by H-NS and activated by LeuO (Stratmann *et al.*, 2008). A *yjjQ*::Tn*5* insertion mutation attenuates the virulence of APEC (Li *et al.*, 2008) while mini-Tn*10* insertions upstream of *bglJ*, causing the constitutive expression of *bglJ*, relieve the silencing of the *bgl* operon (Giel *et al.*, 1996, Madhusudan *et al.*, 2005). The *yjjP* gene encodes a membrane protein of unknown function.

1.4 Aims of this thesis

Thus far, the only known regulatory target of RcsB-BglJ is the *bgl* operon. LeuO is a global regulator involved in the regulation of stress responses and pathogenicity determinants. Moreover, LeuO activates transcription of the *bglJ* gene. Both transcription factors, RcsB-BglJ and LeuO, antagonize H-NS-mediated repression. The aims of this thesis were:

- To identify novel putative targets of RcsB-BglJ and LeuO by microarray analyses and to confirm the obtained microarray data for selected targets,
- to study regulation of the newly identified RcsB-BglJ target *leuO* in detail, and
- to identify additional factors that may affect the feedback loop regulation of RcsB-BglJ and LeuO.

2. Results

2.1 Analysis of LeuO and RcsB-BglJ target loci

The heterodimer RcsB-BglJ activates the *bgl* operon, its only known regulatory target to date (Venkatesh *et al.*, 2010). LeuO is a pleiotropic regulator which regulates transcription at several loci (Shimada *et al.*, 2011). To identify novel target loci of RcsB-BglJ and LeuO, I performed DNA microarray analyses and overexpressed BglJ or LeuO in different genetic backgrounds to measure transcriptome-wide changes in response to expression of RcsB-BglJ and of LeuO, repectively (Figure 5).
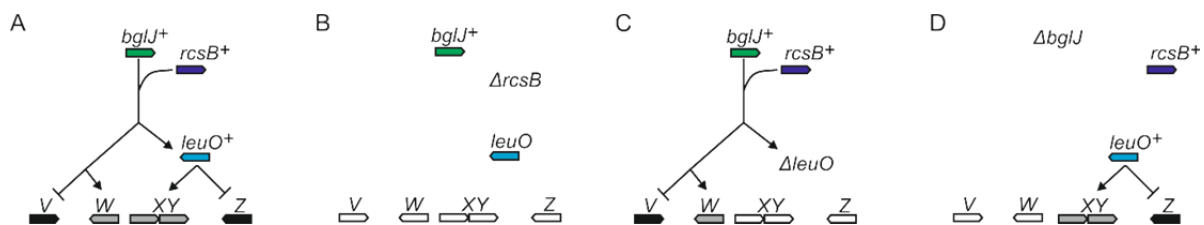
Figure 5: Microarray analysis of RcsB-BglJ and LeuO targets.

(A) In presence of *bglJ* (*bglJ⁺*), *rcsB* (*rcsB⁺*), and *leuO* (*leuO⁺*) all putative targets of RcsB-BglJ or LeuO either upregulated (grey) or downregulated (black) could be identified by microarray analysis. For this, BglJ was expressed from plasmid pKETS1 in strain T75 (*ΔyjjPQ-bglJ*) and expression levels were compared to T75 carrying control vector pKESK22. Chromosomal *rcsB* is constitutively expressed in this strain. (B) Deletion of *rcsB* (*ΔrcsB*) abolished regulation of RcsB-BglJ targets (white). For this, BglJ was expressed from plasmid pKETS1 in strain T175 (*ΔyjjPQ-bglJ ΔrcsB*) and expression levels were compared to T175 carrying control vector pKESK22. In this strain *leuO* is repressed by H-NS. (C) Analysis was performed in *ΔleuO* strain T177 to exclude targets of LeuO from the analysis. For this, BglJ was expressed from plasmid pKETS1 in strain T177 (*ΔyjjPQ-bglJ ΔleuO*) and expression levels were compared to T177 carrying control vector pKESK22. (D) Expression of LeuO (*leuO⁺*) from plasmid pKEDR13 in *ΔyjjPQ-bglJ* strain T75 revealed *bglJ*-independent targets of LeuO.

2.1.1 RcsB-BglJ activates transcription of several targets

For the microarray analysis of RcsB-BglJ targets, BglJ was expressed from low-copy vector pKETS1 in *E. coli* strain T75 carrying a deletion of the *yjjP-yjjQ-bglJ* locus (termed *ΔyjjPQ-bglJ* in the following, Table 3) and expression levels were compared to T75 harboring empty vector pKESK22 as control (Figure 5A). To this end, transformants of the respective strains were grown to mid-exponential growth phase and used for RNA isolation and analysis on Affymetrix GeneChip® E. coli Genome 2.0 microarrays. The microarray data revealed that

overexpression of BglJ lead to a significant (> 4-fold, p value < 0.05) upregulation of 39 loci (summarized in Table 1, detailed list in appendix Table 7).

Table 1: Microarray analysis of BglJ target loci.

Number of loci	**39**
RcsB-dependent	38
LeuO-dependent	5
co-regulated	2
H-NS binding	22

Gene function known	*leuO,* *bgl, chiA,* *cas, setA, sfsB, csrB,* *rhsA, rhsB, rhsC, rhsE,* *elfA, osmB, btuB, blc*

Gene function unknown/predicted	**24**
inner/outer membrane and cell surface	13

Strikingly, the *leuO* gene was one of the genes most strongly affected by BglJ expression, showing a 45-fold upregulation. The known target of RcsB-BglJ, the *bgl* operon, was also strongly activated (29-fold for *bglG*). To 22 of these 38 loci, binding of H-NS has been shown (Uyar *et al.*, 2009). Moreover, microarray analysis in Δ*rcsB* strain T175 revealed that activation of *leuO,* of *bgl,* and of all other target genes was completely dependent on RcsB (Figure 5B, Table 1, Table 7). This suggests that heterodimerization of BglJ and RcsB is in general essential for activation of gene expression. BglJ caused down-regulation of only one locus, *csrB,* encoding the CsrA regulating non-coding RNA CsrB. Beside targets with known function such as *bgl*, *leuO*, *chiA* (periplamic endochitinase), and *setA* (sugar efflux system), 24 RcsB-BglJ targets were genes of unknown or predicted function, 13 of which are predicted to be encoding membrane proteins, such as the RhsA, RhsB, and RhsC elements (encoding hydrophilic proteins with repetitive sequence elements) or cell surface proteins. However, since LeuO is a pleiotropic regulator of transcription, I assumed that some of the genes which were upregulated by RcsB-BglJ were targets of LeuO and only indirectly affected by activation of *leuO* through RcsB-BglJ. Therefore, I repeated the microarray analysis and overexpressed BglJ in Δ*leuO* strain T177 to exclude indirect targets (Figure 5C). Surprisingly, only five targets were regulated LeuO-dependently: the CRSIPR-associated *casA* gene, *elfA*

14

(encoding a fimbrial-like adhesion protein), the predicted fimbrial-like adhesin protein YadN, the RhsE cluster, and the predicted protein YhjX. All other loci were activated by RcsB-BglJ independently of *leuO* (Table 1, Table 7)

2.1.2 LeuO regulates transcription of several targets

To identify LeuO targets which are regulated independently of RcsB-BglJ, LeuO was expressed from low-copy vector pKEDR13 in *E. coli* strain T75 (Figure 5D). In accordance with previously published studies, LeuO showed pleiotropic function (Shimada *et al.*, 2011). Results of the LeuO microarray are summarized in Table 2, and a detailed list of LeuO targets is given in the appendix, Table 8. Overexpression of LeuO lead to the significant (> 4-fold, p value < 0.05) upregulation of 119 genes, whereas 61 genes were downregulated. For the 88 of the upregulated genes, binding of LeuO to the regulatory regions of the respective transcription units has been shown, as demonstrated by a comparison of the LeuO microarray results with the published genome-wide binding data of LeuO (Shimada *et al.*, 2011) (Table 2, Table 8). Of the 61 downregulated genes, only 19 showed also binding of LeuO. All targets which showed binding of LeuO are also bound by H-NS as evident from comparison with the study by Shimada *et al.* (2011). Most interestingly, the regulatory sRNA MicC was upregulated almost 200-fold. Other strongly upregulated targets were the CRISPR-associated *cas* operon, *chiA* (periplasmic endochitinase), and the *bgl* operon as known targets, among others. Please note that in strain T75 that was used for the microarray, the *yjjP-yjjQ-bglJ* region was deleted, so that these genes were not detected in the microarray results. A downregulation was observed for the known LeuO targets *dsrA* as well as the acid stress system *cadAB.* The five LeuO-dependend targets detected in the RcsB-BglJ micoarray were also found to be clearly regulated by LeuO (these were *casA*, *elfA*, *yadN*, RhsE cluster, *yhjX*). In general, the notion of LeuO as regulator of efflux systems and cell surface structures as suggested before (Shimada *et al.*, 2009, Shimada *et al.*, 2011) was confirmed by the results.

Table 2: Microarray analysis of RcsB-BglJ-independent LeuO targets.

Number of genes (LeuO binding shown)	**180 (101)**
upregulated	119 (88)
downregulated	61 (13)
Previously described LeuO targets	*bgl, chiA, cas, rhsE, dsrA acrEF, sdsRQP*
Gene function unknown/predicted	**83**
fimbria/pili	8
membrane	24
intergenic	16

To sum up, a comparison with the RcsB-BglJ microarray results reveals that most of the LeuO-regulated loci were not affected indirectly by BglJ expression. Interestingly, only two loci, *bgl* and *chiA* (encoding enzymes for β-glucoside utilization and a periplasmic endochitinase, respectively), are activated by RcsB-BglJ as well as by LeuO independently of each other. In the following, binding of RcsB-BglJ to the *bgl* regulatory region was shown. Additionally, activation of the CRISPR-*cas* operon by LeuO was analyzed. Moreover, transcriptional regulation of *leuO* was analyzed in detail as described in chapter 2.2.

2.1.3 RcsB-BglJ binds to regulatory region of *bgl*

Recently it has been shown that BglJ requires RcsB as a heterodimerization partner to activate *bgl* transcription (Figure 6) (Venkatesh *et al.*, 2010). The finding that RcsB-BglJ heterodimers counteract repression of *bgl* by H-NS indicates binding of RcsB-BglJ next to the *bgl* promoter. However, the location of a presumptive binding site so far was unknown. For RcsA-RcsB heterodimers, a consensus sequence of the binding sites has been proposed (Majdalani & Gottesman, 2005, Wehland & Bernhard, 2000). The RcsAB consensus sequence (also RcsAB box) is non-palindromic (Figure 7A) and presumably recognized by binding of RcsB to one half-site and by binding of RcsA to the other half-site (Francez-Charlot *et al.*, 2003). Interestingly, within the *bgl* regulatory region a perfect match to one half-site of the RcsAB box is located at position -88 to -95 (relative to the transcription start site). Assuming that the right half-site of the RcsAB box is bound by RcsB, this match indicates that the RcsB

subunit of the RcsB-BglJ heterodimer may bind to this motif and that BglJ contacts adjacent base pairs.
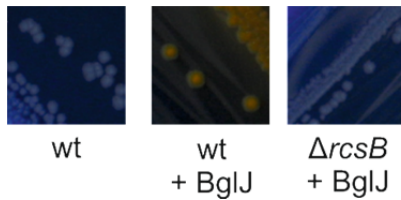
Figure 6: Activation of the *bgl* operon is dependent on *rcsB*.

Bgl phenotype on BTB salicin plates of wild-type strain T28 (Bgl⁻), of wild-type T28 expressing BglJ from plasmid pKETS1 (Bgl⁺) and of Δ*rcsB* strain T30 expressing BglJ from pKETS1 (Bgl⁻). Strains were grown on BTB salicin plates supplemented with 0.2 mM IPTG.

To test the relevance of this presumptive RcsB-BglJ binding site for derepression of *bgl* by RcsB-BglJ, site-specific mutations were introduced in the most conserved bases matching the right half site of the RcsAB box (mutant 1 in Figure 7A). In addition, the left half-site of the presumptive RcsB-BglJ box was mutated (mutant 2 in Figure 7A), and mutations in both half-sites were combined (mutant 3 in Figure 7A). The effect of these mutations on derepression of *bgl* by RcsB-BglJ was tested using a *bgl-lacZ* reporter fusion, which carries all elements required for repression by H-NS (Figure 7B). However, expression of this reporter is independent of regulatory elements for β-glucoside-specific regulation as it carries a mutation of terminator t1 (Nagarajavel *et al.*, 2007, Radde *et al.*, 2008). Note that sugar-specific regulation of the *bgl* operon is promoter-independent and mediated by the specific transcriptional antiterminator BglG, whose activity is regulated by phosphorylation dependent on the availability of the substrate and other sugars. BglG allows transcription read-through at terminator t1 in the leader of the operon and another terminator located within the operon (not present in the *lacZ* reporter gene fusion) (Görke, 2003).

For expression analyses, the *bgl-lacZ* reporter fusion with the putative wild-type and mutated RcsB-BglJ binding sites, respectively, were integrated at the chromosomal phage λ *attB* site of strain T314 (Δ*lacZ* Δ*yjjPQ-bglJ* Δ*leuO*) (Figure 7B). This strain carries deletions of the *lacZ* gene, of the *yjjP-yjjQ-bglJ* locus, and of the *leuO* gene (remember that LeuO also de-represses the *bgl* operon). To analyze derepression of *bgl* by RcsB-BglJ, BglJ was provided *in trans* using low-copy plasmid pKETS1 carrying *bglJ* under control of the inducible *tac* promoter. Empty vector pKESK22 was used as control (absence of BglJ). β-galactosidase expression levels directed by the *bgl-lacZ* fusion were determined of exponential cultures

grown in LB supplemented with kanamycin to an OD_{600} of 0.5. Please note that there is some ambiguity about the translation start codon of *bglJ*. Plasmid pKETS1 includes the most N-terminal AUG which maps within *yjjQ*. This plasmid directs the expression of active BglJ protein while plasmids pKETS9 and pKETS10, which include only the second or third start codon, respectively, provide no functional BglJ (data not shown). This suggests that translation of the *bglJ* gene begins at the very first start codon of the open reading frame.
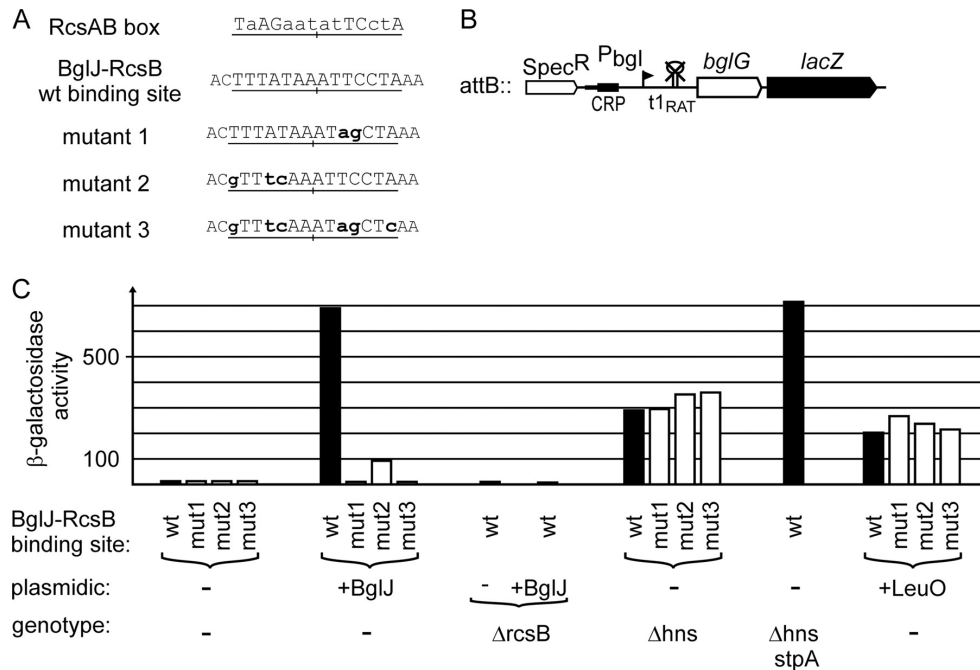
Figure 7: Mapping of RcsB-BglJ binding site at the *bgl* regulatory region.

The expression level directed by *bgl-lacZ* fusions (schematically shown in B) with wild-type and mutant RcsB-BglJ binding sites (B) was determined of exponential cultures grown in LB (with appropriate antibiotics and 1 mM IPTG) (C). The *bgl-lacZ* fusions were integrated at the phage λ *attB* site (strains listed in Table 3). Expression levels were determined in the 'wild-type' strain T314 (*ΔyjjPQ-bglJ ΔleuO*) transformed with the empty vector pKESK22 (-, black bars), with plasmid pKETS1 for expression of BglJ *in trans* (+BglJ), or with plasmid pKEDR13 for expression of LeuO (+LeuO). In addition, the expression level of the *bgl-lacZ* fusions was analyzed in transformants of *Δhns*, *ΔrcsB*, and *Δhns stpA* mutant derivatives, as indicated.

The *bgl-lacZ* reporter fusion with the presumptive wild-type RcsB-BglJ box directed low levels of β-galactosidase activity, as expected (12 units of β-galactosidase activity, Figure 7C). When BglJ was provided *in trans* (using plasmid pKETS1 with *bglJ* under control of the *lacI^q tac* promoter cassette) expression of the *bgl-lacZ* reporter increased 57-fold to 690 units (Figure 7C). In a *ΔrcsB* mutant, expression was low (9 units) and expression remained low (8

units) when BglJ was provided *in trans* confirming again that derepression of *bgl* by BglJ requires RcsB (Figure 7C).

Next, the expression levels directed by the RcsB-BglJ binding-site mutants 1 to 3 (Figure 7A) were tested in the absence or presence of BglJ. In case of mutants 1 and 3, which both carry exchanges corresponding to the conserved bases of the right half-site, induction of plasmid-encoded BglJ had no effect (10 to 13 units in all cases, Figure 7C). This demonstrates that mutations in the presumptive RcsB-BglJ binding site abrogate derepression of *bgl* by RcsB-BglJ. Interestingly, also binding site mutant 2 affected derepression of the *bgl* promoter *lacZ* fusion by RcsB-BglJ, as the expression level increased merely 8-fold from 12 to 92 units when BglJ was expressed (Figure 7C). Mutant 2 carries mutations in the left half of the putative RcsB-BglJ box which is presumably contacted by the BglJ subunit of the RcsB-BglJ heterodimer (Figure 7A). Taken together these data demonstrate that the putative RcsB-BglJ motif is important for de-repression of *bgl* by RcsB-BglJ heterodimers.

As further control, expression of the *bgl-lacZ* reporter constructs with the wild-type RcsB-BglJ box and its mutants was also tested in isogenic Δ*hns* strains. Expression levels were high (290 to 360 units, Figure 7C), as expected, as H-NS represses the *bgl* promoter. Further, in the Δ*hns* mutant the activity was similarly high, irrespective of whether the RcsB-BglJ box was mutated or not, demonstrating that the site-specific mutations do not affect the promoter activity or repression by H-NS (Figure 7C). Interestingly, the expression level directed by the *bgl-lacZ* fusion was lower in the Δ*hns* mutant (290 units) than when plasmid encoded BglJ was provided in the wild-type (690 units). This indicated that the *bgl* promoter is not fully active in the *hns* mutant. In agreement with previous studies, which demonstrated that StpA partially represses *bgl* in *hns* mutants (Free *et al.*, 2001, Muller *et al.*, 2010, Wolf *et al.*, 2006), the expression level directed by the *bgl-lacZ* fusion was 715 units in the Δ*hns stpA* double mutant and thus similarly high as upon de-repression of *bgl* by RcsB-BglJ. However, growth of the Δ*hns stpA* double mutant was significantly slower than that of the Δ*hns* mutant. Similarly, expression of plasmidic BglJ resulted in significantly slower growth in the Δ*hns* mutant and caused a severe growth reduction in the Δ*hns stpA* double mutant (data not shown). Therefore, I could not test whether RcsB-BglJ further enhances *bgl* promoter activity in the absence of H-NS and StpA. However, taken together, the data suggest that the RcsB-BglJ heterodimer binds to the mapped site within the

upstream regulatory region of *bgl* (Figure 8) and antagonizes repression of *bgl* by H-NS, and also by StpA.

Since the *bgl* operon has been shown to be regulated by RcsB-BglJ and by LeuO, I also tested whether de-repression of *bgl* by LeuO is independent of BglJ, whose expression is activated by LeuO, and whether the mutations in the RcsB-BglJ binding site interfere with derepression of *bgl* by LeuO, expression levels were in addition tested with LeuO provided *in trans*. For this, plasmid pKEDR13 carrying *leuO* under control of the inducible *tac* promoter was used. Induction of plasmid encoded LeuO caused derepression of the *bgl-lacZ* fusion (directing 200 units of β-galactosidase activity, Figure 7C) demonstrating that LeuO activates *bgl* independently of RcsB-BglJ (remember that the strain in which expression was tested is Δ*yjjPQ-bglJ* Δ*leuO*).

Similarly high expression levels were directed by the RcsB-BglJ binding-site mutants when LeuO was present (200 units for the wild type compared to 215 to 265 units for the mutants) (Figure 7C). This demonstrates that the mutations of the presumptive RcsB-BglJ box do not interfere with derepression of *bgl* by LeuO. However, LeuO did not cause full activation (approximately 200 units in the presence of LeuO compared to 690 units in the presence of BglJ). Nonetheless, the data suggest that LeuO de-represses *bgl* by directly binding to the upstream regulatory region of the *bgl* promoter. Importantly, these data suggest that mutations in the presumptive RcsB-BglJ binding site do not abolish LeuO binding. Moreover, the position of the LeuO binding site at the *bgl* promoter has been mapped in our laboratory (Venkatesh *et al.*, 2010). The LeuO footprint showed protection of approximately 60 bp, extending from positions −101 to −160 relative to the *bgl* transcription start site. Thus, the LeuO binding site maps just adjacent to the RcsB-BglJ site (Figure 8). Such extended footprints are typical of LeuO (De la Cruz *et al.*, 2007, Hernandez-Lucas *et al.*, 2008, Westra *et al.*, 2010) and other LysR-type transcription factors (Maddocks & Oyston, 2008). However, it remains unknown whether LeuO and RcsB-BglJ can bind simultaneously to the *bgl* regulatory region. The results presented in this chapter have been published in (Venkatesh *et al.*, 2010).
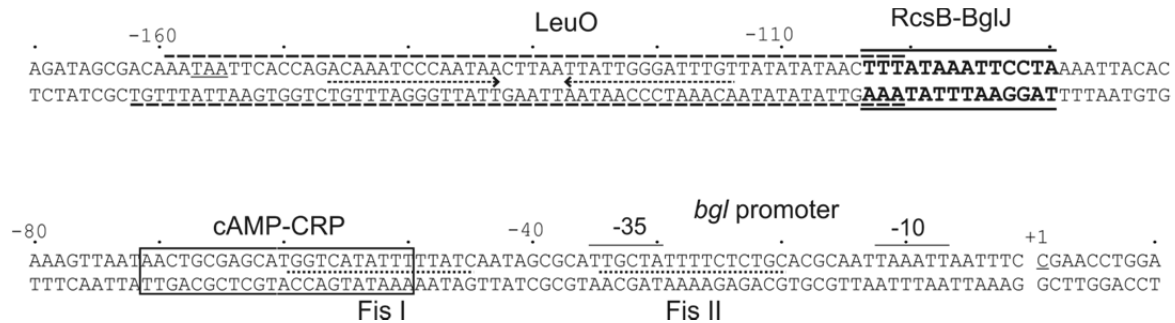
Figure 8: Sequence of the *bgl* promoter and upstream regulatory region.

Indicated are the -35, -10, and transcription start sites of the *bgl* promoter; a CRP binding site (boxed) (Reynolds *et al.*, 1986); and a Fis binding sites (dotted lines) (Caramel & Schnetz, 2000), as well as the LeuO (dashed lines) and RcsB-BglJ (solid lines) binding sites. H-NS binds to the upstream regulatory element and the promoter, but the H-NS nucleation sites have so far not been mapped. The stop codon of the phoU gene located upstream of *bgl* is underlined, and the inverted arrows indicate an inverted repeat that may represent a transcriptional terminator. Figure from (Venkatesh *et al.*, 2010).

2.1.4 LeuO activates the *cas* operon

Among other targets, the microarray analysis revealed that overexpression of LeuO led to an upregulation the CRISPR-associated *cas* operon encoding genes for the bacterial immunity system against foreign DNA (chapter 2.1.2, appendix Table 8). RNA samples isolated from *ΔyjjPQ-bglJ* strain T75 containing LeuO expression vector pKEDR13 were compared to RNA isolated from T75 containing the empty vector pKESK22. Comparison of *cas* gene transcription levels between the LeuO-expressing strain and the control strain in the microarray experiment revealed a significant upregulation of transcription of *casABCDE*, *cas1* and *cas2*, showing a gradual decrease from *casA* (65-fold) to *cas2* (5-fold) (Figure 9B, Table 8). No change in the transcription level of *cas3* was detected. These results are consistent with a polycistronic transcription of the *casABCDE* and possibly the *cas1* and *cas2* genes, with polar effects for the transcription of the more downstream genes. To confirm the effect of LeuO on *cas* gene expression detected in the microarray experiment, transcript levels of the *E. coli* K12 *cas* genes in exponential growth phase were examined using reverse transcription followed by quantitative PCR (RT-qPCR). For this, RNA was isolated from the same strains as described for the microarray analysis and was reverse-transcribed using random hexameric oligonucleotides as primers. The expression of the *cas* operon was measured by qPCR with primers specific for either *casA*, *casC*, *cas2*, or *cas3*, respectively (Figure 9C). The measured activation was 31.6-fold for casA, 16.7-fold for casC, and 3.3-fold

21

for cas2. Transcription of cas3 was not activated. Thus, the RT-qPCR confirmed the microarray data (Figure 9C). A detailed functional analysis of *cas* regulation has been published in (Westra *et al.*, 2010).
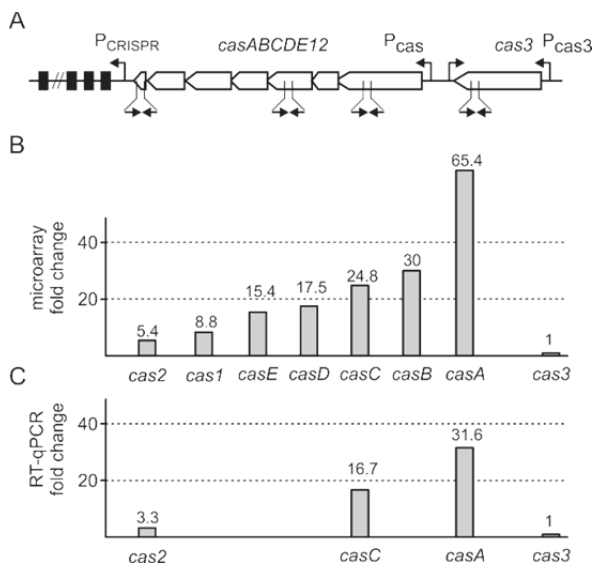
Figure 9: LeuO activates transcription of *cas* genes.

(A) Schematic illustration of the CRISPR/Cas locus in *E. coli* K12 (pos. in NC_000913: 2,885,241 to 2,875,640) that consists of the eight genes *cas3*, *casABCDE12* and a downstream CRISPR locus containing 12 spacers and 13 repeats (CRISPR I, black rectangles). The *cas3*, *cas* and CRISPR promoters are indicated with bent arrows. Small arrows below the genes show the map positions of primer pairs used for RT-qPCR. (B) The fold change of *cas* expression was determined by microarray analysis. RNA was harvested from cultures of *ΔyjjPQ-bglJ* strain T75 harboring either LeuO expression vector pKEDR13 (+, grey bars) or empty control pKESK22 (-) from exponential growth phase in LB supplemented with kanamycin and 1 mM IPTG. RNA was used for hybridization on Affymetrix E. coli 2.0 array. Expression level is given as fold-change compared to the control T75/pKESK22. (C) Analysis of expression of *cas2, casC, casA*, and *cas3* by RT-qPCR to confirm microarray data. RNA was isolated as described in (B). After reverse transcription, qPCR was performed using dilutions of cDNA and the following primer pairs: T411/T412 for *cas2*, T413/T414 for *casC*, T415/T416 for *casA*, and T417/T418 for *cas3*. C_t values were normalized to *rpoD* expression determined with primers T247 and T248. Expression level is given as fold-change compared to the control T75/pKESK22.

2.2 Transcriptional control of *leuO*

The microarray data showed that *leuO* was one of the genes that is most strongly activated by RcsB-BglJ. Since LeuO is regarded as a pleiotropic regulator of stress responses and as an important H-NS antagonist, transcriptional control of *leuO* was analyzed in detail. Results presented in this chapter have been published in Stratmann *et al.* (2012).

2.2.1 Transcription of *leuO* is activated by RcsB-BglJ

To study the regulatory effect of RcsB-BglJ on transcription of *leuO*, I used a *leuO* promoter *lacZ* reporter fusion and integrated it into the chromosomal phage λ attachment site *attB* of isogenic derivatives of *ΔlacZ* strain S4197 (Table 3). The *lacZ* fusion encompasses the complete 659 bp intergenic region between the *leu* operon and *leuO* (Figure 10). In the wild-type strain (T28) this *leuO* promoter *lacZ* fusion directed only 3 Miller units of β-galactosidase activity (Figure 10B). Low expression is in agreement with repression of *leuO* by H-NS (Chen *et al.*, 2001). However, when BglJ was expressed from plasmid pKETS1, the expression level increased to 338 Miller units (Figure 10B). Note that in this strain the chromosomal copy of *bglJ* is repressed by H-NS (Stratmann *et al.*, 2008). Similar results were obtained in the *ΔyjjPQ-bglJ ΔleuO* double mutant T308. In this strain background, BglJ caused an increase in expression from 3 units to 406 units (Figure 1B). Accordingly, the expression analyses demonstrate a more than 100-fold activation of *leuO* by expression of BglJ, confirming the microarray data.
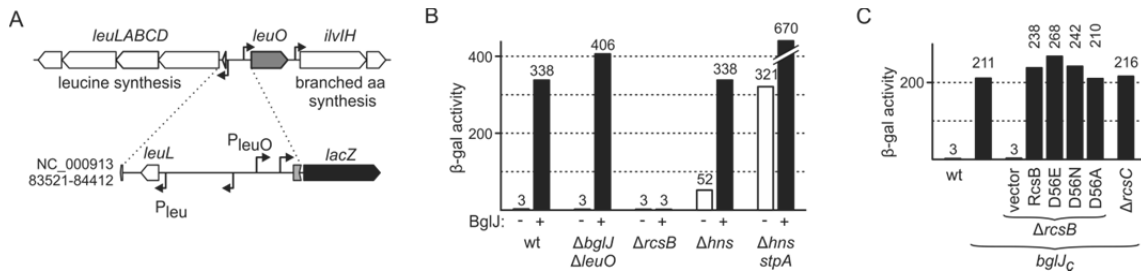
Figure 10: RcsB-BglJ activates transcription of *leuO*

(A) Schematic representation of the chromosomal *leu* operon-*leuO* locus and a *leuO* promoter *lacZ* fusion integrated at the phage λ *attB* site. (B) The expression level directed by the *leuO* promoter *lacZ* fusion was determined in wild-type strain T28, *ΔyjjPQ-bglJ ΔleuO* strain T308, *ΔrcsB* strain T30, *Δhns* strain T288, and *Δhns stpA* strain T352. BglJ was expressed from plasmid pKETS1 (+, black bars). Empty vector pKESK22 served as control (-, white bars). Cultures for β-galactosidase assays were grown in LB medium to an OD_{600} of 0.5 supplemented with 1 mM IPTG and 25 µg/ml of kanamycin. (C) Expression levels directed by the *leuO* promoter *lacZ* fusion in strains carrying a miniTn10 transposon insertion in *yjjQ* which leads to constitutive expression of downstream *bglJ* (*bglJ$_C$*). β-galactosidase activity was determined in strains *bglJ$_C$* T570, *bglJ$_C$ ΔrcsB* T572, and *bglJ$_C$ ΔrcsC* T574. Wildtype RcsB and RcsB mutants D56E, D56N and D56A were provided *in trans* using plasmids pKETS6, pKETS7, pKETS8, and pKES235, respectively, as indicated. Empty cloning vector pKESK22 served as control (vector).

2.2.2 *leuO* is activated by an RcsB-BglJ heterodimer independently of the Rcs phosphorelay

BglJ requires RcsB as dimerization partner to activate transcription of the *bgl* operon (Venkatesh *et al.*, 2010), and the microarray data suggested that BglJ requires RcsB for activation of *leuO* and other target genes. I therefore tested the expression of the *leuO* promoter *lacZ* fusion in the *ΔrcsB* mutant T30. Indeed, in the *ΔrcsB* mutant expression of BglJ from plasmid pKETS1 did not cause activation of the *leuO* promoter *lacZ* fusion and only background expression levels of 3 units were detected (Figure 10B). This shows that both proteins, RcsB and BglJ, are required for activation of *leuO* transcription. Previously, it has been shown that activation of the *bgl* operon by RcsB-BglJ is independent of phosphorylation of RcsB by the Rcs two-component phosphorelay system (Venkatesh *et al.*, 2010). I therefore tested whether activation of *leuO* by RcsB-BglJ is also independent of phosphorylation of RcsB. For this analysis, I used a *ΔrcsB* mutant carrying a miniTn10 transposon insertion causing constitutive expression of *bglJ* (*bglJ$_C$*, strain T572). In this *bglJ$_C$ ΔrcsB* mutant the *leuO* promoter *lacZ* fusion was not expressed (3 units), while in the *rcsB* wild-type background constitutive expression of BglJ from allele *bglJ$_C$* resulted in an expression level of 211 units (Figure 10C). The *ΔrcsB* mutant was complemented with low-copy plasmids encoding wild-type RcsB (pKETS6), or mutants RcsB-D56E (pKETS7), RcsB-

D56N (pKETS8), and RcsB-D56A (pKES235), respectively. Mutation of the presumptive phosphorylation site D56 mimics the active phosphorylated form of RcsB (D56E) or the non-phosphorylated form of RcsB (D56A and D56N) (Scharf, 2010). Complementation with wild-type RcsB restored activation of the *leuO* promoter *lacZ* fusion by BglJ, with an increase of the expression level to 238 units. Similarly, 267 units were determined for complementation with RcsB-D56E, 242 units for RcsB-D56N, and 210 units for RcsB-D56A (Figure 10C). These data demonstrate that there is no significant difference between wild-type RcsB, and the D56 mutants, suggesting that activation of *leuO* by RcsB-BglJ is independent of the phosphorylation status of RcsB at D56. This conclusion is further supported by the result that activation of the *leuO* promoter by RcsB-BglJ was not dependent on RcsC, the upstream sensor kinase of the Rcs phosphorelay. In the $\Delta rcsC$ *bglJ$_C$* mutant (T574) the expression level remained as high (216 units) as in the *bglJ$_C$* background (211 units, Figure 10C).

2.2.3 Transcription of *leuO* is repressed by H-NS and StpA

Previous studies have shown that transcription of *leuO* is repressed by the nucleoid-associated protein H-NS. To elucidate the role of the H-NS paralog StpA for regulation of *leuO*, I determined the activity of the *leuO* promoter *lacZ* fusion in Δhns mutant T316 and Δhns *stpA* double mutant T352. In the Δhns mutant the expression level increased to 52 Miller units (Figure 10B). Intriguingly, in the Δhns *stpA* double mutant expression was even 6-fold higher and reached 321 units (Figure 10B). These results confirm that transcription of *leuO* is repressed by H-NS, and further show that StpA contributes to this repression. Activity of the *leuO* promoter *lacZ* fusion was even 2-fold higher (669 units) when additionally BglJ was expressed from plasmid pKETS1 in the Δhns *stpA* double mutant (Figure 10B). However, I cannot rule out that this additional increase of expression is due to pleiotropic effects, as expression of BglJ in the Δhns *stpA* double mutant led to severe growth deficiencies (data not shown).

2.2.4 RcsB-BglJ binds to regulatory region of *leuO*

Next I assessed whether activation of the *leuO* promoter by RcsB-BglJ is mediated by binding to the *leuO* regulatory region. However, so far I was not successful in purifying active BglJ protein. Therefore, I searched the *leuO* regulatory sequence for possible RcsB-BglJ binding

25

sites by comparing it to the only known RcsB-BglJ binding site located at the *bgl* locus (Chapter 2.1.3, Figure 7, Figure 11A). In addition, I compared the sequence to the consensus sequence of the RcsB-RcsA heterodimer (Wehland & Bernhard, 2000). Three candidate sequence motifs were mutated, and the effect of the mutations on activation of the *leuO* promoter *lacZ* fusion by BglJ was tested (mut1, mut2, and mut3, Figure 11B). Mutation of the best candidate sequence motif (mut3, mapping at NC_00913 position 84239 to 84252) completely abrogated activation by BglJ (Figure 11C). In the *bglJ$_C$* strain expressing BglJ constitutively, the expression level dropped from 184 units obtained with the wild-type *leuO* promoter *lacZ* fusion (strain T862) to 4 units of RcsB-BglJ site mutant mut 3 in strain T1075 (Figure 11C). The same low activity was measured in a strain carrying the two mutations mut1 and mut3, but not in the mut1 and mut2 single mutants, respectively (Figure 11C). In mut2, the expression level was higher (305 units) than in the the wild-type strain (184 units). Since mut2 maps to the H-NS nucleation site, the mutations introduced at mut2 may abrogate binding of H-NS to this site and lead to de-repression of the reproter fusion. As a control, I confirmed that another RcsB-BglJ target (the *bgl* operon) remained activate in all tested strains (data not shown). Importantly, the mutation mut3 of the RcsB-BglJ site did not affect expression in the Δ*hns stpA* mutant T1107. In the absence of H-NS and StpA the *leuO* promoter *lacZ* fusion with the mutant RcsB-BglJ site was expressed at high levels (222 units). Taken together, these data suggest that RcsB-BglJ activates *leuO* transcription by binding to the mapped site at mut3 (RcsB-BglJ site in the following, Figure 12).
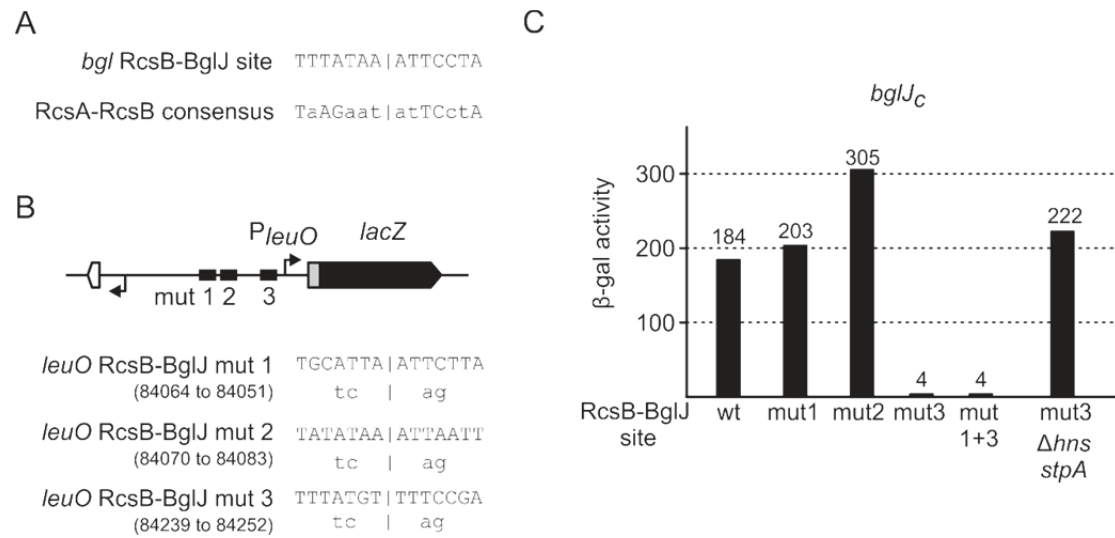
Figure 11: Mapping of RcsB-BglJ binding site at the *leuO* promoter region.

(A) RcsB-BglJ binding site at the *bgl* promoter (chapter 2.1.3) and RcsA-RcsB consensus sequence (Wehland & Bernhard, 2000). (B) The *leuO* promoter region was searched for sites showing high similarity to the RcsB-BglJ binding site mapped at the *bgl* promoter and to RcsA-RcsB consensus binding site. Point mutations (lower case) were introduced into three putative binding sites (black rectangles) located at the indicated positions and fused to a *lacZ* reporter by CCR (mut 1, mut 2, and mut 3). (C) Mutation of the putative RcsB-BglJ binding site (mut 3) abrogates activation of the *leuO* promoter *lacZ* fusion by RcsB-BglJ. Activities directed by the *leuO* promoter *lacZ* fusion in *bglJ$_C$ ΔleuO* strain T862 (wt), by the RcsB-BglJ site mutants T1072 (mut 1), T1073 (mut 2), T1075 (mut 3), T1077 (mut 1+3), and by mut 3 in the *Δhns stpA* derivative (strain T1107) were determined in cultures grown in LB to an OD$_{600}$ of 0.5.

```
83501   GTATCGAAAA TAATGACTTG CTGGCTCATG GTTTGGGTCC TTGTCTCTTT TAGAGCGCCT CGCTTCGGGC ATAAAAAAAC CCGCGCAATG GCGCGGGTTT
        CATAGCTTTT ATTACTGAAC GACCGAGTAC CAAACCCAGG AACAGAGAAA ATCTCGCGGA GCGAAGCCCG TATTTTTTTG GGCGCGTTAC CGCGCCCAAA
        .. D  F   I   I   V   Q   Q   S   M
```

```
83601   TTTGTTTGAC TGCGTGCTGG CTTAATGCTG GATGCCGCTC ACTCGTCTAC CGCGCAAAGA AGATGCGTTT AGTAGTAGTA GACCGATAAA GCGAACGATG
        AAACAAACTG ACGCACGACC GAATTACGAC CTACGGCGAG TGAGCAGATG GCGCGTTTCT TCTACGCAAA TCATCATCAT CTGGCTATTT CGCTTGCTAC
                  *  H   Q   I   G   S   V   R   R   G   R   L   S   A   N   L   L   L   L   G   I   F   R   V   I   .
```

```
                                                                       h
83701   TGAGTCATTA AATCAGCTCC AGATGAATGC GATATGCTTT TAGAGTTACT GGATACAAAA ACGGATGTCA ACCCTGACGC AATAAAAACG TCCCGCCAGC
        ACTCAGTAAT TTAGTCGAGG TCTACTTACG CTATACGAAA ATCTCAATGA CCTATGTTTT TGCCTACAGT TGGGACTGCG TTATTTTTGC AGGGCGGTCG
        H  T   M                                        Pleu
               leuL
```

```
                                  g
83801   GTGAGTTCTG CATCCGTAAA ATTAGCTAAT TGTGGTGCGG TGGTTAAAGT AAGCGATATT AATTTCTGCT TAACTACCGA CGCTTTTCAT CGGTTGACAT
        CACTCAAGAC GTAGGCATTT TAATCGATTA ACACGACGCC ACCAATTTCA TTCGCTATAA TTAAAGACGA ATTGATGGCT GCGAAAAGTA GCCAACTGTA
```

```
            f                                                                                           e
83901   ATTTCAGCAT AAATTTTTGC ATCTAATCAA CGAGGAAAAA GGGGACAAAA TGCACGCGTT GCAAAACCTA TCCTGATGAT TTGTATTGAA TTATATGTTT
        TAAAGTCGTA TTTAAAAACG TAGATTAGTT GCTCCTTTTT CCCCTGTTTT ACGTGCGCAA CGTTTTGGAT AGGACTACTA AACATAACTT AATATACAAA
                                                                                      H-NS nucleation site
```

```
                                            d
84001   TGCGATTTTT TTTGATATTG ATTTGGTGAA TATTATTGAT CAATTAATGT TAAGAATTAA TGCATTAAAT ATATAAATTA ATTATTAAAT AAGCACATTT
        ACGCTAAAAA AAACTATAAC TAAACCACTT ATAATAACTA GTTAATTACA ATTCTTAATT ACGTAATTTA TATATTTAAT TAATAATTTA TTCGTGTAAA
                            P2leu  LeuO site I                 PleuO
```

```
84101   AATCCATTTT GTAGATGATT GAGTATTCGC GGTAGTTATG ATTAGATTGT TTTCGCAACA AAACCATTAT GGATTATTAT GCTGTGGTAA ATGACTCATT
        TTAGGTAAAA CATCTACTAA CTCATAAGCG CCATCAATAC TAATCTAACA AAAGCGGTTGT TTTTGTAATA CCTAATAATA CGACACCATT TACTGAGTAA
                   LeuO site II                                  c
```

```
                                      tc      ag
84201   CCACGGCAAT GGATTCTGTT TTTATCAGAA CCCGTATCTT TATGTTTTCC GAATTTTACT CATTTTGCTT TTTCTTATTT TATATGCATG ATAAATCATA
        GGTGCCGTTA CCTAAGACAA AAATAGTCTT GGGCATAGAA ATACAAAAGG CTTAAAATGA GTAAAACGAA AAAGAATAAA ATATACGTAC TATTTAGTAT
                                          RcsB-BglJ site                                               b
```

```
        P2leuO                                                                      leuO
                                                                          M  P   E   V   Q   T   D   H   P   E   T
84301   TTCTTCAGGA TTATTTCTCT GCATTCCAAT AAGGGAAAGG GAGTTAAGTG TGACAGTGGA GTTAAGTATG CCAGAGGTAC AAACAGATCA TCCAGAGACG
        AAGAAGTCCT AATAAAGAGA CGTAAGGTTA TTCCCTTTCC CTCAATTCAC ACTGTCACCT CAATTCATAC GGTCTCCATG TTTGTCTAGT AGGTCTCTGC
                                                                            a
```

```
        A   E   L   S   K   P   Q   L   R   M   V   D   L   N   L   L   T   V   F   D   A   V   M   Q   E   Q   N   I   T   R   A   A   H   V
84401   GCGGAGTTAA GCAAACCACA GCTACGCATG GTCGATCTCA ACTTATTAAC CGTTTTCGAT GCCGTGATGC AGGAGCAAAA CATTACTCGT GCCGCTCATG
        CGCCTCAATT CGTTTGGTGT CGATGCGTAC CAGCTAGAGT TGAATAATTG GCAAAAGCTA CGGCACTACG TCCTCGTTTT GTAATGAGCA CGGCGAGTAC
```
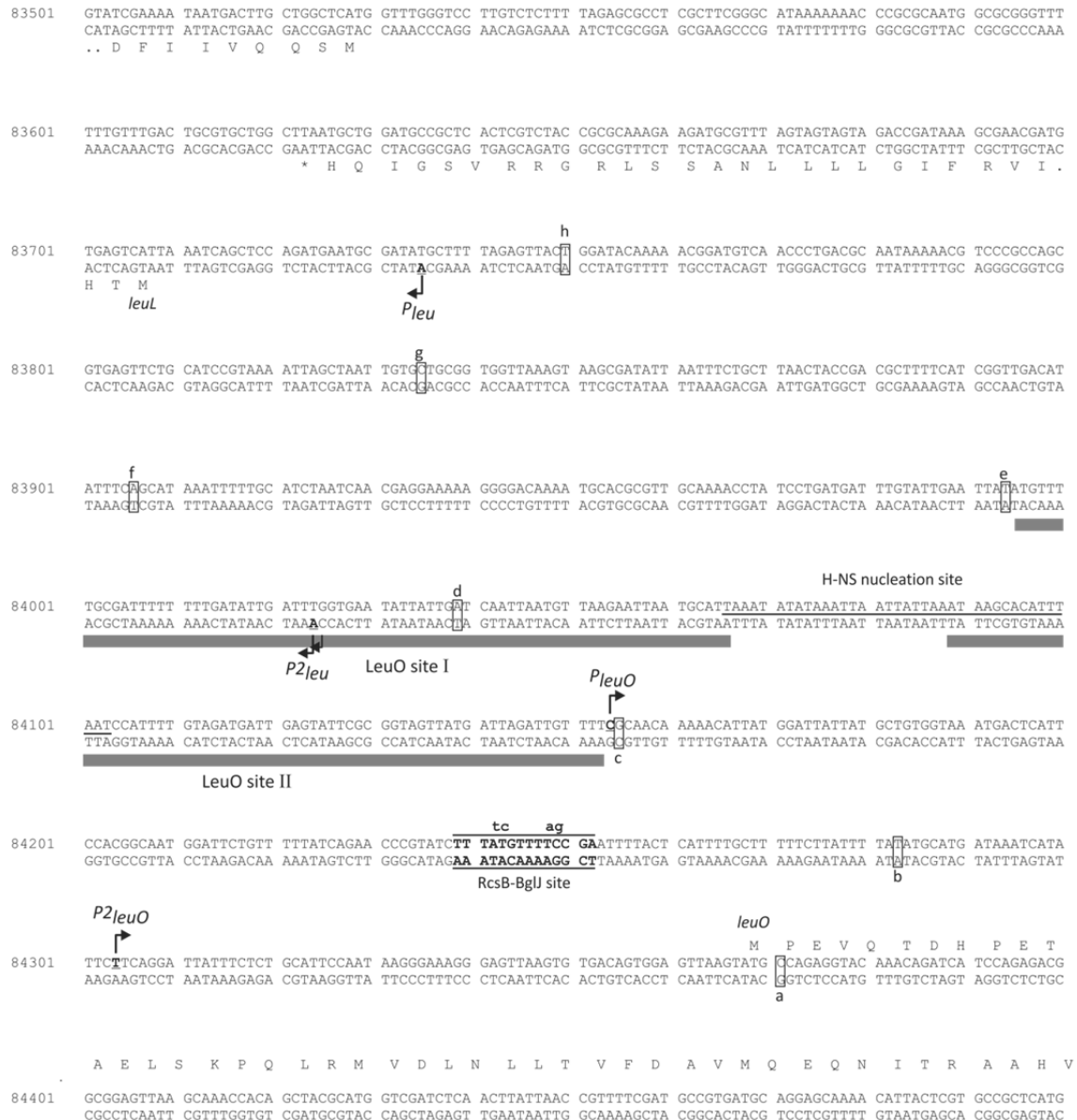
Figure 12: Sequence of *leu-leuO* intergenic region with mapped regulatory features.

The sequence of the *leu-leuO* intergenic region is shown with the coordinates according to the reference genome sequence NC_000913. Bent arrows indicate the transcription start sites termed P*leu*, P2*leu*, P*leuO* and P2*leuO* which were mapped *in vivo* by 5'RACE. Grey bars show the regions protected by LeuO in DNase I footprinting analysis. Rectangles indicate KMnO$_4$ sensitive sites at positions 'a' to 'h' which were mapped by KMnO$_4$ footprinting. Further, the RcsB-BglJ binding site and the mutations used to map this site (mut3 in Figure 11) are indicated. The H-NS nucleation site has been mapped before (Chen & Wu, 2005).

2.2.5 RcsB-BglJ activates one of two H-NS-StpA repressed *leuO* promoters in vivo

To map *in vivo* transcription start sites in the intergenic region between *leuO* and the *leu* operon, I performed 5'RACE analyses. I isolated RNA from Δ*yjjPQ-bglJ* strain T75, from

28

Δ*hns stpA* mutant T447, and from Δ*hns stpA* Δ*yjjPQ-bglJ* mutant T1048. In the Δ*hns stpA* mutants, I expected the *leuO* promoter to be active. In addition, BglJ should be present in the Δ*hns stpA* (chromosomal *bglJ* derepressed) but not in the Δ*hns stpA* Δ*yjjPQ-bglJ* mutant. For 5'RACE analysis, half of each RNA sample was treated with tobacco acid pyrophosphatase (TAP) to distinguish between primary 5' mRNA ends (transcription start sites) and processed 5' mRNA ends. Then 5'RACE products were analyzed on agarose gels, the fragments of TAP treated samples were cloned and at least 4 clones each were sequenced to map the transcription start sites (Figure 13).
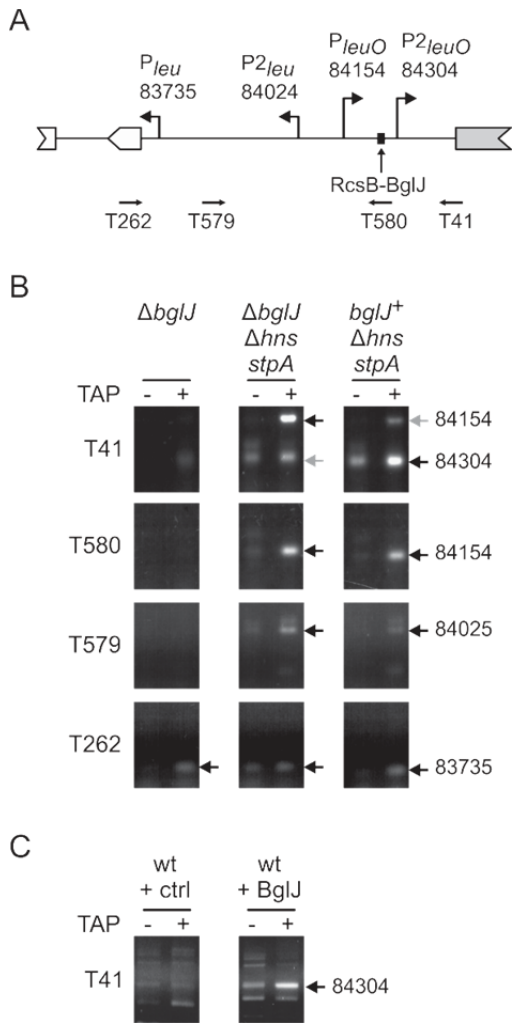
A

Figure 13: RcsB-BglJ activates one of two H-NS/StpA-repressed *leuO* promoters *in vivo.*

(A) Schematic summary of 5'RACE mapping of promoters in the *leu-leuO* intergenic region. Indicated are the primers used for 5'RACE, the mapped transcription starts (given as coordinates of sequence reference file NC_000913), and the RcsB-BglJ binding site. (B) Gel electrophoresis of 5'RACE PCR products. For 5'RACE analysis, total RNA was extracted from strains *ΔyjjPQ-bglJ* (*ΔbglJ*) T75, *Δhns stpA ΔyjjPQ-bglJ* T1048, and *Δhns stpA* (*bglJ*+) T447. To map primary 5'ends of transcripts, half of each RNA sample was treated with tobacco acid pyrophosphatase (+TAP). Then RNA oligo T268 was ligated to RNA 5'ends of TAP treated and untreated samples, and the RNA was used for first-strand cDNA synthesis. For PCR amplification of *leu-leuO* specific cDNA, oligonucleotides T262, T579, T580, and T41, respectively, were used in combination with adapter-specific DNA oligonucleotide T265. TAP-dependent 5'RACE products were cloned into pUC12 and at least four clones each were sequenced. The position of the most 5' nucleotide neighboring the RACE adapter was taken as transcription start site (arrows). Two transcription starts oriented toward the *leu* operon were mapped to NC000_913 positions 83,735 (P$_{leu}$) and 84,024 (P2$_{leu}$) using primers T262 and T579, respectively, confirming the previously published transcription start mapped to position 83,735 (Wessler & Calvo, 1981). Two transcription start sites oriented toward *leuO*, were mapped to positions 84,155 (P$_{leuO}$) and 84,304 (P2$_{leuO}$) using primers T580 and T41, respectively. In strain *Δhns stpA* (BglJ present, derepressed in absence of H-NS), P2$_{leuO}$ at 84,304 is more prominent than in strain *Δhns stpA ΔyjjPQ bglJ* (no BglJ, grey arrow). P2$_{leu}$, P$_{leuO}$, and P2$_{leuO}$ were only detected in the *Δhns stpA* mutant strains. Experiments were carried out twice and typical 2 % agarose gel images are shown. (C) Gel electrophoresis of 5'RACE PCR products using wild-type strain S3974 harboring control vector pKESK22 (wt + ctrl) or BglJ expression vector pKETS1 (wt + BglJ) and primer T41. Procedure as described in (B).

Two transcription start sites of the *leuO* gene were detected when 5'RACE was performed with primers T580 and T41 (Figure 13A). One of these transcription start sites mapped to position 84,155 and corresponds to the *leuO* promoter previously mapped in *S. enterica* (Fang & Wu, 1998a). This promoter is designated P$_{leuO}$. The second novel transcription start of *leuO*, P2$_{leuO}$, was mapped to position 84,304 using primer T41 (sequence shown in Figure

12). Both transcription starts were only detectable in the Δ*hns stpA* mutants indicative of repression by H-NS and StpA. Moreover, the TAP-dependent band corresponding to the newly identified transcription start site at position 84,304 was much more prominent in the Δ*hns stpA* strain, in which chromosomal *bglJ* is de-repressed (i.e. in the presence of BglJ), than in the Δ*hns stpA* Δ*yjjPQ-bglJ* mutant (absence of BglJ). These results show that expression of *leuO* is directed by two H-NS and StpA repressed promoters (P_{leuO} and $P2_{leuO}$) and they suggest that RcsB-BglJ activates transcription from promoter $P2_{leuO}$ at position 84,304. Correspondingly, the center of the RcsB-BglJ binding site maps at -58.5 bp relative to this transcription start (Figure 13B). Further, transcription initiation at $P2_{leuO}$ was detected by 5'RACE in a wild-type strain in which BglJ was overexpressed from a plasmid (Figure 13C).

In parallel, I performed 5'RACE analyses using primers specific for *leu* operon transcripts (Figure 13). In all three strain backgrounds, I detected a band that corresponded to the P_{leu} promoter with the transcription start site at pos. 83,735, which was mapped previously (Figure 13A) (Wessler & Calvo, 1981). An additional transcription start of the *leu* operon was mapped to position 84,024 using PCR primer T579 (Figure 13A). This transcription start site was only detectable in the Δ*hns stpA* mutants, indicative of repression of this newly identified promoter $P2_{leu}$ by H-NS and/or StpA.
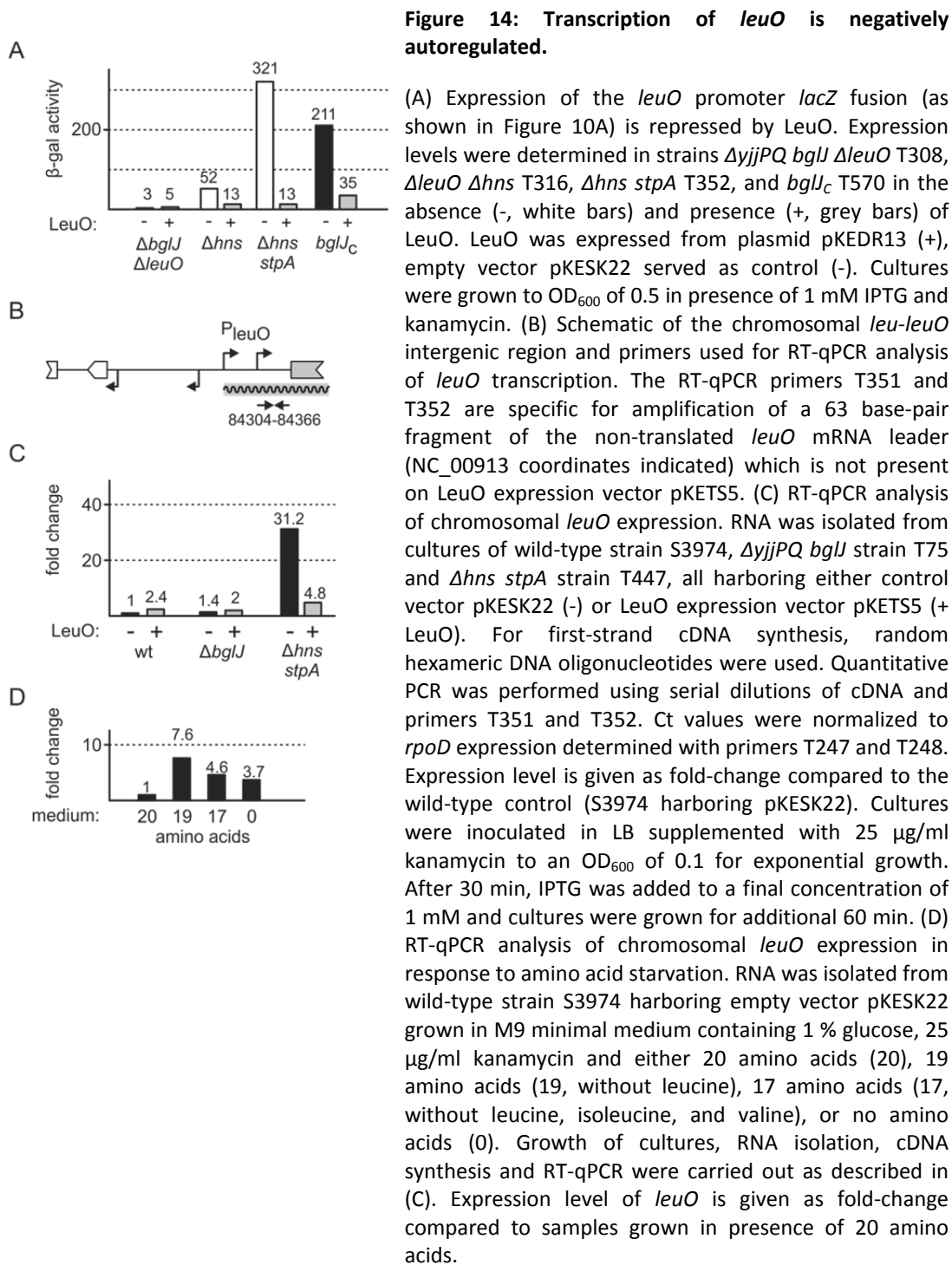

2.2.6 Transcription of *leuO* is negatively autoregulated

Previous studies suggested that LeuO might act as an activator of its own transcription by antagonizing H-NS-mediated repression (Chen *et al.*, 2003, Chen & Wu, 2005). Therefore, I also tested the autoregulatory effect of LeuO *in vivo*. Firstly, LeuO was expressed from low-copy plasmid pKEDR13 and measured activity of the *leuO* promoter *lacZ* fusion in the Δ*leuO* Δ*yjjPQ-bglJ* double mutant T308. In this strain the *leuO* promoter *lacZ* fusion is repressed by H-NS and StpA, while BglJ is absent. In the presence of plasmidic LeuO, expression of the *leuO* promoter *lacZ* fusion increased slightly from 3 units to 5 units (Figure 14A), demonstrating a marginal approximately 2-fold upregulation by LeuO. Secondly, I measured expression of the *leuO* promoter *lacZ fusion* in Δ*hns* mutant T316 and in Δ*hns stpA* double mutant T352, respectively, in which the *leuO* promoter is partially or fully derepressed. When plasmidic LeuO was provided *in trans*, the expression level dropped from 52 units (Δ*hns*) to 13 units (Δ*hns* +LeuO, Figure 14A). Even more strikingly, in the Δ*hns stpA*

double mutant expression also decreased to 13 units as compared to 321 units (Figure 14A). Finally, to investigate whether LeuO can downregulate its expression in the presence of RcsB-BglJ, I performed the experiments using $bglJ_C$ strain T570. Here, the *leuO* promoter *lacZ* fusion directed an expression level of 211 Miller units in absence of LeuO but only of 35 units when LeuO was expressed *in trans* (Figure 14A). This 6-fold down-regulation of *leuO* promoter activity by LeuO in the presence of RcsB-BglJ suggests that LeuO counteracts activation of P2$_{leuO}$ by RcsB-BglJ.

The above data suggest that LeuO is an autoregulator that may have a small positive autoregulatory effect, but that strongly represses *leuO* transcription in the absence of H-NS and StpA and that counteracts activation of *leuO* by RcsB-BglJ. The moderate positive autoregulation is in agreement with previous data (Fang & Wu, 1998a, Chen *et al.*, 2003). These authors further demonstrated that LeuO can hinder spreading of a repressing H-NS complex and assumed that binding of LeuO to the *leu-leuO* region results in positive regulation in a process that involves supercoiling-dependent transcriptional coupling in the chromosomal context (Figure 3)(Chen & Wu, 2005). However, autoregulation of *leuO* so far was not tested in *hns* and *hns stpA* mutants. Therefore, I additionally analyzed autoregulation of *leuO* in its natural chromosomal context by RT-qPCR to test whether autorepression of *leuO* by LeuO was an artifact based on the *leuO* promoter *lacZ* fusion. To this end, I used plasmid pKETS5 for ectopic expression of LeuO. This plasmid encompasses the *leuO* coding region from position -20 (relative to the ATG, NC_00913: 84348 to 85332) and thus allows quantification of transcription of chromosomal *leuO* using primers that are specific for the non-translated leader of the native *leuO* mRNA (Figure 14B, NC_00913: 84,304 to 84,366).

Figure 14: Transcription of *leuO* is negatively autoregulated.

(A) Expression of the *leuO* promoter *lacZ* fusion (as shown in Figure 10A) is repressed by LeuO. Expression levels were determined in strains *ΔyjjPQ bglJ ΔleuO* T308, *ΔleuO Δhns* T316, *Δhns stpA* T352, and *bglJ*_C T570 in the absence (-, white bars) and presence (+, grey bars) of LeuO. LeuO was expressed from plasmid pKEDR13 (+), empty vector pKESK22 served as control (-). Cultures were grown to OD_{600} of 0.5 in presence of 1 mM IPTG and kanamycin. (B) Schematic of the chromosomal *leu-leuO* intergenic region and primers used for RT-qPCR analysis of *leuO* transcription. The RT-qPCR primers T351 and T352 are specific for amplification of a 63 base-pair fragment of the non-translated *leuO* mRNA leader (NC_00913 coordinates indicated) which is not present on LeuO expression vector pKETS5. (C) RT-qPCR analysis of chromosomal *leuO* expression. RNA was isolated from cultures of wild-type strain S3974, *ΔyjjPQ bglJ* strain T75 and *Δhns stpA* strain T447, all harboring either control vector pKESK22 (-) or LeuO expression vector pKETS5 (+ LeuO). For first-strand cDNA synthesis, random hexameric DNA oligonucleotides were used. Quantitative PCR was performed using serial dilutions of cDNA and primers T351 and T352. Ct values were normalized to *rpoD* expression determined with primers T247 and T248. Expression level is given as fold-change compared to the wild-type control (S3974 harboring pKESK22). Cultures were inoculated in LB supplemented with 25 µg/ml kanamycin to an OD_{600} of 0.1 for exponential growth. After 30 min, IPTG was added to a final concentration of 1 mM and cultures were grown for additional 60 min. (D) RT-qPCR analysis of chromosomal *leuO* expression in response to amino acid starvation. RNA was isolated from wild-type strain S3974 harboring empty vector pKESK22 grown in M9 minimal medium containing 1 % glucose, 25 µg/ml kanamycin and either 20 amino acids (20), 19 amino acids (19, without leucine), 17 amino acids (17, without leucine, isoleucine, and valine), or no amino acids (0). Growth of cultures, RNA isolation, cDNA synthesis and RT-qPCR were carried out as described in (C). Expression level of *leuO* is given as fold-change compared to samples grown in presence of 20 amino acids.

For RT-qPCR analysis of the native *leuO* locus, I isolated RNA from the wild-type strain S3974, from *ΔyjjPQ-bglJ* mutant T75 and from *Δhns stpA* mutant T447, both harboring either plasmid pKETS5 (+LeuO) or empty vector pKESK22 (-LeuO). The lowest level of chromosomal

leuO leader mRNA was measured in the wild-type strain in the absence of LeuO, as expected (Figure 14C). Upon expression of plasmidic LeuO *in trans*, we again observed a moderate 2-fold increase of *leuO* expression (Figure 14C). Rather similar results were obtained in the *ΔyjjPQ-bglJ* mutant (Figure 14C). In comparison, expression of the chromosomally encoded *leuO* mRNA was elevated approximately 31-fold in the Δ*hns stpA* mutant, confirming derepression of *leuO* in absence of H-NS and StpA. However, when LeuO was expressed *in trans* in the Δ*hns stpA* background, transcription of chromosomal *leuO* decreased to a level only 5-fold higher than that obtained in the wild-type strain. This demonstrates strong repression of *leuO* transcription by LeuO in the Δ*hns stpA* mutant within the chromosomal context.

Previous studies have shown that *leuO* expression is elevated in response to starvation for branched-chain amino acids (Fang *et al.*, 2000, Majumder *et al.*, 2001). Therefore, I additionally tested by RT-qPCR whether *leuO* expression changes in minimal medium supplemented with different sets of amino acids. I isolated RNA from strain S3974 grown in M9 minimal glucose medium containing either all 20 amino acids (20 aa), all amino acids but leucine (19 aa), all amino acids but the three branched-chain amino acids (17 aa), or no amino acids (0 aa). Note that strain S3974 is *ilvG$^+$* and thus valine-resistant in contrast to K12 strain MG1655 (Salmon *et al.*, 2006). Compared to medium containing all 20 amino acids (Figure 14C, 20), I measured the highest level of 7.6-fold elevated expression in medium lacking leucine (19 aa), a 4.6-fold elevated expression in medium lacking all three branched-chain amino acids (17 aa), and a 3.7-fold elevated expression in medium containing no amino acids (0). These results confirm that branched-chain amino acid starvation leads to higher expression of *leuO*. Finally, analysis of a *leu* promoter *lacZ* reporter fusion in a wild-type strain and a *ΔleuO* mutant confirmed that LeuO has only a small (2.5-fold) effect on expression of the divergent *leu* operon (Figure 15).
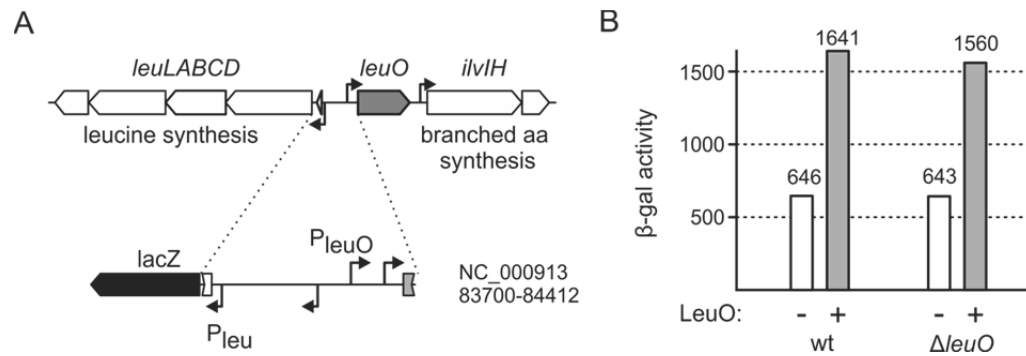
Figure 15: LeuO activates transcription of *leu* operon max 3-fold.

(A) Schematic representation of the chromosomal *leu-leuO* intergenic region and a *leu* promoter *lacZ* reporter fusion integrated at the phage λ *attB* site. (B) Expression was determined in wild-type strain T324 and *ΔleuO* strain T328. LeuO was expressed from plasmid pKEDR13 (+, grey bars). Empty vector pKESK22 served as control (-, white bars). Cultures were grown in LB medium to an OD_{600} of 0.5 in presence of 1 mM IPTG and 25 µg/ml of kanamycin for transformants and assayed for β-galactosidase activity.

2.2.7 In vitro mapping of promoters in the *leuO-leu* operon intergenic region

The above shown data suggest that LeuO acts predominantly as an autorepressor. Furthermore, I mapped two promoters directing expression of *leuO* of which the newly identified $P2_{leuO}$ promoter is activated by RcsB-BglJ. In addition, a second promoter $P2_{leu}$ directing expression of the *leu* operon was mapped here. To further characterize the *leuO-leu* intergenic region and autoregulation of *leuO,* I mapped RNA polymerase binding sites *in vitro* by $KMnO_4$ footprinting in the absence and presence of LeuO protein. In addition I performed *in vitro* transcription assays, and I re-mapped the LeuO binding sites by DNase I footprinting (for a summary of the results see Figure 16). The footprinting experiments were carried out in collaboration with the group of Prof. Rolf Wagner at the Heinrich-Heine-Universität Düsseldorf.
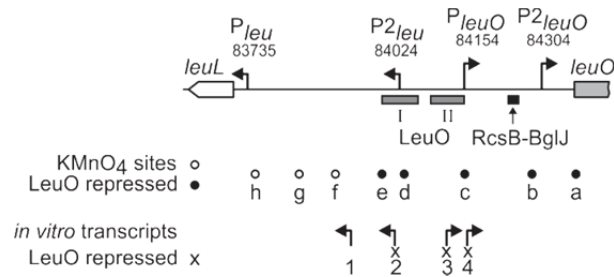
Figure 16: *In vitro* mapping of promoters in the *leu-leuO* intergenic region.

Schematic summary of regulatory features mapped to the 659 bp *leu-leuO* intergenic region. Four transcription start sites were mapped in vivo by 5'RACE termed P_{leu}, $P2_{leu}$, P_{leuO} and $P2_{leuO}$, positions are given as NC_000913 coordinates (Figure 13). The RcsB-BglJ binding site is drawn as black rectangle (Figure 11). In addition, LeuO binding sites were mapped in vitro by DNase I footprinting assays and are represented as grey rectangles termed LeuO I and II (see Figure 17 for details). To detect the formation of putative open complexes, KMnO4 footprinting experiments were performed in presence and in absence of LeuO protein (see Figure 17 for details). Eight KMnO4-sensitive sites (unfilled/filled circles) were detected (termed 'a' to 'h'). Formation of sites a to e is repressed by LeuO (filled circles). In vitro transcription in presence and in absence of LeuO protein was performed to roughly map start sites and orientation of transcripts (see Figure 18 for details). Four transcripts were detected (arrows). Transcription starts 1 and 2 are oriented toward the *leu* operon, transcription starts 3 and 4 are oriented toward *leuO*. Transcripts 2, 3, and 4 are repressed by LeuO (marked with "x", see Figure 18 for details).

For DNase I and KMnO$_4$ footprinting the *leuO-leu* operon intergenic region was sub-cloned so that the whole region was covered by overlapping fragments (Figure 17A). DNase I footprinting using LeuO$_{His6}$ protein revealed two LeuO binding sites, LeuO I and LeuO II (Figure 17B, Figure 16, and Figure 12.). The LeuO binding sites correspond to sites previously mapped (Chen *et al.*, 2003, Chen & Wu, 2005). The binding sites overlap with the *P2$_{leu}$* and *P$_{leuO}$* promoters (Figure 16 and Figure 12). The footprinting analysis also showed that LeuO prevents binding of RNA polymerase (Figure 17B). No additional LeuO binding site was detected by DNase I footprinting and by gel retardation assays (data not shown).
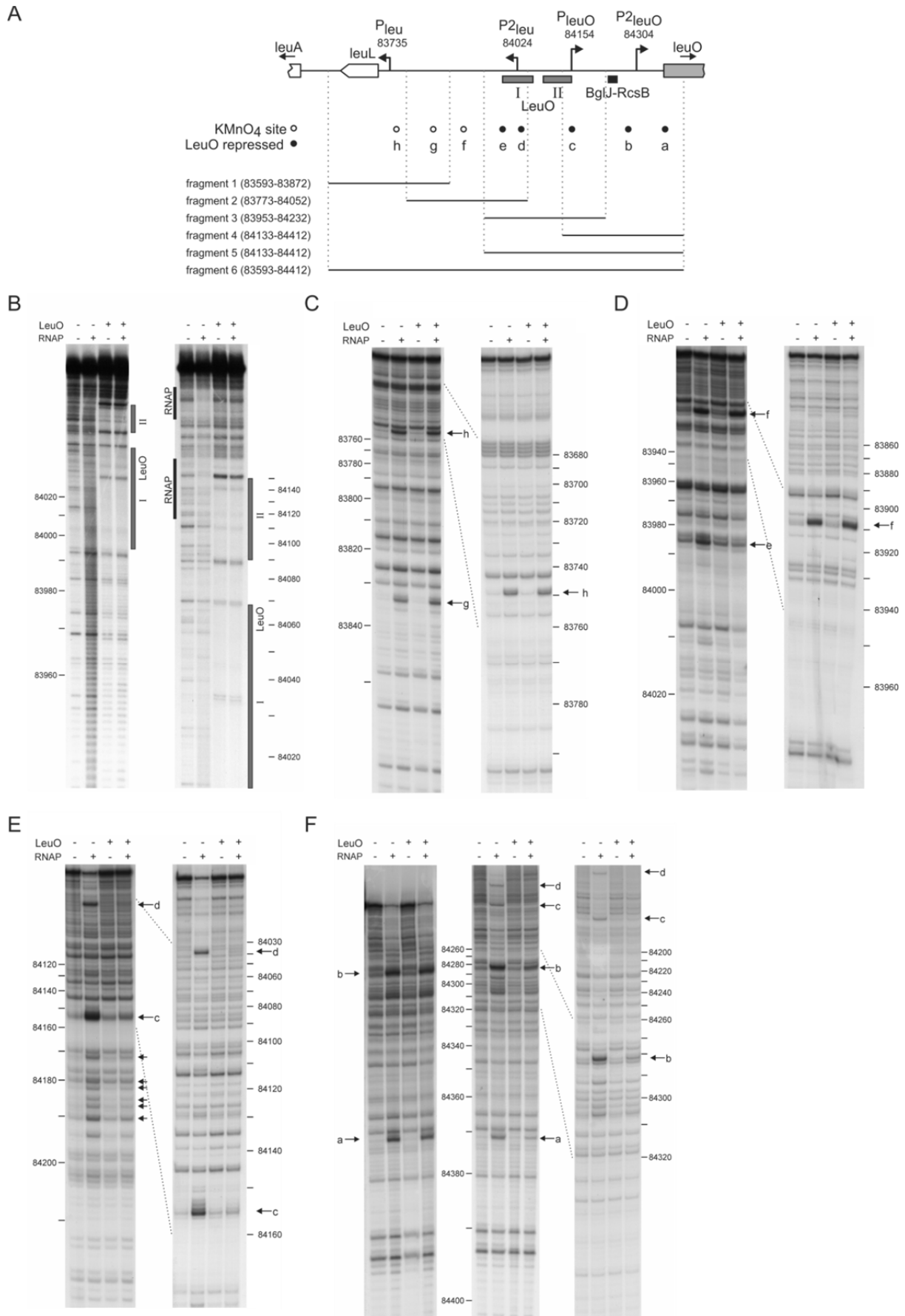
Figure 17: DNase I and KMnO₄ footprinting of the *leu-leuO* intergenic region.

(A) Schematic summary of mapping of LeuO binding sites and open complexes formed by RNA polymerase in the 659 bp *leu-leuO* intergenic region. LeuO binding sites were mapped by DNase I footprinting (panel B) and are represented as grey rectangles termed LeuO I and II. Putative open complexes formed by RNA polymerase were mapped by $KMnO_4$ footprinting experiments in the presence and absence of LeuO protein, as indicated (panels C, D, E, and F). $KMnO_4$-sensitive sites are depicted as circles, with black filled circles indicating open complexes which are repressed by LeuO. For DNase I and $KMnO_4$ footprinting, overlapping fragments 1 to 6 were used (positions given as NC_000913 coordinates). For fragment isolation plasmids pKETS13 to 18 were digested with either PstI/EcoRI or HindII/Ecl136II for 3' end labelling of the top strand (EcoRI filled in) or bottom strand (HindIII filled in), respectively. (B) DNase I footprinting assays to map LeuO binding sites in the *leu-leuO* intergenic region. Fragment 5, which was 3' end labelled at the bottom strand, was incubated with 0.5 mU/µl of DNaseI, 50 nM of RNAP σ70, and 1 µM of LeuO-His$_6$, where indicated. Samples were separated on polyacrylamide gels. Shown are the autoradiograms of a short run (left) and a long run (right). LeuO-protected sites are indicated by grey bars (LeuO I and LeuO II). Sites protected by RNAP are shown as black bars. Positions were counted according to a G+A sequencing reaction that served as size standard (not shown) and are given as NC_000913 coordinates. (C) to (F) $KMnO_4$ footprinting to detect formation of RNA polymerase open complexes in the *leu-leuO* intergenic region. Radiolabeled fragments were incubated in the presence of 50 nM of RNAP σ70, and 1 µM of LeuO$_{His6}$, where indicated and treated with $KMnO_4$. Positions are given as NC_000913 coordinates. Arrows and letters indicate the positions of $KMnO_4$-sensitive sites. Formation of sites a and b was inhibited by LeuO on fragment 6 (comprising the whole region including LeuO binding sites), but not on fragment 4 (LeuO binding sites missing). Formation of sites c, d and e was inhibited by LeuO on fragments 2 (open complex e), 3 (open complexes c and d), and 6 (open complexes a, b, c, and d).

$KMnO_4$ footprinting in the absence and presence of LeuO and sigma70-RNA polymerase revealed the presence of several $KMnO_4$-sensitive sites at which RNA polymerase may form open complexes (labeled 'a' to 'h' in Figure 16 and Figure 17). The map positions of three of these $KMnO_4$-sensitive sites correspond well with the mapped promoter of the *leuO* gene (P$_{leuO}$, site c), the divergent *leu* operon (P$_{leu}$, site h), and the second *leu* operon promoter (P2$_{leu}$, site d). However, $KMnO_4$ sensitive site b maps 20 bp upstream of the transcription start site of P2$_{leuO}$. Further, one site was mapped to the coding region of *leuO* (site a), and three sites were mapped between the two *leu* operon promoters (sites e, f and g). Interestingly, formation of $KMnO_4$-sensitive sites 'a' to 'e' was inhibited when LeuO was added to the reactions (Figure 16 and Figure 17). Suppression of formation of these putative open complexes by LeuO supports the finding that LeuO acts as an autorepressor. Intriguingly, formation of site b, mapping next to the RcsB-BglJ activated P2$_{leuO}$ promoter was repressed by LeuO when the fragment included the LeuO I and LeuO II binding sites but not when a shorter fragment was probed (Figure 17F, compare fragments 4 and 6). This may indicate that binding of LeuO results in an extended complex which prevents open complex formation at a distal site.

To determine whether transcription is initiated at the mapped open complexes and to corroborate repression by LeuO, I additionally performed *in vitro* transcription assay in the

absence and presence of LeuO protein. To this end, I used a set of four DNA fragments of the *leuO-leu* region as templates (fragments 1 to 4, Figure 18) that allowed to simultaneously monitor transcription oriented toward the *leu* operon and toward *leuO* (see Figure 18 for details). Four major RNA transcripts were detected in the *in vitro* transcription assays performed in the absence of LeuO protein but only one transcript was detected in the presence of LeuO protein (Figure 18). Two transcripts were oriented toward the *leu* operon (transcripts 1 and 2, Figure 16 and Figure 18) and two start sites directed transcription toward *leuO* (transcripts 3 and 4, Figure 16 and Figure 18). *In vitro* transcripts 2, 3 and 4 were repressed in the presence of LeuO protein. The starts sites of these transcripts and the LeuO binding sites overlap and the result suggests that binding of LeuO represses transcription. Roughly mapped transcripts 2 and 4 correspond to $P2_{leu}$ and P_{leuO} while the presence of transcripts 1 and 3 suggests that additional promoters may exist in this region. Interestingly, no *in vitro* transcript corresponding to transcription initiation at the $P2_{leuO}$ promoter was detected. This may indicate that $P2_{leuO}$ is RcsB-BglJ dependent. Taken together, the *in vitro* and *in vivo* data suggest that the *leuO-leu* intergenic region represents a complex regulatory promoter region and they support autorepression of *leuO*.
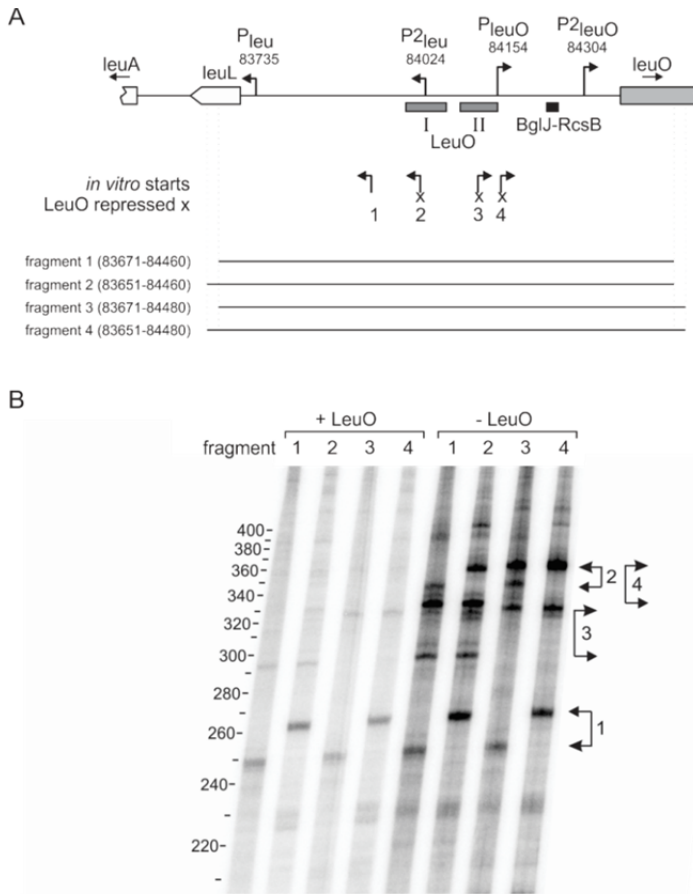
Figure 18: LeuO represses *leuO* transcription *in vitro*.

(A) Schematic summary of regulatory features and in vitro transcript mapping. For in vitro transcription, four different DNA fragments of the *leu-leuO* intergenic region were used to distinguish transcripts oriented toward the *leu* operon (to the left) and toward the *leuO* gene (to the right). I expected a transcript oriented toward the *leu* operon (to the left) to have the same length in assays with fragment 1 and 3 (short) and with fragments 2 and 4 (long), respectively. Accordingly, I expected a transcript oriented toward the *leuO* gene (to the right) to have the same length in assays with fragment 1 and 2 (short) and with fragments 3 and 4 (long), respectively. (B) Autoradiogram of *in vitro* transcripts separated on denaturing polyacrylamide gel. Reactions were carried out in the presence and absence of 1 µM of LeuO protein (+/- LeuO) using fragments 1 to 4, respectively, and separated next to a sequencing reaction that served as size standard for estimation of transcript lengths necessary for rough mapping of the transcript. On the right side, arrows indicate the transcript orientation derived from the gel band pattern (e. g. transcript 1 is shorter with fragments 1 and 3 than with fragment 2 and 4 and thus oriented towards the *leu* operon (to the left)).

2.3 Screen for additional factors and upstream signals of *leuO* and *bglJ* transcription

Activation of *leuO* by RcsB-BglJ, as shown here, and, in turn, activation of the *yjjQ-bglJ* operon by LeuO (Stratmann *et al.*, 2008) indicated a feedback loop regulation. To identify additional factors and possible upstream signals that may regulate transcription of *leuO* or *bglJ*, I performed transposon mutagenesis and screened for mutants in which the *yjjQ-bglJ* promoter or the *leuO* promoter were activated, respectively. Additionally, I performed a genomic library screen to search for factors that activate the *yjjQ-bglJ* promoter.

2.3.1 Transposon insertions activating the *leuO* promoter or the *yjjQ-bglJ* promoter

For transposon mutagenesis, I used the *leuO* promoter *lacZ* fusion and the *yjjQ-bglJ* promoter *lacZ* fusion as reporters to screen mutants that activate the *leuO* or the *yjjQ-bglJ* promoter. For the transposon mutagenesis, plasmid pKESK18 was used (Figure 19A) (Madhusudan *et al.*, 2005). This plasmid encodes a miniTn10-*cat* transposon conferring chloramphenicol resistance and the transposase under control of the temperature-sensitive cI$_{857}$ repressor mutant. In addition, the replication origin of the plasmid is temperature-sensitive. Upon temperature shift to 42°C, transposition is initiated and the plasmid is lost. Transposition occurs in approximately 1 to 5 % of cells. To select for mutants carrying transposon insertions, cells were plated on LB plates supplemented with chloramphenicol. To screen for mutants activating transcription of the *leuO* promoter *lacZ* fusion, plates were additionally supplemented with X-gal. After incubation overnight at 42°C, Lac-positive colonies (blue phenotype) were picked and re-streaked on LB containing chloramphenicol and X-gal to confirm the Lac-positive phenotype (Figure 19A). To locate the transposon insertion site, a semi-random, two-step PCR was performed (ST-PCR, chapter 4.2.11) (Chun *et al.*, 1997). Of these PCR products, the most prominent bands were excised from agarose gels and sequenced. The sequences were analyzed by BLAST to map the transposon insertion sites. Results of the screen are summarized in Figure 19.

When the *leuO* promoter *lacZ* fusion was used, several transposon insertions mapped to the *leuO* promoter *lacZ* fusion rendering its expression constitutive, and one mutation mapped to the chromosomal *lac* locus (data not shown). These mutations thus directly targeted the reporter system. Moreover, several transposon insertions mapped to the *rfa* locus encoding

genes for synthesis and export of lipopolysaccharides (LPS) (Figure 19B). Three insertions mapped to *rfaD* and to *rfaC*, respectively, which belong to the *rfaDFCL* operon. One insertion was found in the *rfaG* gene which is part of the divergent *rfaQGPSBIJYZ-waaU* operon. Interestingly, mutations in the *rfa* locus have been shown to activate capsule synthesis through the Rcs phosphorelay system (Parker *et al.*, 1992, Majdalani & Gottesman, 2005, Majdalani *et al.*, 2005). Another transposon insertion mapped to the *envC* gene encoding a murein hydrolase. To sum up, the identified transposon insertion sites indicate that changes in the bacterial cell surface like LPS structure or cell wall integrity may play a role in activating the *leuO* promoter. However, the activation of the Rcs phoshorelay may affect *leuO* indirectly, as activation by RcsB-BglJ was shown to be independent of RcsB phosphorylation.

To confirm activation of the *leuO* promoter *lacZ* fusion by insertion of the mTn10 transposon in *envC* and *rfa* genes, the respective alles of *rfaG*, *rfaC*, and *envC* were re-transduced using the same strain background as recipient that had been used for the screen (T28). Then, β-galactosidase activity was determined with the respective mutants and compared to the wild-type strain. However, the *leuO* promoter activity was only marginally higher in the mutants than in the wild-type, with each mutant directing a 1.4 to 1.7-fold elevated β-galactosidase activity. Thus, the activation of the *leuO* promoter in these mutants was only marginal in liquid culture.

To find mutants that activate the *yjjQ-bglJ* promoter, transposon mutagensis was additionally performed with strain T413 carrying a *yjjQ-bglJ* promoter *lacZ* fusion (Figure 19C). This screen yielded transposon insertions in *bglH* (carbohydrate-specific outer membrane porin of the *bgl* operon), in *acrA* (periplasmic lipoprotein component of the AcrAB-TolC multidrug efflux pump), and interestingly in *rfaP*, again indicating that cell surface-related factors may play a role in transcriptional regulation of *leuO* and *bglJ*.
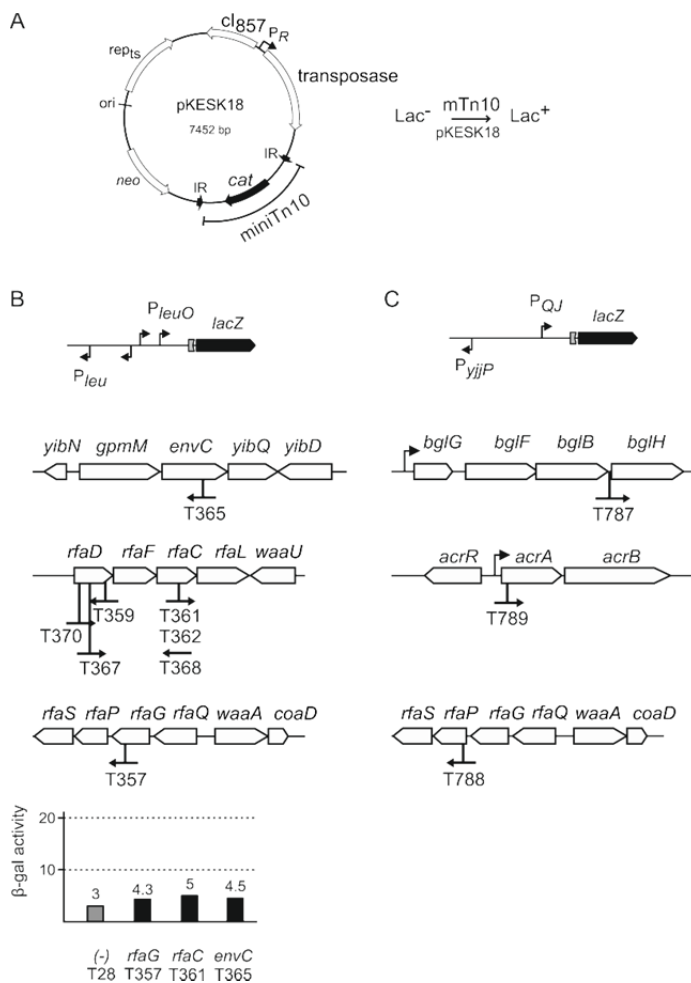
2. Results

Figure 19: Transposon mutants activating *bglJ* or *leuO*.

(A) Plasmid pKESK18 was used to perform a transposon-mutagenesis screen to isolate activators of the *yjjQ-bglJ* promoter and of the *leuO* promter, respectively. Plasmid pKESK18 is a replication temperature-sensitive (rep$_{ts}$) pSC101 derivative, which carries a mini-Tn10 transposon (miniTn10) with a chloramphenicol-resistance gene (*cat*), the Tn10 transposase gene under control of the λ P$_R$ promoter and the λ cl$_{857}$ gene. Transposition was induced by a temperature shift from 28 to 42°C and single miniTn10-*cat* transposon mutants were selected at 42°C on chloramphenicol plates and screened for Lac-positive mutants. (B) For screening, strain T28 carrying the *leuO* promoter *lacZ* reporter fusion was transformed with pKESK18. Mutants were selected at 42°C on LB supplemented with chloramphenicol for selection and X-gal screening of Lac-positive phenotypes. Lac-positive clones were picked and restreaked on the same medium. Transposon insertion sites were mapped using a semi-specific two-step PCR (ST-PCR) described in (Chun *et al.*, 1997) followed by sequencing and BLAST search. Insertion sites were then confirmed by PCR analysis using specific primers. Transposon insertion sites are depicted schematically. Arows indicate the orientation of the *cat* gene, numbers represent the strain numbers of the mutants. Mutant alleles of *rfaG*, *rfaC*, and *envC* were re-transduced into T28 and ß-galactosidase activity was measured. (C) Same as (B) using *yjjQ-bglJ* promoter *lacZ* fusion integrated in strain T413.

2.3.2 Genomic library clones activating the *yjjQ-bglJ* promoter

For the genomic library screen, I isolated genomic DNA from wild-type strain S3974 and restricted this genomic DNA partially with *Sau*3AI. This restriction yielded fragments between 1.5 kb and 5 kb in size. Fragments were cloned into expression vector pKESK22 in

which transcription of inserts is tightly regulated by the IPTG-inducible *tac* promoter (Figure 20B). I used this genomic library (pKETS11) for transformation of strain T413 harboring a *yjjQ-bglJ* promoter *lacZ* fusion integrated in the chromosomal λ *attB* site and screened for Lac-positive clones on selective medium containing X-gal (Figure 20A). The screen yielded four clones (Figure 20C): One mutant carried the 5' part of *envR* (transcriptional repressor of *acrAB* multidrug efflux pump (Hirakawa *et al.*, 2008)). Another mutant carried the *folD* gene encoding a bifunctional 5, 10-methylene- tetrahydrofolate dehydrogenase/ 5, 10-methylene-tetrahydrofolate cyclohydrolase involved in methionine synthesis (D'Ari & Rabinowitz, 1991, Dimri *et al.*, 1991) and the *ybcJ* gene encoding a protein with a S4-like RNA binding domain yet of unknown function (Volpon *et al.*, 2003). Two mutants carried the *cynR* gene encoding a LysR-type transcription factor which activates the *cynTS* operon (Sung & Fuchs, 1988, Sung & Fuchs, 1992). This operon is involved in utilization of cynate as nitrogen source.

The plasmids were recovered from the isolated clones and re-transformed into strain T413 to confirm the Lac-positive phenotype on LB X-gal plates. Additionally, transformants were streaked on BTB salicin plates to analyze their Bgl phenotypes. The *cynR* and *folD-ybcJ* transformants exhibited a clearly Lac-positive phenotype and a weakly Bgl-positive phenotype indicative of activation of the *yjjQ-bglJ* promoter and an RscB-BglJ target, *bgl* promoter. The *envR* transformant showed a weak Lac-positive phenotype and a Bgl-negative phenotype.
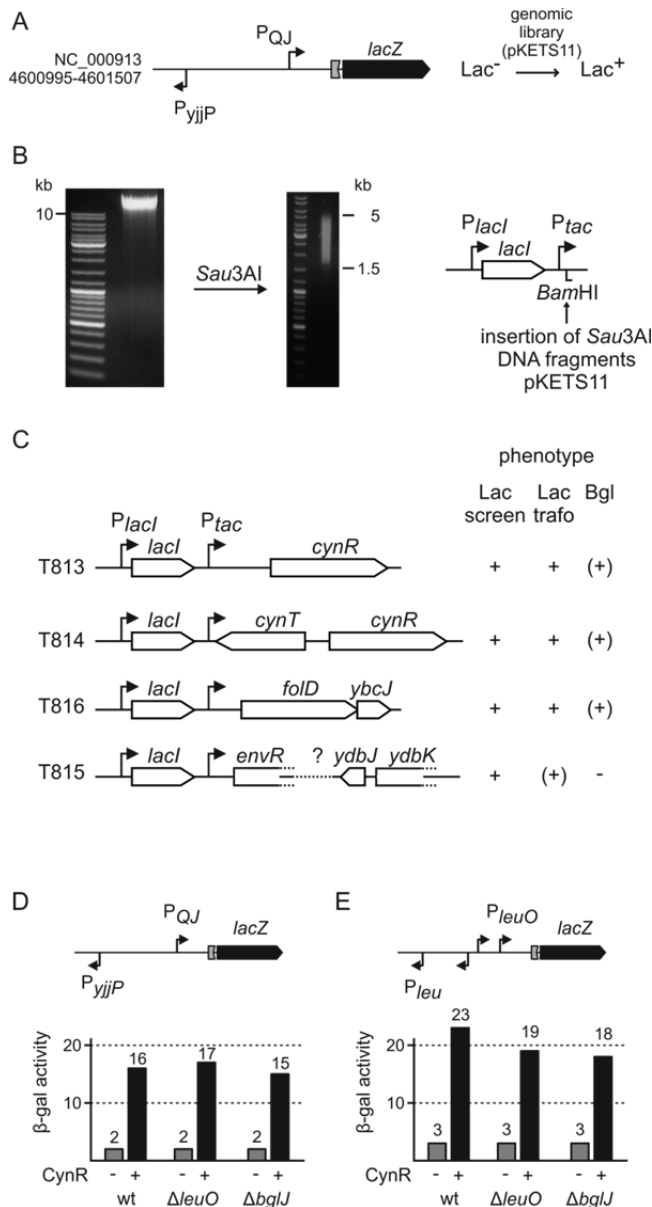
Figure 20: Genomic library clones activating transcription of *yjjQ-bglJ* promoter.

(A) *yjjQ-bglJ* promoter *lacZ* fusion used as reporter to screen for factors that activate the *yjjQ-bglJ* promoter. Strain T413 harboring this construct inserted at the chromsosomal λ *attB* site was used for the screen. (B) Cloning of genomic library. Genomic DNA was isolated from wt strain S3974 and partially restricted with *Sau*3AI. Restriction fragments between 1.5 kb and 5 kb in size were cloned into *Bam*HI site of vector pKESK22 yielding genomic library pKETS11. Inserts are under transcriptional control of the IPTG-inducible *tac* promoter. (C) For screening, strain T413 carrying the *yjjQ-bglJ* promoter *lacZ* fusion (A) was transformed with genomic library pKETS11 (B). Transformants were plated on LB suplemented with kanamycin for selection and X-gal and 0.2 mM IPTG for screening of Lac-positive phenotypes. Lac-positive clones were picked and restreaked on the same medium (Lac screen). Plasmids were isolated from these clones and retransformed into strain T413 to confirm the Lac-positive phenotype (Lac trafo) and to analyze the Bgl phenotype on BTB plates (Bgl). Genomic DNA inserts cloned into *Bam*HI site of pKETS11 were analyzed by PCR and sequenced. Genes present on the inserts are drawn schematically on the left side. Clones were stored under the indicated strain numbers T813 to T816. (D) Analysis of CynR effect on *yjjQ-bglJ* promoter *lacZ* fusion. The *cynR* gene was subcloned into expression vector pKESK22 yielding pKETS23. β-galactosidase activity was determined in strain T413 (wt), strain T414 (*ΔbglJ*), and strain T30 (*ΔleuO*) transformed with pKETS23 (+) or pKESK22 as control (-). (E) Analysis of CynR effect on *leuO* promoter *lacZ* fusion. β-galactosidase activity was determined in strain T28 (wt), strain T32 (*ΔbglJ*), and strain T87 (*ΔleuO*) transformed with pKETS23 (+) or pKESK22 as control (-).

45

I analyzed the effect of the potential activator CynR on the *yjjQ-bglJ* promoter in more detail. To this end, I subcloned the *cynR* gene into low-copy expression vector pKESK22 resulting in plasmid pKETS23 for expression of CynR *in trans*. I then performed β-galactosidase assays with a *yjjQ-bglJ* promoter *lacZ* fusion and a *leuO* promoter *lacZ* fusion, respectively (Figure 20D,E). To analyze whether activation of the *yjjQ-bglJ* promoter was dependent on *leuO*, I measured β-galactosidase activities in the wild-type strain T413, the *leuO* mutant T414 and in *bglJ* mutant T416. In all three strain backgrounds, expression of CynR lead to an approximately 8-fold upregulation of the *yjjQ-bglJ* promoter showing that activation was independent of *leuO* (Figure 20D). I also tested whether activation of *bglJ* by CynR caused activation of the RcsB-BglJ target *leuO*. To this end, I measured the β-galactosidase activity directed from the *leuO* promoter *lacZ* fusion integrated in wild-type strain T28, in *leuO* mutant T87 and in *bglJ* mutant T87. Surprisingly, upon expression of CynR an approximately 6 to 7-fold activation of the *leuO* promoter was observed in all three strain backgrounds showing that also activation of the *leuO* promoter was independent of *bglJ* (Figure 20E).

3. Discussion

H-NS-mediated repression is most commonly relieved by transcription factors which function as H-NS antagonists. In the present study, potential novel target genes of the transcription factors and H-NS antagonists LeuO and RcsB-BglJ were characterized. The results show that BglJ requires RcsB as dimerization partner for its activating function and that the RcsB-BglJ heterodimer activates several genes in *E. coli*, in addition to the only known target thus far, the *bgl* operon. One of these targets is the pleitropic transcription factor and H-NS antagonist LeuO. Detailed analysis of the regulation of *leuO* transcription revealed that *leuO* is strongly activated by the RcsB-BglJ heterodimer, independently of signaling by the Rcs two-component phosphorelay, and further shows that StpA, the H-NS paralog, can cause repression of *leuO* in an *hns* mutant. Moreover, the data suggest that LeuO acts predominantly as a negative autoregulator in absence of H-NS, with a moderate positive effect on transcription of *leuO* and the divergent *leu* operon in the wild-type. Regulation of *leuO* by RcsB-BglJ and LeuO, as shown here, and activation of the *yjjQ-bglJ* by LeuO indicate a feedback loop control mechanism of these two global transcriptional regulators that may ensure turn on of their expression in response to specific environmental signals. Screens performed using a transposon mutagenesis approach and expression of a genomic library indicate that additional factors may be involved in the regulation of a *leuO-bglJ* feedback loop, such as the *rfa* genes or the transcription factor CynR.

3.1 What are the functions of RcsB-BglJ and of LeuO?

Activation of *bgl* and of *leuO* by RcsB-BglJ is independent of phosphorylation of the Rcs two-component system response regulator RcsB (Venkatesh *et al.*, 2010)(Figure 6, Figure 10), in contrast to phosphorylation-dependent activity of RcsA-RcsB (Majdalani & Gottesman, 2005). The microarray data presented here suggest that regulation by BglJ in general requires RcsB (chapter 2.1.1) and further analysis demonstrated that activation of *leuO* by RcsB-BglJ is also independent of the Rcs phoshorelay system. This extra level of combinatorial control of the response regulator RcsB is likely to have an impact on the regulatory repertoire attributable to transcriptional regulation by RcsB. The data further suggest that RcsB-BglJ acts as a global transcriptional regulator with a distinct set of mainly

H-NS-repressed targets, many of which putatively relate to membrane and surface functions (Table 1). Thus, the set of RcsB-BglJ targets is expanded beyond activation of the *bgl* operon. However, it remains to be elucidated which targets are activated directly by binding of RcsB-BglJ. To this end, the newly identified RcsB-BglJ binding sites at the *bgl* promoter (Figure 7) and the *leuO* promoter (Figure 11) may be helpful in defining a consensus binding site of RcsB-BglJ similarly to the RcsAB box (Majdalani & Gottesman, 2005, Wehland & Bernhard, 2000).

The LeuO microarray confirms pleiotropic effects of this transcription factor (chapter 2.1.2, Table 2, appendix Table 8). For most upregulated loci, binding of LeuO has been shown, and at all of these LeuO-bound loci H-NS binding was observed (Shimada *et al.*, 2011). This finding is in accordance with LeuO functioning as H-NS antagonist. Despite this common notion of LeuO, more than 60 genes were downregulated when LeuO was overexpressed, suggesting that LeuO may itself repress transcription at other targets than the *leuO* gene. Interestingly, LeuO was found to bind only to 13 of the repressed loci (Shimada *et al.*, 2011). This indicates that downregulation of these genes may be caused by indirect effects of LeuO overexpression rather than directly. Moreover, loci at which LeuO acts itself as repressor may possibly not have been identified by the microarray approach of the present study since the strains used here carried wild-type *hns* and *stpA* genes. This suggests that the potential repressor function of LeuO by shutting off expression of active (derepressed) promoters may have been masked. For example, it has been shown previously that LeuO downregulates the promoter of the *yjjP* gene, encoding a membrane protein of unknown function, in absence of H-NS (Stratmann *et al.*, 2008), and in the present study, expression analyses in *hns* mutants and *hns stpA* double mutants revealed that LeuO is a negative auto-regulator (Figure 14). Interestingly, the *cadAB* operon (acid stress) was found to be downregulated by LeuO. It has been shown before that downregulation of *cadAB* is mediated through downregulation of *cadC*, the transcriptional activator of *cadAB* (Watson *et al.*, 1992, Shi & Bennett, 1995). Downregulation of *cadC*, however, was not detected in the LeuO microarray with the threshold limit set here. In general, LeuO apparently functions as H-NS antagonist to activate a number of genes, many of which are related to cell surface and adherence structures and to membrane-bound efflux systems.

Furthermore, the LeuO protein does not significantly contribute to the activation of the *leu* operon as no significant upregulation of *leu* genes has been observed in the microarray experiment (data not shown) and only a comparably slight upregulation of the leu promoter was determined in the expression analysis of the *leu* promoter *lacZ* fusion (Figure 15).

3.2 How do LeuO and RcsB-BglJ regulate transcription?

BglJ and RcsB have been shown to interact and form heterodimers as demonstrated by two-hybrid analysis and co-immunoprecipitation (Venkatesh *et al.*, 2010). The site-specific mutations of a sequence motif 'TTTATAA|ATTCCTA' at the *bgl* promoter (chapter 2.1.3, Figure 8), and 'TTTATGT|TTTCCGA' at the *leuO* promoter region (chapter 2.2.4, Figure 12) show that RcsB-BglJ binds proximal to the *bgl* promoter and the *leuO* P2$_{leuO}$ promoter, respectively. However, at the *bgl* promoter the binding site is located at position -95.5 bp (respective to transcription start site) whereas at the *leuO* promoter the binding site is found at position -58.5 bp. In both cases, the right half site of the indentified RcsB-BglJ binding motifs is similar to the right half site of the RcsAB box. This suggests that the RcsB subunit binds more proximal to the transcription start site and may be involved in interaction with RNA polymerase. However, direct experimental evidence for this hypothesis is missing.

For transcription of *leuO*, a published model proposed that *leuO* is moderately upregulated in response to starvation for branched-chain amino acids and in the stationary phase (Fang *et al.*, 2000, Majumder *et al.*, 2001, Shimada *et al.*, 2011). Further, it was proposed that LeuO acts as a positive regulator of the *leu* operon and *leuO* gene with activation based on transcription induced changes in DNA supercoiling and delimiting of H-NS spreading by LeuO (Fang & Wu, 1998b, Chen *et al.*, 2003, Chen & Wu, 2005, Chen *et al.*, 2005). Data presented in the present study confirm the moderate (2 to 3-fold) positive effect of LeuO on expression of the *leu* operon and the H-NS/StpA-repressed *leuO* gene, respectively, as well as a moderate upregulation in response to the availability of branched-chain amino acids (Figure 14, Figure 15). However, my further data suggest that LeuO acts predominantly as an autorepressor on the *leuO* promoter P$_{leuO}$ and the newly identified promoters P2$_{leuO}$ and P2$_{leu}$ (for a model see Figure 21). P$_{leuO}$ corresponds to a promoter previously mapped in *Salmonella enterica* while the P2$_{leuO}$ promoter is activated by RcsB-BglJ. Both of these promoters are repressed by LeuO, and LeuO acts antagonistically to activation by RcsB-BglJ

(Figure 21). Repression of P$_{leuO}$ by LeuO is presumably direct as the two LeuO binding sites mapped by DNase I footprinting are located next to this promoter and closely flank the H-NS nucleation site. One of the sites overlaps with the core sequence of P$_{leuO}$ (Figure 12). Repression of the second P2$_{leuO}$ promoter also requires the LeuO I and II binding sites and it is open whether repression might be caused by formation of a more extended LeuO-DNA complex. Extended protein-DNA complexes and restructuring of the DNA have been proposed for LysR-type transcription factors (Maddocks & Oyston, 2008).
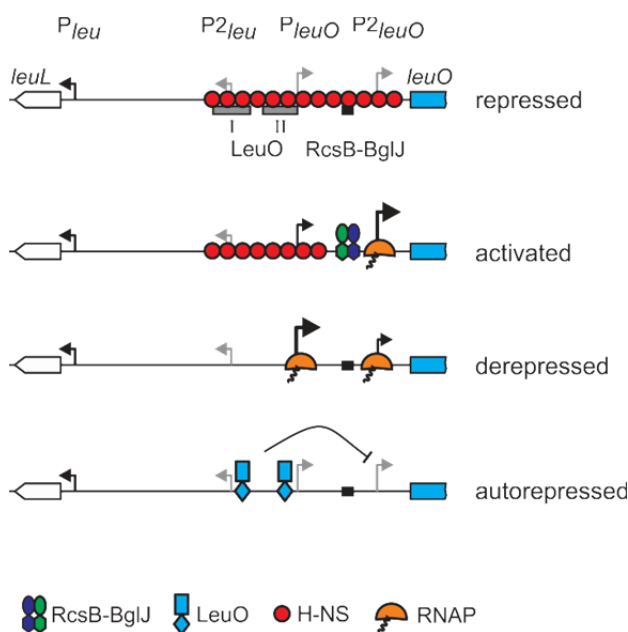
Figure 21: Model of transcriptional regulation of *leuO*.

Under standard laboratory growth conditions, transcription of *leuO* is repressed by H-NS and/or StpA (repressed). Transcription can be activated by binding of RcsB-BglJ upstream of P2$_{leuO}$ (activated). It remains unclear how RcsB-BglJ interferes with repression by H-NS/StpA and whether RcsB-BglJ acts as class I regulator and recruits RNA polymerase to P2$_{leuO}$. In absence of H-NS, StpA, and RcsB-BglJ, RNA polymerase can access both P$_{leuO}$ and P2$_{leuO}$ and initiate transcription (derepressed). In this case P$_{leuO}$ is favored over P2$_{leuO}$. In case of high LeuO concentration (e.g. by overexpression) LeuO may bind to the two central binding sites and repress transcription from promoter P2$_{leu}$ and P$_{leuO}$ that overlap with LeuO binding sites (autorepressed). In addition it represses transcription from the more distal P2$_{leuO}$.

Previous studies mapped binding sites of LeuO at the regulatory regions of *yjjP-yjjQ-bglJ*, the *bgl* operon, and the *cas* operon by electrophoretic mobility shift assays or DNase I footprinting (Stratmann *et al.*, 2008, Venkatesh *et al.*, 2010, Westra *et al.*, 2010). Similar to the *in vitro* data presented here (Figure 12), LeuO binding caused the formation of extended footprints on the DNA of 60 bp or more. In case of the LeuO binding region at the *yjjP* promoter, LeuO binding overlaps with the *yjjP* core promoter and LeuO represses *yjjP* in an *hns* mutant background. In case of the LeuO-activated *yjjQ-bglJ* promoter, the *cas* promoter, and the *bgl* promoter LeuO binds to sites more distal upstream and/or downstream of the core promoters. For the *cas* promoter it has been proposed that LeuO delimits spreading of the H-NS nucleoprotein complex into the core promoter region and does not compete with

H-NS for binding (Westra *et al.*, 2010). These findings indicate that the position of the LeuO binding site(s) determines whether LeuO acts as an activator (H-NS antagonist) or as a repressor.

Another possibility for the regulation of LeuO function may be that in general, LysR-type transcription factors like LeuO require small co-effector molecules. Such molecules bind to a co-effector binding pocket in the C-terminal domain, cause a conformational change and, thus, may alter the regulatory function of the transcription factor. This has been shown e. g. for CynR, ArgP, and IlvY (Lamblin & Fuchs, 1994, Laishram & Gowrishankar, 2007, Maddocks & Oyston, 2008, Momany & Neidle, 2012). For CynR it has been shown that binding to cyanate activates transcription of the *cynTS* operon presumably by changing the DNA bending properties of the CynR protein (Lamblin & Fuchs, 1994). In case of ArgP (regulator of arginine metabolism), binding of arginine enables the protein to recruit RNA polymerase to initiate transcription of some target genes, whereas binding of lysine appears to inhibit transcription initiation (Laishram & Gowrishankar, 2007). Note that in case of CynR and ArgP, DNA binding of the protein is not affected by binding of the co-inducer molecule. For IlvY, a regulator involved in branched-chain amino acid metabolism, it has been demonstrated that it is a negative autoregulator independently of binding of its co-effector, α-aceto-lactate. However, binding of α-aceto-lactate is essential for transcriptional activation of the IlvY target *ilvC*. The IlvC protein encodes an α-acetohydroxy isomeroreductase for which the IlvY co-effector α-aceto-lactate is a substrate. Thus, accumulation of α-aceto-lactate leads to increased expression of IlvC via IlvY (Salmon *et al.*, 2006).

However, a co-effector has not yet been identified for LeuO. Transcription of *leuO* is slightly elevated in response to starvation for branched-chain amino acids and has been shown to be coupled to transcription of the downstream *ilvIH* opero. Thus, one might search for such a co-inducer among small metabolites that are part of branched-chain amino acid anabolic pathways. A promising candidate might be α-ketoisovaleric acid (KIV) which is a substrate of the 2-isopropylmalate synthase LeuA, the first enzyme encoded in the *leuLABCD* operon, or other intermediates in this pathway. Initial experiments have shown that neither the presence of 1 mM of the intermediates α-ketoisocaproic acid (KIC), α-ketoisoleucine (KIL), or KIV nor of leucine, isoleucine, or valine, respectively, altered the binding of LeuO to fragments of the *leu-leuO* intergenic region in electrophoretic mobility shift assays (not

shown). In addition, KIV did not alter binding of LeuO to the *yjjP* promoter region (not shown). However, since binding of a co-effector may not influence the DNA binding properties of a LysR-type protein but may change its regulatory function (as shown for ArgP and CynR) the effect of KIV, KIL, and KIC should be analyzed by transcription assays, e. g. by *in vitro* transcription or KMnO$_4$ footprinting using the *leu-leuO* regulatory region and other targets as templates.

3.3 How does the feedback control of *bglJ* and *leuO* work?

Activation of *leuO* by RcsB-BglJ as shown here (chapter 2.2) as well as activation of the *yjjQ-bglJ* operon by LeuO (Stratmann *et al.*, 2008) constitutes a regulatory double-positive-feedback loop that connects the two global regulators and H-NS antagonists, LeuO and RcsB-BglJ (for network motifs and terminology see (Shoval & Alon, 2010, Alon, 2007)) (Figure 22). Moreover, negative autoregulation of *leuO* was shown above. Remarkably, RcsB-BglJ has rather mild effects on the expression of only five LeuO target loci, while the vast majority of LeuO targets are not at all affected by RcsB-BglJ (chapter 2.1.1). In contrast to an initial hypothesis in which RcsB-BglJ leads to the sequential activation of LeuO targets in a positive cascade (RcsB-BglJ→LeuO→target, Figure 5), this finding indicates that a negative feedback mechanism exists which operates in addition to the mutual positive control of *leuO* and *bglJ* expression and switches off regulation of LeuO targets. Such a feedback may provide a tightly controlled switch of LeuO and/or BglJ expression in response to specific environmental signals. Further, the microarray data show that out of dozens of targets only two genes are regulated by both LeuO and RcsB-BglJ independently of each other (*bgl* and *chiA*). This suggests that RcsB-BglJ and LeuO have individual sets of distinct targets. One hypothesis might be that the *bglJ-leuO* feedback loop operates only transiently. Activation of *leuO* by RcsB-BglJ may lead to accumulation of LeuO protein which in return results in shut-down of *leuO* transcription, as LeuO antagonizes activation by RcsB-BglJ (negative autoregulation). In addition to this feedback loop, mechanisms that regulate expression of BglJ or of LeuO on a post-transcriptional level may exist, e. g. by a regulatory sRNA. Moreover it is possible that expression of BglJ and/or LeuO changes the physiological status within the cell. Such a physiological modification may indirectly influence BglJ and/or LeuO expression through an unknown mechanism.
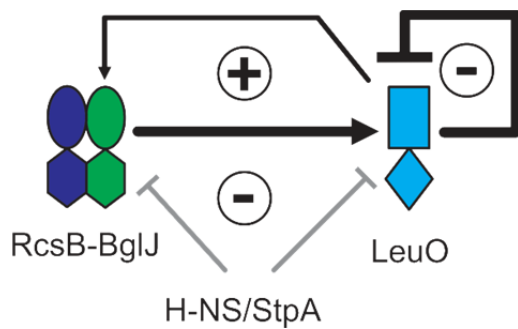
Figure 22: Schematic model of feedback loop regulation of RcsB-BglJ and LeuO.

LeuO antagonizes H-NS-mediated repression of *bglJ*. In turn, RcsB-BglJ antagonizes H-NS/StpA-mediated repression of *leuO* (double-positive feedback). Excess LeuO protein switches its own expression off (negative autoregulation).

It is still unknown how the double-positive feedback loop of RcsB-BglJ and LeuO is activated since both, *bglJ* and *leuO,* are repressed by H-NS under standard growth conditions. In the genomic library screen, CynR, the regulator of the *cynTS* operon involved in cyanate metabolism (Sung & Fuchs, 1988, Sung & Fuchs, 1992), was found to activate the *yjjQ-bglJ* promoter (Figure 20). Further experiments revealed that CynR activates the *yjjQ-bglJ* promoter *lacZ* fusion independently of LeuO and that it also activates the *leuO* promoter *lacZ* fusion independently of BglJ. It remains to be tested whether this activation of both promoters is an artifact based on the promoter *lacZ* fusions used here. Interestingly, one of the three genomic library clones (*envR*) and all of the transposon insertions are involved in cell membrane or cell surface processes, indicative of a role for BglJ and LeuO in these processes. Insertion of the miniTn10 transposon in the *acrAB* operon, encoding a multidrug efflux pump (transposon mutant T789, Figure 19), or overexpression of a truncated EnvR, the negative regulator of *acrAB* (genomic library clone T815, Figure 20) (Hirakawa *et al.*, 2008), caused activation of the *yjjQ-bglJ* promoter *lacZ* fusion.Remarkably , transcription of *envR* is 48-fold upregulated when LeuO is overexpressed as revealed by the microarray analysis (appendix Table 8). One might speculate that EnvR and the AcrAB efflux system may be involved in activation of *yjjQ-bglJ*. Another genomic library clone contained the genes *folD* and *ycbJ*. The enzyme 5, 10-methylene- tetrahydrofolate dehydrogenase/ 5, 10-methylene- tetrahydrofolate cyclohydrolase encoded by *folD* is a component of C1 metabolism (D'Ari & Rabinowitz, 1991). The S4-like RNA binding domain of the YbcJ protein is potentially involved in binding of structured RNA molecules (Volpon *et al.*, 2003).

As shown by transposon mutagenesis (Figure 19), transposon insertions in the *rfa* genes (LPS synthesis) as well as in *envC* (murein hydrolase) caused a Lac-positive phenotype of the *leuO* promoter *lacZ* fusion on agar plates. Transposon insertions in *bglH*, *acrA*, and *rfaP* caused a Lac-positive phenotype of the *yjjQ-bglJ* promoter *lacZ* fusion. Intriguingly, mutations in the *rfa* genes which are involved in the synthesis and export of lipopolysaccharides have been described to activate the Rcs phosphorelay system (Parker *et al.*, 1992, Majdalani & Gottesman, 2005, Majdalani *et al.*, 2005). However, complementation studies as presented in chapter 2.2.2 show that activation of *leuO* by RcsB-BglJ is independent of the phosphorylation status of RcsB. It is still an open question how these *rfa* mutants contribute to the regulation of *bglJ* and *leuO* that requires further investigation. Moreover, activation of the *leuO* promoter by *rfaG*, *rfaC*, and *envC* was only marginal in liquid culture (Figure 19). This may be due to the different growth conditions on agar plate and in culture. On plate, these insertions may exert regulatory function on the *yjjQ-bglJ* operon or the *leuO* promoter by rendering expression of downstream genes constitutive, or disruption of the genes may lead to intracellular physiological conditions that indirectly influence activity of the promoters. It is also possible that the expression level directed by the promoter *lacZ* fusion on plate is close to the threshold from a Lac-negative to a Lac-positive phenotype. In this case such small factors as determined by β-galactosidase assays in liquid culture would result in a Lac-positive phenotype on X-gal plates.

4. Material and Methods

4.1 Material

4.1.1 Bacterial strains, plasmids and oligonucleotides

Escherichia coli K12 strains used in this study are listed in Table 3, plasmids are summarized in Table 4, and sequences of oligonucleotides are given in Table 5.

Table 3: *Escherichia coli* **K12 strains**

Strain	Relevant genotype	Reference/Construction[a]
MG1655	K12 wild-type strain (CGSC #6300)	(Guyer *et al.*, 1981)
BW30270	MG1655 *rph*$^+$	CGSC #7925
S159	M182 *stpA*::Tet^R	(Zhang *et al.*, 1996)
S1734	*yjjQ/bglJ*-Y6::miniTn*10-cat* (= *bglJ$_C$*)	(Madhusudan *et al.*, 2005)
S3010	CSH50 Δ*lacZ*-Y217 Δ*bgl*-AC11 Δ*hns$_{KD4-Kan}$*	(Nagarajavel *et al.*, 2007)
S3754	MG1655 Δ*hns$_{KD4-Kan}$*	laboratory strain collection
S3974	BW30270 *ilvG*$^+$	(Venkatesh *et al.*, 2010)
S4197	S3974 Δ*lacZ*-Y217	× pFDY217
T21	S4197 Δ*rcsB$_{FRT}$* (NC_000913: 2314199-2314846)	× PCR S819/S820 (pKD3) × pCP20
T23	S4197 Δ*yjjPQ-bglJ$_{FRT}$* (NC_000913: 4600115-4602857)	× PCR S676/S783 (pKD3) × pCP20
T28	S4197 *attB*::(Spec^R P$_{leuO}$ *lacZ*)	× pKES200
T30	S4197 *attB*::(Spec^R P$_{leuO}$ *lacZ*) Δ*rcsB$_{FRT}$*	T21/pLDR8 × pKES200
T32	S4197 *attB*::(Spec^R P$_{leuO}$ *lacZ*) Δ*yjjPQ-bglJ$_{FRT}$*	T23/pLDR8 × pKES200
T70	S3974 Δ*yjjPQ-bglJ$_{KD3-Cm}$*	× PCR S676/S783 (pKD3)
T71	S4197 Δ*leuO$_{FRT}$* (NC_000913: 84368-85312)	× PCR S676/S783 (pKD3)
T73	S3974 Δ*rcsB$_{FRT}$*	× PCR T209/T210 (pKD3) × pCP20
T75	S3974 Δ*yjjPQ-bglJ$_{FRT}$*	T69 × pCP20
T77	S3974 Δ*leuO$_{FRT}$*	× PCR T209/T210 (pKD3) × pCP20
T87	S4197 *attB*::(Spec^R P$_{leuO}$ *lacZ*) Δ*leuO$_{FRT}$*	T71/pLDR8 × pKES200
T175	S3974 Δ*rcsB$_{FRT}$* Δ*yjjPQ-bglJ$_{FRT}$*	T73 × T4GT7 (T70) × pCP20
T177	S3974 Δ*leuO$_{FRT}$* Δ*yjjPQ-bglJ$_{FRT}$*	T77 × T4GT7 (T70) × pCP20
T208	S3974 Δ*hns$_{KD4-kan}$*	× T4GT7 (S3754)
T221	S3974 Δ*hns$_{FRT}$* (NC_000913: 1292145-1291735)	× T4GT7 (S3754) × pCP20
T288	S4197 *attB*::(Spec^R P$_{leuO}$ *lacZ*) Δ*yjjPQ-bglJ$_{FRT}$* Δ*hns$_{FRT}$*	T32 × T4GT7 (S3754) × pCP20
T290	S3974 Δ*yjjPQ-bglJ$_{FRT}$* Δ*hns$_{FRT}$*	T75 × T4GT7 (S3754) × pCP20

Strain	Relevant genotype	Reference/Construction[a]
T292	S4197 *attB*::(Spec^R P$_{leuO}$ *lacZ*) Δ*leuO*$_{FRT}$ Δ*hns*$_{FRT}$	T87 × T4GT7 (S3754) × pCP20
T308	S4197 *attB*::(Spec^R P$_{leuO}$ *lacZ*) Δ*leuO*$_{FRT}$ Δ*yjjPQ-bglJ*$_{FRT}$	T87 × T4GT7 (T70) × pCP20
T314	S4197 Δ*leuO*$_{FRT}$ Δ*yjjPQ-bglJ*$_{FRT}$	T71 × T4GT7 (T70) ×pCP20
T316	S4197 *attB*::(Spec^R P$_{leuO}$ *lacZ*) Δ*leuO*$_{FRT}$ Δ*hns*$_{FRT}$ Δ*yjjPQ-bglJ*$_{FRT}$	T292 × T4GT7 (T70) × pCP20
T324	S4197*attB*::(Spec^R P$_{leuLABCD}$ *lacZ*)	× pKETS3
T328	S4197 *attB*::(Spec^R P$_{leuLABCD}$ *lacZ*) Δ*leuO*$_{FRT}$	T71/pLDR8 × pKETS3
T352	S4197 *attB*::(Spec^R P$_{leuO}$ *lacZ*) Δ*yjjPQ-bglJ*$_{FRT}$ Δ*leuO*$_{FRT}$ Δ*hns*$_{FRT}$ *stpA*::Tet^R	T316 × T4GT7(S159)
T357	S4197 *attB*::(Spec^R P$_{leuO}$ *lacZ*) *rfaG*::mTn10-*cat*	T28 × pKESK18 Lac$^+$
T359	S4197 *attB*::(Spec^R P$_{leuO}$ *lacZ*) *rfaD*::mTn10-*cat*	T28 × pKESK18 Lac$^+$
T361	S4197 *attB*::(Spec^R P$_{leuO}$ *lacZ*) *rfaC*::mTn10-*cat*	T28 × pKESK18 Lac$^+$
T362	S4197 *attB*::(Spec^R P$_{leuO}$ *lacZ*) *rfaC*::mTn10-*cat*	T28 × pKESK18 Lac$^+$
T365	S4197 *attB*::(Spec^R P$_{leuO}$ *lacZ*) *envC*::mTn10-*cat*	T28 × pKESK18 Lac$^+$
T367	S4197 *attB*::(Spec^R P$_{leuO}$ *lacZ*) *rfaD*::mTn10-*cat*	T28 × pKESK18 Lac$^+$
T368	S4197 *attB*::(Spec^R P$_{leuO}$ *lacZ*) *rfaC*::mTn10-*cat*	T28 × pKESK18 Lac$^+$
T370	S4197 *attB*::(Spec^R P$_{leuO}$ *lacZ*) *rfaD*::mTn10-*cat*	T28 × pKESK18 Lac$^+$
T413	S4197 *attB*::(Spec^R P$_{yjjQ}$ *lacZ*)	S4197/pLDR8 × pKES111
T414	S4197 *attB*::(Spec^R P$_{yjjQ}$ *lacZ*) Δ*yjjPQ-bglJ*$_{FRT}$	T23/pLDR8 × pKES111
T416	S4197 *attB*::(Spec^R P$_{yjjQ}$ *lacZ*) Δ*leuO*$_{FRT}$	T71/pLDR8 × pKES111
T447	S3974 Δ*hns*$_{FRT}$ *stpA*::Tet^R	T221 × T4GT7 (S159)
T453	S3974 Δ*rcsC*$_{KD3-Cm}$	× PCR T331/T332 (pKD3)
T468	S4197 *attB*::(Spec^R P$_{leuO}$ *lacZ*) *rfaG*::mTn10-*cat*	T28 × T4GT7 (T357)
T469	S4197 *attB*::(Spec^R P$_{leuO}$ *lacZ*) *rfaC*::mTn10-*cat*	T28 × T4GT7 (T361)
T470	S4197 *attB*::(Spec^R P$_{leuO}$ *lacZ*) *envC*::mTn10-*cat*	T28 × T4GT7 (T365)
T538	S4197 *attB*::(Spec^R P$_{leuO}$ *lacZ*) Δ*rcsC*$_{FRT}$ (NC_000913: 2315049-2317930)	T28 × T4GT7 (T453) × pCP20
T568	S4197 *attB*::(Spec^R P$_{bgl}$ t1$_{RAT}$ *bglG lacZ*) Δ*leuO*$_{FRT}$ Δ*yjjPQ-bglJ*$_{FRT}$	T314/pLDR8 × pKENV61
T576	S4197 *attB*::(Spec^R P$_{bgl}$ -mut2 t1$_{RAT}$ *bglG lacZ*) Δ*leuO*$_{FRT}$ Δ*yjjPQ-bglJ*$_{FRT}$	T314/pLDR8 × pKES220
T578	S4197 *attB*::(Spec^R P$_{bgl}$ -mut3 t1$_{RAT}$ *bglG lacZ*) Δ*leuO*$_{FRT}$ Δ*yjjPQ-bglJ*$_{FRT}$	T314/pLDR8 × pKES221
T580	S4197 attB::(Spec^R P$_{bgl}$ -mut1 t1$_{RAT}$ *bglG lacZ*) Δ*leuO*$_{FRT}$ Δ*yjjPQ-bglJ*$_{FRT}$	T314/pLDR8 × pKES222
T570	S4197 *attB*::(Spec^R P$_{leuO}$ *lacZ*) *bglJ*$_C$	T28 × T4GT7 (S1734)
T572	S4197 *attB*::(Spec^R P$_{leuO}$ *lacZ*) Δ*rcsB*$_{FRT}$ *bglJ*$_C$	T30 × T4GT7 (S1734)
T574	S4197 *attB*::(Spec^R P$_{leuO}$ *lacZ*) Δ*rcsC*$_{FRT}$ *bglJ*$_C$	T538 × T4GT7 (S1734)
T727	S4197 attB::(Spec^R P$_{bgl}$ t1$_{RAT}$ *bglG lacZ*) Δ*leuO*$_{FRT}$ Δ*yjjPQ-bglJ*$_{FRT}$ Δ*rcsB*$_{FRT}$	T568 × T4GT7 (T15) × pCP20
T729	S4197 attB::(Spec^R P$_{bgl}$ t1$_{RAT}$ *bglG lacZ*) Δ*leuO*$_{FRT}$ Δ*yjjPQ-bglJ*$_{FRT}$ Δ*hns*$_{FRT}$	T568 × T4GT7 (S3010) × pCP20
T731	S4197 attB::(Spec^R P$_{bgl}$ -mut2 t1$_{RAT}$ *bglG lacZ*) Δ*leuO*$_{FRT}$ Δ*yjjPQ-bglJ*$_{FRT}$ Δhns$_{FRT}$	T576 × T4GT7 (S3010) × pCP20
T733	S4197 attB::(Spec^R P$_{bgl}$ -mut3 t1$_{RAT}$ *bglG lacZ*) Δ*leuO*$_{FRT}$ Δ*yjjPQ-bglJ*$_{FRT}$ Δhns$_{FRT}$	T578 × T4GT7 (S3010) × pCP20
T735	S4197 attB::(Spec^R P$_{bgl}$ -mut1 t1$_{RAT}$ *bglG lacZ*) Δ*leuO*$_{FRT}$ Δ*yjjPQ-bglJ*$_{FRT}$ Δhns$_{FRT}$	T580 × T4GT7 (S3010) × pCP20
T757	S4197 attB::(Spec^R P$_{bgl}$ t1$_{RAT}$ *bglG lacZ*) Δ*leuO*$_{FRT}$ Δ*yjjPQ-bglJ*$_{FRT}$ Δ*hns*$_{FRT}$ *stpA*::*tet*	T729 × T4GT7 (S159)
T787	S4197 *attB*::(Spec^R P$_{yjjQ}$ *lacZ*) *bgl*::mTn10-*cat*	T413 × pKESK18 Lac$^+$
T788	S4197 *attB*::(Spec^R P$_{yjjQ}$ *lacZ*) *rfaP*::mTn10-*cat*	T413 × pKESK18 Lac$^+$

Strain	Relevant genotype	Reference/Construction[a]
T789	S4197 *attB*::(Spec[R] P*yjjQ* *lacZ*) *acrA*::mTn10-*cat*	T413 × pKESK18 Lac[+]
T813	S4197 *attB*::(Spec[R] P*yjjQ* *lacZ*)/pKESK22::*cynR* (NC_000913: 358547-355838)	T413 x pKEST11 Lac[+]
T814	S4197 *attB*::(Spec[R] P*yjjQ* *lacZ*)/pKESK22::*cynT-cynR* (NC_000913: 358725-356766)	T413 x pKEST11 Lac[+]
T815	S4197 *attB*::(Spec[R] P*yjjQ* *lacZ*)/pKESK22::*envR-?-ydbJ-ydbK* (NC_000913: 3412107-XXX-1438267)	T413 x pKEST11 Lac[+]
T816	S4197 *attB*::(Spec[R] P*yjjQ* *lacZ*)/pKESK22::*folD* (NC_000913: 557681-555881)	T413 x pKEST11 Lac[+]
T849	S4197 Δ*leuO*FRT *attB*::(Spec[R] P*bgl* t1RAT *bglG lacZ*)	T71/pLDR8 × pKENV61
T851	S4197 Δ*leuO*FRT *attB*::(Spec[R] P*bgl* -mut2 t1RAT *bglG lacZ*)	T71/pLDR8 × pKES220
T853	S4197 Δ*leuO*FRT *attB*::(Spec[R] P*bgl* -mut3 t1RAT *bglG lacZ*)	T71/pLDR8 × pKES221
T855	S4197 Δ*leuO*FRT attB::(Spec[R] P*bgl* -mut1 t1RAT *bglG lacZ*)	T71/pLDR8 × pKES222
T862	S4197 *attB*::(Spec[R] P*leuO* *lacZ*) Δ*leuO*FRT *bglJ*C	T87 × T4GT7 (S1734)
T1032	S4197 Δ*leuO*FRT *bglJ*C	T71 × T4GT7 (S1734)
T1048	S3974 Δ*yjjPQ-bglJ*FRT Δ*hns*FRT *stpA*::Tet[R]	T290 × T4GT7 (S159)
T1072	S4197 *attB*::(Spec[R] P*leuO* RcsB-BglJmut1 *lacZ*) Δ*leuO*FRT *bglJ*C	T1032/pLDR8 × pKETS19
T1073	S4197 *attB*::(Spec[R] P*leuO* RcsB-BglJmut2 *lacZ*) Δ*leuO*FRT *bglJ*C	T1032/pLDR8 × pKETS20
T1075	S4197 *attB*::(Spec[R] P*leuO* RcsB-BglJmut3 *lacZ*) Δ*leuO*FRT *bglJ*C	T1032/pLDR8 × pKETS21
T1077	S4197 *attB*::(Spec[R] P*leuO* RcsB-BglJmut1+3 *lacZ*) Δ*leuO*FRT *bglJ*C	T1032/pLDR8 × pKETS22
T1106	S4197 *attB*::(Spec[R] P*leuO* RcsB-BglJmut3 *lacZ*) Δ*leuO*FRT *bglJ*C Δ*hns*KD4-Kan	T1075 × T4GT7 (T208)
T1108	S4197 *attB*::(Spec[R] P*leuO* RcsB-BglJmut3 *lacZ*) Δ*leuO*FRT *bglJ*C Δ*hns*Kan *stpA*::Tet[R]	T1106 × T4GT7 (S159)

a) Construction of strains by cointegrate formation (x pFDY217), by transduction (x T4GT7), by λ-Red mediated recombination (x PCR x pCP20), and by chromosomal integration (pLDR8) briefly described below were performed as described (Hamilton *et al.*, 1989, Wilson *et al.*, 1979, Datsenko & Wanner, 2000, Diederich *et al.*, 1992). Transposon mutagenesis (x pKESK18 Lac[+]) (Madhusudan *et al.*, 2005) and genomic library screens (x pKETS11 Lac[+]) are described below. Strains were stored as DMSO stocks (50 μl of DMSO, 1.5 ml of overnight culture).

Table 4: Plasmids

Plasmid	Features	Use/Reference
pUC12	standard cloning vector *lacZ*-alpha bla pBR-ori	(Vieira & Messing, 1987)
pCP20	cI857 λ-PR flp in pSC101 rep[ts] bla	(Cherepanov & Wackernagel, 1995)
pKD3	FRT-cat - FRT oriRγ bla	(Datsenko & Wanner, 2000)
pKD4	FRT-neo - FRT oriRγ bla	(Datsenko & Wanner, 2000)
pKD46	araC P*ara* γ-β-exo in pSC101 rep[ts] bla	(Datsenko & Wanner, 2000)
pLDR8	cI857 PR λ-int in pSC101 rep[ts] neo	(Diederich *et al.*, 1992)

Plasmid	Features	Use/Reference
pFDY217	lacI lacOP [Δ*lacZ*] lacYA in pSC101-rep$_{ts}$ Tet^R	(Dole *et al.*, 2002)
pKEAP21	lacI^q P$_{tac}$ *leuO* (NC_000913: 84170-85309) His$_6$ in pMB1 bla	(Stratmann *et al.*, 2008)
pKEDR13	lacI^q P$_{tac}$ *leuO* (NC_000913: 84170-85331) in p15A neo	(Stratmann *et al.*, 2008)
pKENV61	P$_{bgl}$ t1$_{RAT}$ bglG *lacZ* in p15A neo λ-attP aadA	(Nagarajavel *et al.*, 2007)
pKES220	P$_{bgl}$ mut1 t1$_{RAT}$ bglG *lacZ* in p15A neo λ-attP aadA	laboratory collection
pKES221	P$_{bgl}$ mut2 t1$_{RAT}$ bglG *lacZ* in p15A neo λ-attP aadA	laboratory collection
pKES222	P$_{bgl}$ mut3 t1$_{RAT}$ bglG *lacZ* in p15A neo λ-attP aadA	laboratory collection
pKESK18	cI$_{857}$ P$_R$ transposase miniTn10-cat neo in pSC101-rep$_{ts}$	(Madhusudan *et al.*, 2005)
pKESK22	lacI^q P$_{tac}$ MCS in p15A neo	(Stratmann *et al.*, 2008)
pKES111	P$_{yjjQ\text{-}bglJ}$ (NC_000913: 4600995-4601507) *lacZ* in p15A neo λ-attP aadA	(Stratmann *et al.*, 2008)
pKES148	MCS *lacZ* in p15A neo λ-attP aadA	laboratory collection
pKES200	P$_{leuO}$ *lacZ* (NC_000913: 83521-84412) in p15A neo λ-attP aadA	this work[a]
pKES235	lacI^q P$_{tac}$ rcsB-D56A in p15A neo	laboratory collection

Plasmid	Features	Use/Reference
pKETS1	lacI^q P$_{tac}$ *bglJ* (NC_000913: 4602168-4602867) in p15A neo	this work[b]
pKETS3	P$_{leu}$ (NC_000913: 84412-83700) *lacZ* in p15A neo λ-attP aadA	this work[a]
pKETS5	lacI^q P$_{tac}$ *leuO* (NC_000913: 84348-85331) in p15A neo	this work[b]
pKETS6	lacI^q P$_{tac}$ rcsB (NC_000913: 2314174-2314849) in p15A neo	this work[b]
pKETS7	lacI^q P$_{tac}$ rcsB-D56E in p15A neo	this work[b]
pKETS8	lacI^q P$_{tac}$ rcsB-D56N in p15A neo	this work[b]
pKETS9	lacI^q P$_{tac}$ *bglJ* (NC_000913: 4602217-4602867) in p15A neo	this work[a]
pKETS10	lacI^q P$_{tac}$ *bglJ* (NC_000913: 4602313-4602867) in p15A neo	this work[a]
pKETS11	lacI^q P$_{tac}$ Sau3AI gDNA in p15A neo	this work[d]
pKETS13	footprint fragment 1 (NC_000913: 83593-83872) in pUC12 bla	this work[c]
pKETS14	footprint fragment 2 (NC_000913: 83773-84052) in pUC12 bla	this work[c]
pKETS15	footprint fragment 3 (NC_000913: 83953-84232) in pUC12 bla	this work[c]
pKETS16	footprint fragment 4 (NC_000913: 84133-84412) in pUC12 bla	this work[c]
pKETS17	footprint fragment 6 (NC_000913: 83593-84412) in pUC12 bla	this work[c]
pKETS18	footprint fragment 5 (NC_000913: 84133-84232) in pUC12 bla	this work[c]
pKETS19	P$_{leuO}$ mut1 *lacZ* in p15A neo λ-attP aadA	this work[a]
pKETS20	P$_{leuO}$ mut2 *lacZ* in p15A neo λ-attP aadA	this work[a]
pKETS21	P$_{leuO}$ mut3 *lacZ* in p15A neo λ-attP aadA	this work[a]
pKETS22	P$_{leuO}$ mut1+3 *lacZ* in p15A neo λ-attP aadA	this work[a]
pKETS23	lacI^q P$_{tac}$ *cynR* (NC_000913: 357934-357015) in p15A neo	this work[b]

a) For promoter *lacZ* fusions, plasmid pKES148 was used. Plasmid pKES148 is a vector for cloning of promoter *lacZ* fusions and subsequent integration of these fusions into the phage λ *attB* site, as described (Diederich *et al.*, 1992, Dole *et al.*, 2002). It carries a multiple cloning site upstream of the promoter-less *lacZ* gene. In addition, the plasmid carries a cassette with the phage λ *attP* sequence

and gene *aadA* conferring spectinomycin resistance for integration into *attB* and selection of integrants. The plasmid backbone consists of a p15A replication origin and the *neo* gene for selection on kanamycin. For plasmids pKES200 and pKETS3 inserts were amplified by PCR using primer pairs T40/T41 and T251/T262, respectively, as listed in Table 5. PCR fragments were digested with SalI and XbaI for cloning into pKES148. For plasmids pKETS19, pKETS20, and pKETS21, the insert was amplified using the combined chain reaction (CCR) method (Bi & Stambrook, 1998, Hames *et al.*, 2005) as described below. Primers T334/S118 combined with the 5'-phosphorylated oligonucleotides T517, T518, or T519, respectively were used to amplify the insert carrying the mutated RcsB-BglJ binding site from template plasmid pKES200. CCR was followed by digestion with SalI and XbaI for cloning into pKES148.

b) Plasmids pKETS1, pKETS5, pKETS6, pKETS7, pKETS8, pKETS9, pKETS10, and pKETS23 are vectors for expression of moderate levels of the encoded transcription factors under transcriptional control of the *lacI-tac*-IPTG system. These pKESK22-derived plasmids (p15A origin of replication, *neo*) were constructed by insertion of fragments generated by PCR followed by digestion with EcoRI and XbaI.

c) For plasmids pKETS13-18 used for footprinting assays, inserts were amplified by PCR using pKES200 as template and primers as listed in Table 5 for cloning into pUC12.

d) Cloning of genomic library pKETS11 was performed as described below.

Table 5: Oligonucleotides

Oligo	Sequence[a]	Target/application
S2	CGGGATCCTTTAAATTGTCTTAAACCGGAC	*hns* 3' end
S93	CCGGGCCGACAACAAAGTCA	λ-*attB* region
S94	GCTTTACTAAGCTGATCCGGTGGA	λ-*attP* plasmids
S95	CATATGGGGATTGGTGGCGA	λ-*attP* plasmids
S96	CACTCTGCCAGATGGCGCAA	λ-*attB* region
S116	TGGCACGACAGGTTTCCCGA	pUC12
S118	TGCGGGCCTCTTCGCTATTA	*lacZ*
S123	TGTGGAATTGTGAGCGGATA	*tac* promoter
S150	CGACGGGATCAGTACCGACGG	pACYC plasmid
S164	GAGCAGGGGAATTGATCCGGTGGA	*attB* region
S165	GTAACAGTGGCCCGAAGATA	*lacY*
S182	ATAAGATGCCGTGGAACCAA	*stpA*
S183	CGCTTACACTACGCGACGAA	*stpA*

Oligo	Sequence[a]	Target/application
S357	GGCAGGGTCGTTAAATAGCCGCTTATGT	ST-PCR
S358	CGGTATCAACAGGGACACCAGGATTTATTTATTCT	ST-PCR
S359	gcTCTAGAGATCATATGACAAGATGTGTATCCACCTTAACT	ST-PCR *Xba*I
S361	gcTCTAGAGGCCACGCGTCGACTAGTAC	ST-PCR *Xba*I
S540	tcagatctCCACCAGCCCTATCGTTCCGCACCGC	*fhuF* BglII
S602	actctagaTCCTTACATTCCTGGCTATTGCA	*hns* XbaI
S656	ATGTCAAGAGCTTGCTGTAGCAAGG	*rcsB*
S657	GACACTAACGCGTCTTATCTGGCC	*rcsB*
S676	GAAAGCACTGCCGGGGAAGTAAACCCGGCATCATGCGGATTAcatatgaatatcctcccttagttcctattcc	construction of Δ*yjjPQ-bglJ*
S783	GAGGATCATATCCTGCGCCAACGCTAACAGAAATTCGATCAgtgtaggctggagctgcttcg	construction of Δ*yjjPQ-bglJ*
S795	AACACCATCGCAAAGCCGAC	*yjjP*
S819	ATTGACAGTTATGTCAAGAGCTTGCTGTAGCAAGGTAGCCTATTACgtgtaggctggagctgcttcg	construction of Δ*rcsB*
S820	TGCCAGATAAGACACTAACGCGTCTTATCTGGCCTACAGGTGATTAcatatgaatatcctccttagttcctattcc	construction of Δ*rcsB*
T-40	cgacgtcgaCTGGCTCATGGTTTGGGTCCT	*leuO* SalI cloning pKES200, pKETS21
T-41	cgactctagaGCTTAACTCCGCCGTCTCTGG	*leuO* XbaI cloning pKES200, pKETS21 5'RACE
T106	cagggatcctctagattaGTCTTTATCTGCCGGACTTAAGGTCAC	*rcsB* BamHI XbaI cloning pKETS6
T207	gaccgaattcTGGAGATGCCGCAGAATGG	*bglJ* EcoRI cloning pKETS1
T208	ctggtctagaATGCGGATTAATAGGGATGCAA	*bglJ* XbaI cloning pKETS1
T209	ATTCCAATAAGGGAAAGGGAGTTAAGTGTGACAGTGGAGTTAAGTgtgtaggctggagctgcttcg	construction of Δ*leuO*
T210	TGCAGAATAAACCAGACATTCATGTCTGACCTATTCTGCAATCAGcatatgaatatcctccttagttcctattcc	construction of Δ*leuO*
T211	TGTAGATGATTGAGTATTCGCGGTAGTT	*leuO*
T212	TGATAATAAATCGGCTGAATCCCAC	*leuO*
T245	ATGACACGGTAGATAAGCAAGCCAGT	*leuO qPCR*
T246	TTCAGCGAACTCTTCAGCCAGC	*leuO qPCR*
T247	GACGAAGAAGATGGCGATGACGAC	*rpoD* qPCR
T248	TTCCTGAGCGGTAGCGTGACTG	*rpoD* qPCR
T251	cgacgtcgacGCTTAACTCCGCCGTCTCTGG	*leuO* SalI cloning pKETS3
T262	cgattctagaGTGAGTCATTAAATCAGCTCCAGATGAAT	*leuL* XbaI Cloning pKETS3 5'RACE
T265	GCGCGAATTCCTGTAGAACGA	5'RACE EcoRI
T268	AUAUGCGCGAAUUCCUGUAGAACGAACACUAGAAGAAA	5'RACE RNA oligo
T309	GCTGTTCATCGTGGAATAATCCCTC	*envC*
T310	CGCCAACAGAGCGGCAAATG	*envC*
T311	AAGGGATTCGGATGTGATGGTATG	*rfaD*
T312	ATGAGGAATACCCGCGAAGAAAG	*rfaD*

Oligo	Sequence[a]	Target/application
T313	TGGTGATCGGCCCGTCTTG	*rfaF*
T314	GATAACTGCGTCATAGTTCTCTGCTTGTAG	*rfaF*
T315	TTACAAGAGGAAGCCTGACGGATG	*rfaC*
T316	CGCAGAATACCAAATTAAATCAAGCAAG	*rfaC*
T317	GGGTATGGGAAGAATCAGATGGTATGTAG	*rfaL*
T318	CCGAATCATCATAAATCTATACAAATAGTATCC	*rfaL*
T329	GAGAACATTGCGGTAACACGCTTTTACCGCTACCTTAACCACACTgtgtaggctggagctgcttcg	construction of Δ*rcsC*
T330	GCATTTGCACTGAATGCCGGATGCGGCGTAAACGCCTTATCCGTCcatatgaatatcctccttagttcctattcc	construction of Δ*rcsC*
T331	GTGATGATTTCTCGGCGGTGTATC	*rcsC*
T332	GCGTTAGTGTCTTATCTGGCATTTG	*rcsC*
T333	GGCCACGCGTCGACTAGTACNNNNNNNNNNTCAG	ST-PCR
T334	TGGCGAAGTAATCGCAACATCC	λ-*attP* plasmids
T351	CTTAACTCCACTGTCACACTTAACTCCCT	*leuO* leader qPCR
T352	TTCAGGATTATTTCTCTGCATTCCAATA	*leuO* leader qPCR
T353	TGTAATTTTAGGAATTTgaAAcGTTATATATAACAAATCCCAATAATTAAGTTA	RcsB-BglJ site mutant 1 bgl promoter
T354	GTGTAATTTgAGctATTTgaAAcGTTATATATAACAAATCCCAATAATTAAGTTA	RcsB-BglJ site mutant 2 bgl promoter
T355	CTTTGTGTAATTTTAGctATTTATAAcGTTATATATAACAAATCCCAATAATTAAGTTA	RcsB-BglJ site mutant 3 bgl promoter
T358	gaccgaattcTTGCTGTAGCAAGGTAGCCTATTACATG	*rcsB* EcoRI cloning pKETS6
T359	gaccgaattcCACTCATAGAAAAATGCGTCATGAGTAGTAT	*bglJ Eco*RI cloning pKETS9
T360	gaccgaattcAGGAGTCATTTCAGGATGCCATGT	*bglJ Eco*RI cloning pKETS10
T411	AGACACCAACCTTAAACCATCCAAATC	*cas2* qPCR
T412	TCTGGGAACAAATAGCTGGACTGG	*cas2* qPCR
T413	AAAACACCCGATGAAAATTCCTGAG	*casC* qPCR
T414	TGAGTTGGGAAAAGTTGATGGTGC	*casC* qPCR
T415	AATTCAAGAGGACTTTGCGGCG	*casA* qPCR
T416	CCTCCGCACCATCATGGACA	*casA* qPCR
T417	TGGCAACAGGAATCTCAAAACCAG	*cas3* qPCR
T418	TGGACGGATACTTGTCGCAACC	*cas3* qPCR
T435	TGATAGGTCGCAGGATCAATCTGATAG	*acrA*
T436	ATTTGTGAATGTATGTACCATAGCACGAC	*acrA*
T437	cgacggatccCCCCTGACGCAATAAAAACGTCCC	footprint 2 *Bam*HI
T438	cgacgaattcgagctcGCCCTAACATTAATTGATCAATAATATTCACCAAATCA	footprint 2 *Eco*RI SacI
T439	cgacggatccCCCACGCGTTGCAAAACCTATCCT	footprint 3 *Bam*HI
T440	cgacgaattcgagctcGCCCGGTTCTGATAAAAACAGAATCCATTGC	footprint 3 *Eco*RI SacI
T441	cgacggatccCCTAGTTATGATTAGATTGTTTTCGCAACAAA	footprint 4 *Bam*HI
T442	cgacgaattcgagctcGCCCGCTTAACTCCGCCGTCTCTGG	footprint 4 *Eco*RI SacI

Oligo	Sequence[a]	Target/application
T443	cgacggatccCCGCGGGTTTTTTGTTTGACTGCG	footprint 1 *Bam*HI
T444	cgacgaattcgagctcGCCCTAAGCAGAAATTAATATCGCTTACTTTAACCA	footprint 1 *Eco*RI SacI
T517	[PHOS]GAATATTATTGATCAATTAATGTTAActATTAgaGCATTAAATATATAAAT TAATTATTAAATAAGCACATTTAATC	*leuO* RcsB-BglJ site mut1 CCR cloning pKETS19, 22
T518	[PHOS]taatgttaagaattaatgcattaaaTATtcAAATagATTATTAAATAAGCA CATTTAATCCATTTTGTAGAT	*leuO* RcsB-BglJ site mut2 CCR cloning pKETS20
T519	[PHOS]GTTTTTATCAGAACCCGTATCTTTtcGTTTagCGAATTTTACTCATTTTGC TTTTTCTTATTTTATAT	*leuO* RcsB-BglJ site mut3 CCR cloning pKETS21, 22
T530	ATCGAAAACGGTTAATAAGTTGAGATCG	*in vitro* transcription
T531	TTTTGCTCCTGCATCACGGC	*in vitro* transcription
T532	AGTAGTAGTAGACCGATAAAGCGAACGAT	*in vitro* transcription
T533	CGCGCAAAGAAGATGCGTTTA	*in vitro* transcription
T579	cgactctagaTAATTGTGCTGCGGTGGTTAAAGTAAG	*leu-leuO* XbaI 5'RACE
T580	cgactctagaATTCGGAAAACATAAAGATACGGGTTC	*leu-leuO* XbaI 5'RACE
T581	gaccgaattcGATTTACTTATAGGTTGCGAATGCTCTCT	*cynR Eco*RI cloning pKETS22
T582	ctggtctagaGTGTCAGCGGCTACCGTGATTC	*cynR Xba*I cloning pKETS22

a) Oligonucleotides are given in 5' to 3' direction. Matching parts to the indicated targets are printed in upper case, non-matching parts are printed in lower case letters. Sites for restriction endonucleases are underlined.

4.1.2 Media and antibiotics

LB medium (for 1000 ml): 10 g of BactoTryptone, 5 g of YeastExtract, 5 g of NaCl, 15 g of BactoAgar for plates.

SOB medium (for 1000 ml): 20 g of BactoTryptone, 5 g of YeastExtract, 0.5 g of NaCl, 1.25 ml of 2 M KCl. pH adjusted to 7.0 with NaOH, 10 ml of 1M MgCl$_2$ (after autoclaving).

SOC medium: 19.8 ml of 20% Glucose added to 1000 ml of SOB.

M9 minimal medium (for 1000 ml): 50 ml 20 x M9 (140 g Na$_2$HPO$_4$, 60 g KH$_2$PO$_4$, 20 g NH$_4$Cl, H$_2$O ad 1 l), 1 ml of 0.1 M CaCl$_2$, 1 ml of 1 M MgSO$_4$, 0.5 ml of 1 mM FeCl$_3$, 50 ml of 20 % glucose, 300 mM amino amino where indicated, 15 g of BactoAgar for plates.

MacConkey lactose plates (for 1000 ml): 40 g of MacConkeyAgar Base, 20 g of lactose.

BTB agar (for 1000 ml): 15 g BactoAgar, 1 g YeastExtract, 1 g BactoTryptone, 5 g NaCl, 1 ml 1 M $MgSO_4$, 1 ml 0.1 M $CaCl_2$, 1 ml of 1 mg/ml Vitamin B1, 20 ml of 10 % (w/v) casamino acids, 50 ml of 10 % (w/v) salicin, 10 ml bromthymol blue stock solution (2 % bromthymol blue in 50% EtOH, 0.1 N NaOH) (Dole *et al.*, 2002).

T4 top agar (for 1000 ml): 6 g of BactoAgar, 10 g of BactoTryptone, 8 g of NaCl, 2 g of tri-sodiumcitrate dihydrate, 3 g of glucose.

X-gal was used at a final concentration of 40 µg/ml.

Antibiotics were used at the following concentrations: ampicillin 50 µg/ml, chloramphenicol 15 µg/ml, kanamycin 25 µg/ml, spectinomycin 50 µg/ml, tetracyclin 12 µg/ml.

4.1.3 Enzymes, kits and chemicals

A list of suppliers and manufacturers of enzymes, kits and chemicals is provided in Table 6.

Table 6: Manufacturers

Manufacturer	Item
5PRIME, Hamburg, Germany	Agarose GelExtract PCRExtract
Affymetrix, Ohio, USA	GeneChip® E. coli Genome 2.0 Sequenase™ Version 2.0 DNA Sequencing Kit
Ambion, Carlsbad, CA, USA	SUPERAse In RNase Inhibitor
Applied Biosystems, Carlsbad, CA, USA	BigDye Terminator v3.1 Cycle Sequencing Kit
Becton, Dickinson, and Company, Sparks, USA	BactoAgar BactoTryptone YeastExtract Difco MacConkey Agar Base
Epicentre, Madison, WI, USA	Tobacco Acid Pyrophosphatase (TAP) Ampligase E. coli RNA Polymerase sigma70

Manufacturer	Item
Fermentas, St. Leon-Rot, Germany	FastDigest restriction enzymes
	T4 DNA ligase
	HighFidelity Enzyme Mix
	RNase-free DNaseI
	dNTPs
	DNA and RNA ladders
	RNaseH
Hartmann Analytic, Göttingen, Germany	radiolabelled dNTPs
Invitek, Berlin, Germany	MSB Spin PCRapace
Invitrogen, Karlsruhe, Germany	SuperScript III reverse transcriptase
	Platinum Taq DNA polymerase
	RNase OUT
	custom-made oligonucleotides
	NTPs
Molzym, Bremen, Germany	PrestoSpin D Bug
New England Biolabs, Frankfurt am Main, Germany	restriction enzymes
	T4 ssRNA ligase
Promega, Madison, WI, USA	Wizard Plus MaxiPrep
	GoTaq DNA polymerase
Qiagen, Hilden, Germany	QIAquick Gel Extract
	QIAquick PCR extract
	RNeasy MiniKit
	RNAprotect Bacteria Reagent
SERVA Electrophoresis GmbH, Heidelberg, Germany	chemicals
	antibiotics
Sigma-Aldrich, Taufkirchen, Germany	custom-made oligonucleotides
	chemicals

4.2 Methods

4.2.1 Standard molecular techniques

Standard molecular techniques like agarose gel electrophoresis, PCR and cloning work were carried out according to published protocols (Ausubel *et al.*, 2005). Sequencing was either perfomed by the Cologne Center for Genomics (University of Cologne) using the BigDye Terminator v3.1 Cycle Sequencing Kit (Applied Biosystems) or by GATC Biotech AG, Konstanz, Germany. Sequences were analyzed using Vector NTI 11 software (Invitrogen).

4.2.2 Site-specific mutagenesis by combined chain reaction (CCR)

Combined chain reaction (CCR) was performed as described previously (Bi & Stambrook, 1998, Hames *et al.*, 2005). In brief, 1 µl of forward PCR primer T334 (10 pmol/µl) and 1 µl of reverse PCR primer S118 (10 pmol/µl) were used in combination with 4 µl of internal, 5'-phosphorylated mutagenesis primer (10 pmol/µl, Table 5). Plasmid pKES200 was used as template for the *leuO* promoter *lacZ* fusion. 25 µl of dNTP mix (10 mM each), 5 µl of 10 x CCR buffer (200 mM Tris-HCl (pH 8.5), 30 mM $MgCl_2$, 500 mM KCl, 5 mM NAD^+), 2 µl of HighFidelity EnzymeMix (Fermentas), 3 µl of Ampligase (Epicentre), 2 µl of BSA (10 mg/ml), and H_2O were added to a final volume of 50 µl. The PCR cycler program was 5 min 95°C, 35 x (30 s 95°C, 30 s 55°C, 2 min 65°C), 5 min 65°C, hold at 4°C. CCR fragments were excised from agarose gels and used for cloning.

4.2.3 $CaCl_2$-competent cells and transformation

For $CaCl_2$-competent cells, cultures were grown in 25 ml LB to an OD_{600} of 0.3 and pelleted by centrifugation at 3,000 rpm for 10 minutes at 4°C. The pellets were resuspended in 12.5 ml of ice cold 0.1 M $CaCl_2$ and incubated on ice for 20 minutes, followed by centrifugation for 10 minutes at 3000 rpm. The cell pellet was resuspended in 1 ml of 0.1 M $CaCl_2$. For transformation 1 to 20 ng of plasmid DNA or 10 µl of ligations in 50 µl of TEN buffer (20 mM Tris-HCl pH 7.5, 1 mM EDTA, 50 mM NaCl) was mixed on ice with 100 µl of competent cells. The cells were incubated on ice for 20 minutes followed by heat shock at 42°C for 2 minutes and additional 10 minutes of incubation on ice. The competent cells were transferred to 1 ml of LB medium, incubated for 1 hour at 37°C (or appropriate temperature) and 100 µl of the culture was plated on suitable selective medium. TEN buffer: 20 mM Tris-HCl pH 7.g, 1 mM EDTA, 50 mM NaCl.

4.2.4 Electrocompetent cells and electroporation

For preparation of electrocompetent cells, cultures were grown overnight in 3 ml SOB medium with appropriate antibiotics and at appropriate temperature. An aliquot of 200 µl of culture was used to inoculate 50 ml of SOB medium with appropriate antibiotics, and this culture was grown to OD_{600} of 0.6. The culture was kept on ice for 1 hour. The culture was

transferred to prechilled tubes and centrifuged at 4°C for 15 minutes at 3000 rpm. The pellet was resuspended in 50 ml of ice-cold water and centrifuged at 4°C for 15 minutes at 3000 rpm. The pellet was resupended in 25 ml of ice-cold water and centrifuged at 4°C for 15 minutes at 3000 rpm. The cells were resuspended in 2 ml of ice-cold 10% glycerol and pelleted by centrifugation at 4°C for 15 minutes at 6000 rpm. Then, cells were resuspended in 200 µl of ice-cold 10 % glycerol. The cells were either used immediately for electroporation or, for long-term storage, further incubated for 1 hour on ice and stored as 40 µl aliquots at -80°C. For transformation, 40 µl of competent cells were mixed with 1 µl of DNA (50-100 ng/µl solution in water) and incubated for 10 minutes on ice. The mixture was transferred to a prechilled electroporation cuvette with a 1 mm electrode gap (Bio-Rad). The cuvettes were placed in the electroporator (Gene Pulser, Bio-Rad) and the electric shock was given for 3 seconds at 1.8 kV. Then 1 ml of SOC medium was immediately added to the cuvettes, and the cells were transferred to culture tubes and incubated at 37°C for 1 hour. After incubation 100 µl of culture was plated on suitable selection medium. Alternatively, 1 ml of culture was centrifuged for 1 minute at 5000 rpm, supernatant was decanted, pellet resuspended in 100 µl of SOC and plated.

4.2.5 Gene deletion by cointegrate formation

Construction of a Δ*lacZ* mutant was performed using plasmid pDFY217 (*lacI lacOP* [Δ*lacZ*] *lacYA* in pSC101-rep$_{ts}$ Tet[R]) as described (Hamilton *et al.*, 1989, Dole *et al.*, 2002). In brief, strain S3974 was transformed with pFDY217. Transformants were selected on LB tetracylin plates at 28°C. Single colonies were re-streaked on LB tetracylcin plates and grown at 42°C to select for cointegrates (first recombination event). From these plates LB cultures were inoculated and grown overnight at 28°C (second recombination event). Of the overnight cultures several dilutions were plated on MacConkey plates supplemented with 2 % of lactose, incubated at 37°C overnight and screened for Lac-negative colonies. Lac-negative clones were re-streaked on LB plates and incubated at 37°C overnight. Clones were anlyzed by PCR using primer pair S116/S165 to confirm Δ*lacZ* and tested for tetracyclin sensitivity.

4.2.6 Chromosomal integration of promoter *lacZ* fusions

Promoter *lacZ* fusions were integrated into the chromosomal λ attachment site *attB* of derivatives of Δ*lacZ* mutant strain S4197 as described (Diederich *et al.*, 1992)(Dole *et al.*, 2002). In brief, plasmids carrying the *attP* site, the promoter-*lacZ* fusions, and the spectinomycin resistance cassette were digested with enzyme *Bam*HI. The originless fragments were gel-purified and eluted. 10 ng of the originless fragment was self-ligated and half of the ligation mixture was used to transform the strain of interest. The target strain was first transformed with integrase-expressing temperature-sensitive plasmid pLDR8, transformants were selected at 28°C. Overnight cultures of transformants were diluted twenty-fold and grown at 37°C for 90 minutes to induce the expression of integrase and to arrest the replication of pLDR8. These cells were transformed with the self-ligated origin-less fragments carrying the promoter *lacZ* fusions and the spectinomycin resistance gene. Integrase promotes recombination between the λ *attB* site in chromosome and *attP* sites resulting in integration of the circularized DNA fragment into the chromosome. The transformants were selected at 42°C on LB spectinomycin plates to select for the cells carrying the promoter-*lacZ* DNA fragment integrated into attB site. In addition, the replication of pLDR8 is blocked at 42°C. The colonies were analyzed for kanamycin sensitivity (loss of pLDR8), and the correct integration was verified by PCR analysis using primer pairs S93/S164, S95/S96, S95/S164, and T334/S118. Two independent integrants were stored in the strain collection and used in expression analyses.

4.2.7 Transduction

The technique is based on generalized transduction, which makes use of the bacteriophage T4GT7 to transfer DNA between bacteria (Wilson *et al.*, 1979). For production of a bacteriophage lysate, 150 µl of an overnight culture of the donor strain was infected with serial dilutions of wt lysate of T4GT7 and incubated for 15 minutes at room temperature. 1 ml of LB was added and the mixture was transferred to a culture tube containing 3 ml of T4 top agar at 44°C. The warm top agar mix was plated on fresh LB plates and incubated overnight at 37°C. Plates that showed an almost confluent lysis were used for extraction of the phage by chloroform extraction. For transduction of the allele of interest, 100 µl of an overnight culture of the recipient strain were incubated with a range of 0.1 to 10 µl of T4*GT7* lysate prepared from the donor strain. The incubation was carried out for 15 minutes at

room temperature and 100 µl were plated on respective selection plates. The tranductants were restreaked at least four to five times to get rid of the contaminating phages. The transfer of the alleles was verified by PCR.

4.2.8 Gene deletion by λ-Red mediated recombination

Deletion of chromosomal genes was performed according to (Datsenko & Wanner, 2000). This system is based on the λ-Red mediated recombination between linear DNA fragment and the chromosomal locus. The basic strategy is to replace the chromosomal sequence with a selectable antibiotic resistance gene that is generated by PCR and by using primers with 30 to 50 nt homology extensions of the gene to be deleted. Briefly, the cells were transformed with the temperature sensitive plasmid (pKD46) which encodes the λ-Red system under the control of an arabinose-inducible promoter. The PCR product for deletion of a target gene was generated using primers carrying homology to the target chromosomal region and to antibiotic resistance cassettes of plasmids pKD3 and pKD4. This PCR generates a fragment carrying the chloramphenicol or kanamycin resistance genes, flanked by a 40 to 50 bp homology to upstream and downstream sequences of the target gene. In addition, the resistance genes are flanked by FRT sites (Flp recombinase target sites) that allow the deletion of the resistance gene by the Flp recombinase after gene replacement. Gel-purified PCR products (> 100 ng/µl in H_2O) were used for electroporation of cells harboring helper plasmid pKD46 expressing λ-Red recombinase. Electrocompetent cells were prepared from cultures grown at 28°C in LB supplemented with 10 mM L-arabinose for induction of λ-Red recombinase. The recombinants were selected at 37°C on LB plates supplemented with kanamycin or chloramphenicol. The loss of pKD46 was confirmed by sensitivity to ampicillin and the deletion of the target gene was confirmed by PCR using primers flanking the deleted region. Resistance cassettes flanked by FRT sites were excised by transforming the respective strain with helper plasmid pCP20 encoding the Flp recombinase gene and selection on LB supplemented with ampicillin at 28°C. By re-streaking transformants on LB plates and shifting the temperature to 42°C, expression of Flp recombinase was induced, pCP20 was lost and resistance cassettes were excised leaving one FRT site. Loss of antibiotic resistance was confirmed by antibiotic sensitivity of the clones and by PCR.

4.2.9 β-galactosidase assay

β-galactosidase assays were performed as described (Miller, 1992). Briefly, cultures were grown overnight in LB medium with antibiotics. Then, 8 ml-cultures were inoculated to an optical density at 600 nm (OD_{600}) of 0.05 to 0.1 and grown to an OD_{600} of approximately 0.5. IPTG (isopropyl-β-D-thiogalactopyranoside) was added, where indicated, to a final concentration of 1 mM to the overnight and the exponential cultures for induction. The bacteria were harvested, and β-galactosidase activities were determined. The assays were performed in Z-buffer of at least three independent cultures and activity was determined with the following formula: 1 unit = $[OD_{420}$ x dilution factor x 1000]/$[OD_{600}$ x time (minutes)]. Standard deviations were less than 15 %. Z-buffer: 60 mM Na_2HPO_4, 40 mM NaH_2PO_4, 10 mM KCl, 1 mM $MgSO_4$, 100 µg/ml chloramphenicol. ONPG solution: 4 mg/ml in 60 mM Na_2HPO_4, 40 mM NaH_2PO_4.

4.2.10 Genomic library screen

For cloning of an *E. coli* whole genomic library, genomic DNA was isolated from strain BW30270 using the PrestoSpin D Bug kit (Molzym) according to the manufacturer's instructions. In brief, 2 ml of an overnight cultures were processed, and quality and concentration of genomic DNA was determined by agarose gel electrophoresis and UV measurement. For cloning, vector pKESK22 was restricted with *Bam*HI and dephosphorylated. Genomic DNA was partially restricted using *Sau*3AI (New England Biolabs). Partial restriction was monitored by agarose gel electrophoresis and one assay that delivered mainly fragments between 1.5 and 5 kb in size was used for elution of the DNA 'smear' from an agarose gel followed by an additional purification step. Concentration of partially restricted genomic DNA was determined by UV measurement in a NanoDrop spectrophotometer (ThermoFisher Scientific, Waltham, MA, USA) and used for cloning into pKESK22. Ligations were purified using MSB Spin PCRapace (Invitek) columns and eluted in water. Purified ligations were transformed into electrocompetent cells of cloning strain XL1-Blue by electroporation. After electroporation, SOC cultures were used to inoculate 400 ml LB overnight cultures supplemented with kanamycin. These cultures were used for preparation of plasmid DNA (Promega WizardPlus MaxiPrep) und plasmid DNA was stored as pKETS11. Insertion of genomic DNA fragments of varying sizes was verified by re-transforming pKETS11 into XL1-Blue and PCR analysis of several clones. For screening for

trans-activating factors, strains carrying suitable promoter-*lacZ* reporter fusions were transformed with pKETS11. 100 µl of CaCl$_2$-competent cells were transformed with 5 µl of pKETS11 (235 ng/µl) in 45 µl of TEN. To select for transformants and to screen for Lac-positive clones, complete transformation assays were plated on LB plates (100 µl each) supplemented with kanamycin, X-gal and 0.2 mM IPTG. Lac-positive transformants were restreaked, analyzed by PCR and sequenced. The obtained sequences were used for a BLAST analysis to identify the inserted fragment of genomic DNA of the respective clone.

4.2.11 Transposon mutagenesis

Transposon-mutagenesis screens were performed by using pKESK18 carrying a miniTn10-*cat* transposon (Madhusudan *et al.*, 2005). In this plasmid, replication is temperature-sensitive and, also, expression of the transposase is repressed at 28 °C and induced at 42 °C. Thus, at 28 °C, the plasmid replicates, while the transposase is not expressed. Upon a temperature shift, expression of the transposase gene and transposition are induced, while replication of the plasmid stops, allowing the selection of transposon mutants on chloramphenicol plates at 42°C. With this system, transposition takes place in approximately 1 to 5 % of the cells and the mutants characterized carried single miniTn10-cat transposon insertions. Strains carrying the respective promoter *lacZ* reporter fusions were transformed with pKESK18. Transformants were grown at 28 °C in LB medium containing kanamycin and chloramphenicol. To select for transposon mutants and to screen for Lac phenotype mutants, 100 µl of 10^{-3} and 10^{-4} dilutions were plated on pre-warmed (42°C) M9 chloramphenicol plates containing 1 % glucose, X-gal and 0.2 mM IPTG or pre-warmed LB chloramphenicol X-gal IPTG plates. Plates were incubated at 42°C and Lac-positive mutants were restreaked. Of mutants with a clear Lac-positive phenotype, the insertion position of the miniTn10 transposon was determined by a semi-random, two-step PCR protocol as described by (Chun *et al.*, 1997). Briefly, in a first, semispecific PCR, random primer T333 and a miniTn10-specific primer S357, or primer S358, were used. The amplification products of this first PCR were reamplified in a second PCR using primer S361 that matches random primer T333 and the miniTn10-specific primer S359. The PCR products were gel-purified and sequenced. The obtained sequences were used for a BLAST analysis to map the chromosomal transposon insertion sites.

4.2.12 RNA isolation

For isolation of total RNA, exponential cultures were inoculated from fresh overnight cultures to an OD_{600} of 0.1 in LB (with antibiotics for transformants). In case of induction, IPTG was added to a final concentration of 1 mM after 30 min of growth. After an additional 60 min, the bacteria were harvested using RNAprotect and used for RNA isolation using the RNeasy MiniKit system (Qiagen). In brief, 1 ml of each culture (OD_{600} between 0.5 and 0.6) was used and processed according to the manufacturer's instructions including an on-column DNaseI treatment. RNA quality was assayed by denaturing urea PAGE and by measuring the ratio of absorption at 260/280 nm. RNA concentration was determined by measuring UV light absorption at 260 nm. RNA was stored in H_2O at -80°C until further use.

4.2.13 Urea PAGE

Denaturating urea-polyacrylamide gel electrophoresis (urea PAGE) was used to analyze the quality of RNA preparations that were further used for 5' RACE analysis, for microarray analysis, or for RT-qPCR. 0.5 µg of an RNA sample was mixed with 2 x RNA Loading Dye (Fermentas), heat-denatured at 70°C for 10 min and cooled on ice. Samples were separated together with Riboruler High Range RNA ladder (Fermentas) on a denaturing urea-polyacrylamide gel (5 % polyacrylamide from 19:1 acrylamide:bisacrylamide 40 % stock solution, 7 M Urea, 0.5 x TBE) with 0.5 x TBE buffer at 200 V for 1.5-2.5 hours. Gel was stained in 0.5 x TBE with ethidium bromide for 30 min. The presence of intact 2904 nt (23S rRNA) and 1542 nt (16S rRNA) RNA bands without degradation products was interpreted as an indication of a good quality of RNA preparation (Sambrook and Russell, 2001).

10 x TBE stock solution (for 100 ml): 10.8 g Tris base, 5.5 g boric acid, 4 ml of 0.5 M EDTA pH 8.0.

4.2.14 cDNA synthesis

RNA was isolated as described above. For first strand cDNA synthesis, 1 µg of RNA was reverse transcribed using the SuperScript III First Strand Synthesis Kit (Invitrogen) according to the manufacturer's instructions and random hexameric oligonucleotides as primers. In brief, RNA was mixed with primers and dNTPs, denatured by heating to 65°C and then kept

on ice. For the RT reaction, 200 U of SuperScript III reverse transcriptase and 40 U of RNaseOUT were used. The final reaction volume was 20 µl. Samples were first incubated at 25°C for 10 min, then at 50°C for 60 min, then at 85°C for 5 min and put on ice. 1 µl of RNase H (Fermentas) was added and samples were incubated for 20 min at 37°C. cDNA was stored at -20°C.

4.2.15 Microarray analysis

To determine putative target genes of BglJ and LeuO, Δ*yjjPQ-bglJ* strain T75, Δ*yjjPQ-bglJ* Δ*rcsB* strain T175 and Δ*yjjPQ-bglJ* Δ*leuO strain* T177 (Table 3) were transformed with either pKETS1 (BglJ) or pKESK22 (control, Table 4). Strain T75 was additionally transformed with plasmid pKEDR13 (LeuO). From fresh overnight cultures, cultures were inoculated in 15 ml LB supplemented with kanamycin to an OD_{600} of 0.1 and grown to an OD_{600} of approximately 0.15. At this point IPTG was added to the medium to a final concentration of 1 mM. After 60 min, cells were harvested for RNA isolation. RNA isolation was performed as described above. Hybridization to Affymetrix GeneChip®*E. coli* Genome 2.0 microarrays was carried out by the Cologne Center for Genomics, University of Cologne, according to the manufacturer's instructions. Microarrays were scanned using an Affymetrix GeneChip Scanner 3000 7G. Data were processed using Affymetrix apt-probeset-summarize software version 1.10 and RMA algorithm. Samples were normalized using the standard normalization probes present on the Affymetrix GeneChip. Differential expression values were calculated as fold change. Microarray data were submitted to the NCBI Gene Expression Omnibus Website (http://www.ncbi.nlm.nih.gov/geo/) under accession number GSE34023.

4.2.16 RT-qPCR analysis

Quantitative PCR measurements were carried out using gene specific oligonucleotide primers, SYBR Green I and an iQ5 real-time PCR cycler (Bio-Rad), or a C1000 touch thermal cycler with optical reaction module CFX96 (Bio-Rad). RNA isolation and cDNA synthesis were carried out as described above. cDNA derived from 1 µg of total RNA was diluted 1:10 in DEPC-treated water. For one assay, 4 µl of dNTPs (1 mM each), 4 µl of 5 x GoTaq buffer (Promega), 6.8 µl of DEPC-treated water, 0.8 µl of DMSO 0.2 µl of SYBR green (1:1000 in

DMSO), 0.2 µl of GoTaq DNA Polymerase (Promega), and 1 µl of each primer (10 pmol/µl) were used. 2 µl of diluted cDNA served as template. Assays were pipetted on 96 well PCR plates and sealed with optical quality adhesive film (Bio-Rad). The thermal cycler program was 94°C for 3 min, 40 x (94°C for 10 s; 58°C for 30 s; 72°C for 30 s), 72°C for 10 min. A melting curve analysis was carried out starting from 95°C leading to 50°C in steps of 0.5°C. Samples were prepared in triplicate, a pool of cDNA samples of different dilutions served as calibration line for efficiency correction, and the rpoD gene served as reference for data normalization. Data were analyzed using the iQ5 Opitcal System Software 2.0 (Bio-Rad) or CFX Manager Software 2.1 (Bio-Rad), applying an efficiency-corrected, normalized expression ($\Delta\Delta C_t$) algorithm.

4.2.17 5' RACE (rapid amplification of cDNA ends)

5'RACE analysis was performed as described (Wagner & Vogel, 2005) for *in vivo* mapping of transcription start sites. RNA was isolated as described above. For treatment with tobacco acid pyrophosphatase (TAP, Epicentre Biotechnologies), 12 µg of RNA were brought to a volume of 87.5 µl in water. 10 µl of 10 x TAP buffer and 0.5 µl (10 U) of RNase inhibitor SUPERaseIn (Ambion) were added. Then, assays were split in half (treated sample and control, 49 µl each) and 1 µl (10 U) of TAP was added to the treated sample. All samples were incubated at 37°C for 30 min. After incubation 5 µl of RNA adapter oligonucleotide T268 (100 pmol/µl) and 100 µl of water were added. Enzyme and buffer were removed by phenol-chloroform-isoamyl alcohol (25:24:1) extraction followed by ethanol precipitation of RNA. For ligation of RNA adapter oligonucleotide, RNA was dissolved in 14 µl water, heated to 90°C for 5 min and placed on ice for 5 min. 2 µl of 10 x RNA ligation buffer and 2 µl of DMSO were added. Then 1.8 µl of RNA ligase pre-mixed with 0.2 µl of RNase inhibitor SuperaseIn (Ambion) were added and samples were incubated at 17°C over-night. After incubation, 4 µl of random hexameric DNA oligonucleotides (50 ng/µl) and 130 µl of water were added for reverse transcription, final volume 150 µl. Enzyme and buffer were removed by phenol-chloroform-isoamyl alcohol extraction followed by ethanol precipitation. RNA pellets were dissolved in 20 µl of water. 10 µl of RNA solution were used for first-strand cDNA synthesis as described above. For PCR amplification, PlatinumTaq Polymerase (Invitrogen) was used according to the manufacturer's instructions. Either 1 µl of cDNA or

untreated RNA (control), respectively, were used as templates in assays of 25 µl including RNA adapter specific DNA primer T265 and a gene-specific DNA primer as indicated in the results section. PCR products were analyzed on 2 % agarose gels, isolated and cloned into pUC12. At least 4 clones were sequenced for mapping of the primary transcription start sites.

4.2.18 Purification of LeuO$_{His6}$

Purification of C-terminally histidine-tagged LeuO$_{His6}$ was performed as described (Stratmann *et al.*, 2008). In brief, one liter LB cultures supplemented with ampicillin were inoculated to an OD$_{600}$ of 0.1 using a fresh overnight culture of strain S541 harboring plasmid pKEAP21. The cultures were grown to OD$_{600}$ of 0.3, when IPTG was added to a final concentration of 1 mM. Then the cultures were grown for an additional 1 h, and harvested on ice having reached an OD$_{600}$ of 0.8. The cells were spun down and washed twice with Mg-Saline (10 mM MgSO$_4$, 0,85 % NaCl), and the pellets were stored in aliquots at -80°C. For lysate preparation the pellets derived from 5 liter of culture were resuspended in 16 ml lysis buffer (20 mM Tris-HCl pH 7,5 at 4°C, 100 mM KCl, 1 mM DTT, 1 mM PMSF, 5 % glycerol, 50 mM imidazole), the cells were lysed by sonication. The lysates were cleared by high-speed centrifugation and by filtration through a 0.2 µm filter unit. Then 10 ml of the lysate were loaded onto a 1 ml HisTrap HP (GE Healthcare) column equilibrated with the same buffer using an ÄKTA-FPLC system (GE Healthcare). The column was washed with the same buffer containing 100 mM imidazole. LeuO$_{His6}$ was eluted by increasing the imidazole concentration stepwise to 200 mM and 500 mM. A fraction of the eluate with 500 mM imidazole contained the highest LeuO$_{His6}$ concentration of 120 µg/ml (or 3.4 µM) LeuO$_{His6}$ (~37 kDa), and was stored in aliquots at -80°C.

4.2.19 DNase I footprint analysis

DNase I footprinting analysis of free DNA and protein DNA complexes was performed in collaboration with the group of Prof. Rolf Wagner, Heinrich Heine University of Düsseldorf, as described (Pul *et al.*, 2007) In brief, the top strand was labeled by EcoRI/PstI digestion of plasmids pKETS13 to pKETS18 (Table 4), and the bottom strand was labeled by HindIII/Ecl136II digestion of the same plasmids. Both strands were separately end-labeled by

Klenow polymerase (Promega) incorporation of [α-^{32}P]dATP. Samples were incubated in the presence of 0.5 mU/μl of RNase-free DNase I (Fermentas) for 30 s at 25°C. 50 nM of RNAP and 1 μM of LeuO$_{His6}$ were used where indicated. Hydrolysis was stopped by addition of 330 mM NaOAc (pH 4.8), 10 mM EDTA and 10 ng/μl of glycogen followed by a phenol extraction. For the sequence assignment G- and A-specific chemical cleavage reactions were performed. Cleavage products were separated on denaturing 8 % polyacrylamide gels next to sequencing reactions as size standard and visualized by autoradiography.

4.2.20 KMnO$_4$ footprint analysis

KMnO$_4$ footprint analysis was performed in collaboration with the group of Prof. Rolf Wagner, Heinrich Heine University of Düsseldorf, as described (Pul *et al.*, 2010) by the group of Prof. Rolf Wagner, Heinrich Heine University of Düsseldorf. In brief, radioactively labeled DNA fragments were obtained as described above for DNase I footprinting. 40 ng of the labeled DNA fragments in a total volume of 40 μl were incubated for 10 min at 30°C, with 50 nM of RNAP and 1 μM of LeuO$_{His6}$, where indicated. 4 μl of 160 mM KMnO$_4$ were added and the samples were incubated for an additional 2 min at 30°C. The reaction was stopped by addition of 4.8 μl of β-mercaptoethanol (14.3 M) and 5.3 μl 500 mM EDTA and the samples were extracted with phenol/chloroform, followed by precipitation with ethanol. The pellets were dissolved with 70 μl of 10 % piperidine and incubated for 30 min at 90°C. After lyophylization the pellets were washed twice with 30 μl H$_2$O and lyophylized again. The pellets were then dissolved in 50 μl H$_2$O and precipitated with ethanol. The cleavage products were separated on 10 % denaturing polyacrylamide gels and visualized by autoradiography.

4.2.21 *In vitro* transcription

Transcription assays were performed as described previously (Schnetz & Wang, 1996) with minor modifications. DNA fragments were amplified by PCR using MG1655 single colonies as templates and oligonucleotides T530 to T533 as primers (Table 5). In brief, *in vitro* transcription was performed at 37°C in transcription buffer (TB; 30 mM Tris-acetate, pH 7.8, 7 mM magnesium acetate, 150 mM potassium glutamate, 1 mM DTT, 100 μg ml^{-1} BSA, 10 % glycerol). DNA (250 ng in 4 μl TB) was mixed with 10 μl TB containing 1 μM LeuO$_{His6}$, where

indicated. Simultaneously, 3 µl TB containing 0.2 U RNA polymerase saturated with σ^{70} (RNAP; Epicentre) were added. After 20 min of incubation to allow binding of RNAP to DNA, run-off transcriptions were started by the addition of 3 µl of a nucleotide/heparin mixture [final concentrations of 200 µM each of ATP, CTP and GTP, 2 µM [^{32}P]UTP (Hartmann Analytic, Germany, 40 Ci mmol^{-1} final activity)]. Samples were incubated for an additional 10 to 15 min and 12 µl of RNA Loading Dye (Fermentas; 95 % formamide, 0.025 % SDS, 0.025 % bromphenol blue, 0.025 % xylene cyanol FF, 0.025 % ethidium bromide, 0.5 mM EDTA) were added to each reaction mixture. Five microliters of each quenched sample were loaded on a 4 % denaturing polyacrylamide gel [4 % acrylamide:bisacrylamide (19:1), 7 M urea, 72 mM Tris-borate, pH 8.3, 1.6 mM EDTA]. A sequencing reaction was set up using the Sequenase^{TM} Version 2.0 DNA Sequencing Kit (usb-Affymetrix) according to the manufacturer's instructions and loaded to the gel as size standard. Gels were dried onto Whatman 3MM paper and exposed to a Fuji imaging plate for visualization of radioactivity with a Typhoon^{TM} scanner (GE Healthcare).

5. Appendix

5.1 Microarray analysis of RcsB-BglJ targets

Table 7: Significantly regulated BglJ targets.
Summary of all significantly BglJ-regulated loci (> 4-fold, p value < 0.05). Positions of probes and genes are given as NC_000913 coordinates, 'dir' describes the orientation of the probe (<-- for lower strand, --> for upper strand). H-NS binding: +, binding sites of H-NS according to (Uyar *et al.*, 2009). RcsB-BglJ and LeuO-dependence: LeuO-regulated, <4-fold in +BglJ Δ*leuO*. co-regulated, >4-fold in +BglJ Δ*leuO* and >4-fold in +LeuO Δ*bglJ*. CsrB is denoted 'RcsB-independent' since it is also downregulated in +BglJ Δ*rcsB*. Loci mentioned in the text are highlighted in grey.

RcsB-BglJ targets

Probe			Locus				Fold change				RcsB-BglJ and LeuO dependence
from	to	dir.	gene	position	function	H-NS binding	+BglJ wt	+BglJ ΔrcsB	+BglJ Δ*leuO*	+LeuO Δ*bglJ*	
77625	78711	[-->]	setA	[77,621 -> 78,799]	broad specificity sugar efflux system		4,11	1,10	4,80	-1,03	
84380	85128	[-->]	*leuO*	[84,368 -> 85,312]	DNA-binding transcriptional activator	+	44,96	1,12	-1,21	n.a.	
156827	156365	<--	yadN	[156,299 <- 156,883]	predicted fimbrial-like adhesin protein	+	5,95	-1,15	2,64	13,56	LeuO-regulated
177604	177016	<--	yadS	[177,001 <- 177,624]	conserved inner membrane protein		6,02	-1,11	5,23	1,40	
211878	212259	[-->]	yaeR	[211,877 -> 212,266]	predicted lyase		3,11	1,16	5,63	-1,77	
408055	408103	[-->]	ykiA	[407,833 -> 408,174]	putative uncharacterized protein	+	10,19	1,18	13,23	-1,80	
432031	431559	<--	yajI	[431,536 <- 432,075]	predicted lipoprotein		3,57	1,03	4,74	-1,44	
555588	555320	<--	ybcI	[555,255 <- 555,776]	conserved inner membrane protein		4,60	-1,08	2,91	1,28	

RcsB-BglJ targets

Probe			Locus			H-NS binding	Fold change				RcsB-BglJ and LeuO dependence
from	to	dir.	gene	position	function		+BglJ wt	+BglJ ΔrcsB	+BglJ ΔleuO	+LeuO ΔbglJ	
			RhsC locus			+					
729788	731110	[-->]	rhsC	[728,806 -> 732,999]	Rhs family protein	+	11,45	1,08	13,49	1,10	
733015	733311	[-->]	ybfB	[732,999 -> 733,325]	predicted inner membrane protein	+	22,80	-1,09	37,72	1,24	
734401	734820	[-->]	ybfO	[733,443 -> 734,876]	predicted protein	+	9,61	1,04	10,23	-1,02	
734933	735366	[-->]	ybfC	[734,873 -> 735,442]	predicted protein	+	11,33	-1,10	16,02	-1,23	
735447	736153	[-->]	ybfQ	[735,668 -> 735,922]	putative transposase	+	30,35	-1,04	30,32	1,26	
737556	737674	[-->]	ybfD	[737,315 -> 738,076]	putative DNA ligase	+	15,66	-1,09	12,85	1,03	
980510	982071	[-->]	ycbB	[980,270 -> 982,117]	murein L,D-transpeptidase		3,02	1,27	4,14	-2,00	
997117	997516	[-->]	elfA (ycbQ)	[997,091 -> 997,630]	fimbrial-like adhesin protein	+	7,18	-1,04	1,16	58,03	LeuO-regulated
1341616	1341363	<--	osmB	[1,341,134 <- 1,341,352]	lipoprotein (osmotically inducible)	+	4,16	-1,15	3,77	1,51	
1475646	1476213	[-->]	ynbA	[1,475,645 -> 1,476,250]	predicted diacylglycerol choline phospho-transferase	+	11,34	-1,08	18,15	-1,15	
1476287	1477111	[-->]	ynbB	[1,476,250 -> 1,477,146]	predicted CDP-diglyceride synthase	+	5,92	-1,27	6,07	1,21	
			RhsE locus								LeuO-regulated
1525733	1525588	<--		[1,525,914 -> 1,527,962]	yncH/rhsE intergenic	+	5,17	-1,07	1,31	5,96	
1528097	1528050	<--	ydcD	[1,527,946 -> 1,528,428]	predicted protein	+	4,05	-1,27	1,43	2,77	
1528710	1529343	[-->]	yncI	[1,528,610 -> 1,529,356]	predicted protein	+	4,98	-1,12	2,22	3,46	
1529408	1529591	[-->]	yncM	[1,529,400 -> 1,529,600]	predicted protein	+	8,55	-1,07	3,28	5,60	
1842730	1841899	<--	ynjI	[1,841,855 <- 1,842,895]	predicted inner membrane protein		12,32	-1,13	10,57	1,10	
1863601	1862823	<--	yeaE	[1,862,806 <- 1,863,660]	methylglyoxal reductase		4,97	1,13	7,90	-1,50	
1960017	1960481	[-->]	yecT	[1,959,996 -> 1,960,484]	predicted protein	+	10,96	-1,10	10,52	-1,12	

RcsB-BglJ targets

Probe			Locus				H-NS binding	Fold change				RcsB-BglJ and LeuO dependence
from	to	dir.	gene	position	function			+BglJ wt	+BglJ ΔrcsB	+BglJ Δ*leuO*	+LeuO Δ*bglJ*	
2150257	2149741	<--	yegK	[2,149,735 <- 2,150,496]	predicted protein		+	5,02	-1,13	5,67	1,19	
2151143	2150501	<--	yegL	[2,150,493 <- 2,151,152]	conserved protein		+	18,74	1,02	17,62	1,52	
2406921	2407480	[-->]	yfbR	[2,406,884 -> 2,407,483]	deoxyribonucleoside 5'-monophosphatase		+	4,21	1,19	5,49	-1,39	
2463216	2463056	<--	mlaA	[2,462,274 <- 2,463,029]	putative lipoprotein		+	4,09	1,05	3,90	-1,15	
2463423	2464086	[-->]	yfdC	[2,463,323 -> 2,464,255]	predicted inner membrane protein		+	3,20	-1,03	5,31	-1,32	
2662579	2663207	[-->]	yfhR	[2,662,385 -> 2,663,266]	predicted peptidase			4,65	-1,04	3,19	1,25	
2882149	2880661	<--	casA	[2,880,652 <- 2,882,160]	CRISPR-associated		+	4,59	1,10	-1,25	65,38	LeuO-regulated
2922535	2922197	<--	csrB	[2,922,178 <- 2,922,546]	ncRNA			-4,25	-2,99	-3,33	-1,02	RcsB-independent
3097426	3096597	<--	yggM	[3,096,580 <- 3,097,587]	conserved protein			5,81	1,09	6,59	1,60	
3155682	3155948	[-->]	yqhG	[3,155,672 -> 3,156,598]	conserved protein			21,91	1,00	22,88	-1,52	
3156650	3156904	[-->]	yqhH	[3,156,649 -> 3,156,906]	predicted outer membrane lipoprotein			6,63	1,05	7,24	-1,03	
3170144	3169928	<--	ygiZ	[3,169,901 <- 3,170,233]	conserved inner membrane protein		+	19,44	-1,11	25,40	1,06	
3332939	3333203	[-->]	sfsB	[3,332,931 -> 3,333,209]	DNA-binding transcriptional activator of maltose metabolism			7,78	-1,05	8,49	1,11	
3467573	3465855	<--	chiA	[3,465,182 <- 3,467,875]	periplasmic endochitinase		+	18,22	-1,08	9,93	26,77	co-regulated
			<u>RhsB locus</u>									
3620956	3621440	[-->]	rhsB	[3,617,215 -> 3,621,450]	rhsB element core protein RshB			16,74	-1,02	33,30	-1,02	
3621493	3621799	[-->]	yhhH	[3,621,422 -> 3,621,805]	predicted protein			13,63	1,09	33,17	-1,09	
3622256	3621918	<--	yrhC	[3,621,910 -> 3,622,155]	pseudogene			9,60	-1,08	9,41	1,07	

RcsB-BglJ targets

Probe			Locus				H-NS binding	Fold change				RcsB-BglJ and LeuO dependence
from	to	dir.	gene	position	function			+BglJ wt	+BglJ ΔrcsB	+BglJ ΔleuO	+LeuO ΔbglJ	
3709926	3709041	<--	yhjX	[3,708,822 <- 3,710,030]	putative resistance protein			-4,35	1,45	-1,93	-7,29	LeuO-regulated
3725383	3724947	<--	yiaA	[3,724,947 <- 3,725,384]	conserved inner membrane protein		+	15,55	1,12	9,04	1,46	
3725782	3725435	<--	yiaB	[3,725,430 <- 3,725,771]	conserved inner membrane protein		+	58,10	1,02	36,35	3,04	
			RhsA locus				+					
3764533	3765190	[-->]	yibA	[3,764,360 -> 3,765,202]	lyase containing HEAT-repeat		+	7,87	-1,15	13,56	1,06	
3765665	3765938	[-->]	yibJ	[3,765,244 -> 3,765,945]	rhsA core protein with extension		+	16,29	1,02	26,46	1,18	
3766245	3766658	[-->]	yibG	[3,766,200 -> 3,766,661]	conserved protein		+	28,61	-1,29	52,68	-1,03	
3767384	3767668	[-->]	yibV	[3,767,368 -> 3,767,703]	hypothetical protein		+	26,30	-1,35	33,29	1,07	
3854456	3854841	[-->]	yidI	[3,854,438 -> 3,854,887]	predicted inner membrane protein			5,13	1,02	5,37	-1,23	
3858287	3859080	[-->]	yidL	[3,858,276 -> 3,859,199]	putative ARAC-type regulatory protein		+	6,61	1,09	13,26	-1,48	
			bgl operon				+					
3901606	3900446	<--	bglB	[3,900,312 <- 3,901,724]	phospho- β -glucosidase B		+	7,84	1,05	7,66	1,24	
3903261	3901754	<--	bglF	[3,901,743 <- 3,903,620]	β -glucoside-specific PTS permease		+	4,13	1,08	4,60	1,52	
3904536	3903765	<--	bglG	[3,903,754 <- 3,904,590]	transcriptional antiterminator		+	28,65	-1,08	29,15	5,11	co-regulated
4000753	4000469	<--	yigF	[4,000,442 <- 4,000,822]	uncharacterized protein		+	9,40	-1,15	13,06	1,94	
4001251	4000848	<--	yigG	[4,000,836 <- 4,001,216]	inner membrane protein		+	25,75	-1,28	28,10	2,37	
4042286	4043639	[-->]	yihF	[4,042,222 -> 4,043,652]	putative protein		+	8,34	-1,08	6,58	2,49	
4162418	4162709	[-->]	btuB	[4,161,662 -> 4,163,506]	vitamin B12/cobalamin outer membrane transporter			6,76	1,08	5,16	1,29	
4375614	4375267	<--	blc	[4,375,212 <- 4,375,745]	outer membrane lipoprotein			3,30	-1,01	6,64	-3,80	co-regulated ?

5.2 Microarray analysis of LeuO targets

Table 8: Significantly regulated LeuO targets.
Summary of all significantly LeuO-regulated genes (> 4-fold, p value < 0.05). Positions of probes and genes are given as NC_000913 coordinates, 'dir' describes the orientation of the probe (<-- for lower strand, --> for upper strand). LeuO-bound: +, binding of LeuO according to (Shimada *et al.*, 2011) to the regulatory region of the respective transcription unit. Genes mentioned in the text are highlighted in grey.

LeuO targets							
Probe			Locus				
from	to	dir.	gene	gene position	function	Fold change	LeuO-bound
up-regulated							
11762	11391	<--	yaaI	[11,382 <- 11,786]	predicted protein	7,76	+
156126	155462	<--	ecpD	[155,461 <- 156,201]	predicted periplasmic pilin chaperone	4,91	
156827	156365	<--	yadN	[156,299 <- 156,883]	predicted fimbrial-like adhesin protein	13,56	+
237017	237333	[-->]	yafT	[237,335 -> 238,120]	---	7,83	
237975	238116	[-->]	yafT	[237,335 -> 238,120]	predicted aminopeptidase	5,79	
383154	382602	<--	yaiP	[381,963 <- 383,159]	predicted glucosyltransferase	86,87	
383687	383303	<--	yaiS	[383,283 <- 383,840]	conserved protein	110,86	+
490716	491149	[-->]	apt	[490,636 -> 491,187]	adenine phosphoribosyltransferase	4,13	
522076	522480	[-->]	rhsD	[522,485 -> 526,765]	Rhs element	9,39	+
522466	522062	<--	rhsD	[522,485 -> 526,765]	Rhs element	13,97	+
617571	618485	[-->]	fepE	[617,477 -> 618,610]	ferric enterobactin transport	28,74	+
634585	634153	<--	ybdM	[633,970 <- 634,599]	conserved protein	5,23	+
635757	634749	<--	ybdN	[635,939 <- 636,841]	conserved protein	19,44	+
636741	636098	<--	ybdO	[634,572 <- 635,792]	predicted LysR-type transcriptional regulator	22,97	+
650006	649838	<--	citD	[649,710 <- 650,006]	citrate lyase, acyl carrier (gamma) subunit	5,27	+
651180	651393	[-->]	dpiA	[651,458 -> 653,116]	membrane associated sensor kinase	6,23	+
675774	675647	<--	ybeQ	[674,793 <- 675,770]	conserved protein	43,01	+
676242	676618	[-->]	ybeR	[675,934 -> 676,641]	predicted protein	20,14	+
678573	678083	<--	ybeT	[678,075 <- 678,629]	conserved outer membrane protein	22,64	+
678769	679367	[-->]	ybeU	[678,731 -> 679,438]	predicted tRNA ligase	7,59	+
799775	798869	<--	ybhD	[798,845 <- 799,861]	predicted DNA-binding transcriptional regulator	6,20	+
877163	876038	<--	rimO	[875,933 <- 877,258]	predicted SAM-dependent methyltransferase	5,14	
959468	959703	[-->]	ycaL	[959,487 -> 960,251]	putative heat shock protein	17,96	+
997117	997516	[-->]	elfA	[997,091 -> 997,630]	fimbrial-like adhesin protein	58,03	
997864	998408	[-->]	elfD	[997,713 -> 998,414]	putative chaperone	33,17	
998465	999014	[-->]	elfC	[998,439 -> 1,001,039]	predicted outer membrane usher protein	18,12	
1002468	1002606	[-->]	ycbU	[1,002,112 -> 1,002,654]	predicted fimbrial-like adhesin protein	4,12	
1004062	1004098	[-->]	pyrD	[1,003,991 -> 1,005,001]	dihydro-orotate oxidase, FMN-linked	4,76	
1183566	1182877	<--	potB	[1,182,840 <- 1,183,667]	spermidine/putrescine ABC transporter	4,02	
1259967	1258477	<--	ychM	[1,258,347 <- 1,260,026]	putative sulfate transporter YchM	4,62	
1324667	1324875	[-->]	rluB	[1,324,876 -> 1,325,751]	23S rRNA pseudouridylate synthase B	4,84	
1378368	1378807	[-->]	ycjU	[1,378,172 -> 1,378,831]	predicted β-phosphoglucomutase	4,08	+
1378890	1379801	[-->]	ycjV	[1,378,845 -> 1,379,813]	putative ATP-binding component of transporter	5,57	+
1380046	1380817	[-->]	ompG	[1,379,971 -> 1,380,876]	outer membrane porin OmpG	4,39	
1434871	1434568	<--	ompN	[1,433,784 <- 1,434,917]	Outer membrane protein N precursor	73,00	+
1435147	1435245	[-->]	micC	[1,435,145 -> 1,435,253]	ncRNA	199,08	+
1463527	1465888	[-->]	ydbA	[1,463,416 -> 1,465,974]	predicted outer membrane protein (pseudogene)	14,51	+
1525212	1525906	[-->]	"---"	[1,525,914 -> 1,527,962]	RhsE cluster	17,41	+
1525733	1525588	<--	rhsE	[1,525,914 -> 1,527,962]	RhsE protein	5,96	+
1529408	1529591	[-->]	yncI	[1,528,610 -> 1,529,356]	hypothetical protein	5,60	+
1651877	1651135	<--	rspB	[1,650,920 <- 1,651,939]	predicted oxidoreductase	4,93	
1652955	1651964	<--	rspA	[1,651,951 <- 1,653,165]	starvation sensing protein rspA	6,28	
1677585	1678947	[-->]	ydgI	[1,677,581 -> 1,678,963]	putative arginine/ornithine antiporter	5,79	
1944176	1944850	[-->]	yebB	[1,944,275 -> 1,944,877]	predicted protein	4,26	+
1956172	1956542	[-->]	"---"		torY/cutC intergenic	5,11	+
1993842	1994063	[-->]	yecF	[1,993,842 -> 1,994,066]	predicted protein	4,52	+

LeuO targets

Probe			Locus			Fold change	LeuO-bound
from	to	dir.	gene	gene position	function		
2031474	2031280	<--	yedR	[2,031,143 <- 2,031,508]	predicted inner membrane protein	5,55	
2032010	2031555	<--	"---"		yedR/yedS intergenic	6,05	
2032572	2032779	[-->]	yedS	[2,032,075 -> 2,032,560]	putative outer membrane protein (pseudogene)	194,91	+
2084969	2083807	<--	plaP	[2,083,728 <- 2,085,086]	low-affinity putrescine importer	7,36	
2085270	2085093	<--	"---"		plaP/yeeY intergenic	9,84	
2148986	2147255	<--	yegI	[2,147,063 <- 2,149,009]	conserved protein	26,20	+
2149250	2149647	[-->]	yegJ	[2,149,209 -> 2,149,670]	predicted protein	17,95	+
2163762	2164970	[-->]	yegQ	[2,163,692 -> 2,165,053]	predicted peptidase	4,58	
2186401	2185690	<--	yehA	[2,185,402 <- 2,186,436]	predicted fimbrial-like adhesin protein	4,01	
2188796	2187091	<--	yehB	[2,186,452 <- 2,188,932]	putative outer membrane usher protein	4,22	
2189591	2188981	<--	yehC	[2,188,948 <- 2,189,667]	putative fimbrial chaperone	49,58	
2190177	2189765	<--	yehD	[2,189,702 <- 2,190,244]	predicted fimbrial-like adhesin protein	91,68	+
2202694	2203645	[-->]	yehL	[2,202,618 -> 2,203,706]	predicted ATP-binding component of transporter	6,39	
2203775	2205180	[-->]	yehM	[2,203,717 -> 2,205,996]	predicted protein	7,76	
2206597	2206639	[-->]	yehP	[2,205,989 -> 2,207,125]	conserved protein	7,02	
2255274	2254681	<--	yeiM	[2,254,107 <- 2,255,357]	predicted nucleoside transporter	10,79	+
2256354	2255454	<--	pscG	[2,255,451 <- 2,256,389]	predicted pseudouridine 5'-phosphate glycosidase	13,83	+
2257184	2256444	<--	pscK	[2,256,377 <- 2,257,318]	predicted pseudouridine kinase	10,31	+
2383917	2384366	[-->]	yfbL	[2,383,882 -> 2,384,853]	predicted peptidase	6,41	+
2386395	2385752	<--	yfbN	[2,385,732 <- 2,386,448]	predicted protein	14,05	+
2386659	2387073	[-->]	yfbO	[2,386,603 -> 2,387,079]	predicted protein	9,31	
2387214	2387929	[-->]	yfbP	[2,387,135 -> 2,387,986]	predicted protein	7,88	
2453626	2453134	<--	yfcV	[2,453,105 <- 2,453,668]	predicted fimbrial-like adhesin protein	6,24	+
2520741	2520502	<--	xapP	[2,520,751 <- 2,522,007]	predicted xanthosine transporter	4,07	+
2627282	2627186	<--	"---"		yfgG/yfgH intergenic antisense	5,08	+
2627813	2627504	<--	"---"		yfgG/yfgH intergenic antisense	6,09	+
2627826	2628332	[-->]	yfgH	[2,627,814 -> 2,628,332]	predicted outer membrane lipoprotein	33,00	+
2628362	2628827	[-->]	yfgI	[2,628,348 -> 2,628,887]	putative membrane protein	18,66	+
2876877	2876621	<--	cas2	[2,876,591 <- 2,876,875]	predicted endoribonuclease	5,40	+
2877697	2876971	<--	cas1	[2,876,877 <- 2,877,794]	multifunctional nuclease	8,77	+
2878398	2877852	<--	casE	[2,877,810 <- 2,878,409]	CRISPR associated	15,40	+
2879057	2878476	<--	casD	[2,878,396 <- 2,879,070]	CRISPR associated	17,45	+
2880112	2879081	<--	casC	[2,879,073 <- 2,880,164]	CRISPR associated	24,76	+
2880627	2880246	<--	casB	[2,880,177 <- 2,880,659]	CRISPR associated	29,99	+
2882149	2880661	<--	casA	[2,880,652 <- 2,882,160]	CRISPR associated	65,38	+
3131214	3130488	<--	yghR	[3,130,476 <- 3,131,234]	predicted ATP-binding protein	14,70	
3131907	3131289	<--	yghS	[3,131,266 <- 3,131,979]	predicted ATP-binding protein	28,04	
3132191	3132836	[-->]	yghT	[3,132,153 -> 3,132,845]	predicted ATP-binding protein	12,41	+
3133511	3132898	<--	pitB	[3,132,894 <- 3,134,393]	phosphate transporter	31,89	
3134403	3134668	[-->]	"---"		pitB/gss intergenic	8,87	+
3134684	3134404	<--	"---"		pitB/gss intergenic	14,99	+
3157708	3157356	<--	ygiQ	[3,156,949 <- 3,159,168]	conserved protein	4,80	
3183451	3183978	[-->]	ygiL	[3,183,436 -> 3,183,987]	predicted fimbrial-like adhesin protein	57,48	+
3190237	3190833	[-->]	yqiJ	[3,190,230 -> 3,190,859]	putative oxidoreductase	6,38	
3191376	3192314	[-->]	yqiK	[3,190,886 -> 3,192,547]	putative membrane protein	4,88	
3330740	3329817	<--	yhbE	[3,329,792 <- 3,330,757]	conserved inner membrane protein	6,05	
3359299	3359941	[-->]	gltF	[3,359,198 -> 3,359,962]	periplasmic protein	56,13	+
3360181	3360770	[-->]	yhcA	[3,360,134 -> 3,360,808]	predicted periplasmic chaperone protein	100,27	
3361250	3363205	[-->]	yhcD	[3,360,829 -> 3,363,210]	predicted outer membrane protein	6,70	
3408361	3409231	[-->]	dusB	[3,408,302 -> 3,409,267]	tRNA-dihydrouridine synthase B	4,86	
3409296	3409562	[-->]	fis	[3,409,293 -> 3,409,589]	DNA-binding protein Fis	4,29	
3411459	3410894	<--	envR	[3,410,825 <- 3,411,487]	DNA-binding transcriptional regulator EnvR	48,32	+
3411506	3411863	[-->]	"---"		envR/acrE intergenic	6,02	+
3411882	3411514	<--	"---"		envR/acrE intergenic	12,28	+
3411975	3413010	[-->]	acrE	[3,411,886 -> 3,413,043]	cytoplasmic membrane lipoprotein	21,00	+
3414134	3414646	[-->]	acrF	[3,413,055 -> 3,416,159]	multidrug efflux system protein	12,54	+

LeuO targets

Probe			Locus			Fold change	LeuO-bound
from	to	dir.	gene	gene position	function		
3451944	3451559	<--	gspB	[3,451,530 <- 3,451,949]	calcium-binding protein for chromosome replication	4,19	+
3453329	3452021	<--	gspA	[3,451,951 <- 3,453,420]	general secretory pathway component	13,05	+
3453818	3454362	[-->]	gspC	[3,453,600 -> 3,454,415]	general secretion pathway protein C	37,07	+
3455285	3456267	[-->]	gspD	[3,454,399 -> 3,456,351]	general secretory pathway component	22,41	+
3456481	3457724	[-->]	gspE	[3,456,361 -> 3,457,842]	general secretory pathway component	20,70	+
3457901	3458899	[-->]	gspF	[3,457,839 -> 3,459,035]	general secretory pathway component	17,65	+
3459049	3459451	[-->]	gspG	[3,459,045 -> 3,459,482]	general secretory pathway component	11,79	+
3459490	3459945	[-->]	gspH	[3,459,490 -> 3,459,999]	general secretory pathway component	5,51	+
3459992	3460268	[-->]	gspI	[3,459,996 -> 3,460,373]	general secretory pathway component	8,58	+
3460368	3460910	[-->]	gspJ	[3,460,366 -> 3,460,953]	general secretory pathway component	7,03	+
3461029	3461929	[-->]	gspK	[3,460,946 -> 3,461,929]	general secretory pathway component	6,67	+
3467573	3465855	<--	chiA	[3,465,182 <- 3,467,875]	periplasmic endochitinase	26,77	+
3497477	3497615	[-->]	yhfL	[3,497,470 -> 3,497,637]	conserved secreted peptide	14,34	+
3582784	3583066	[-->]	yrhB	[3,582,782 -> 3,583,066]	predicted protein	13,98	+
3744142	3744907	[-->]	yiaO	[3,744,117 -> 3,745,103]	predicted transporter	4,18	
3904536	3903765	<--	bglG	[3,903,754 <- 3,904,590]	transcriptional antiterminator of the bgl operon	5,11	+
4085151	4085661	[-->]	yiiG	[4,085,025 -> 4,086,080]	conserved protein	25,56	+
4276365	4276513	[-->]	yjcD	[4,276,502 -> 4,277,851]	predicted permease	7,48	
4276716	4277848	[-->]	yjcD	[4,276,502 -> 4,277,851]	predicted permease	4,96	
4300712	4300580	<--	sdsQ	[4,299,050 <- 4,301,101]	multidrug efflux pump	8,67	+
4301091	4300949	<--	sdsQ	[4,299,050 <- 4,301,101]	multidrug efflux pump	5,49	+
4301741	4301416	<--	sdsR	[4,301,101 <- 4,302,132]	multidrug resistance protein MdtN	10,13	+
4302423	4302157	<--	ytcA	[4,302,151 <- 4,302,426]	hypothetical protein	13,83	+
4304558	4304077	<--	yjcS	[4,302,635 <- 4,304,620]	predicted alkyl sulfatase	23,00	+
4372250	4371443	<--	yjeJ	[4,371,388 <- 4,372,257]	predicted protein	8,85	+
4408182	4408555	[-->]	yjfI	[4,408,156 -> 4,408,557]	conserved protein	38,69	+
4408608	4409266	[-->]	yjfJ	[4,408,576 -> 4,409,274]	predicted transcriptional regulator effector protein	20,82	+
4409382	4409561	[-->]	yjfK	[4,409,325 -> 4,409,984]	conserved protein	14,42	+
4410319	4410387	[-->]	yjfL	[4,410,002 -> 4,410,400]	conserved inner membrane protein	9,93	+
4410591	4411034	[-->]	yjfM	[4,410,410 -> 4,411,048]	conserved protein	6,94	+
4478021	4478860	[-->]	yjgN	[4,477,753 -> 4,478,949]	conserved inner membrane protein	5,68	+
<u>down-regulated</u>							
345715	345961	[-->]	yahO	[345,708 -> 345,983]	predicted protein	-5,00	
485029	485605	[-->]	acrR	[484,985 -> 485,632]	DNA-binding transcriptional repressor	-4,34	
576047	576002	<--	nmpC	[574,981 <- 576,048]	outer membrane porin	-12,21	+
641087	640712	<--	uspG	[640,662 <- 641,090]	universal stress protein UP12	-51,62	+
644130	643540	<--	rna	[643,420 <- 644,226]	ribonuclease I	-8,91	
849685	850158	[-->]	ompX	[849,673 -> 850,188]	outer membrane protein X	-5,65	
918023	917392	<--	ybjX	[917,351 <- 918,307]	conserved protein	-8,40	
1014965	1015098	[-->]	rmf	[1,014,938 -> 1,015,105]	ribosome modulation factor	-8,31	
1050182	1049767	<--	cspH	[1,050,186 <- 1,050,398]	stress protein, member of the CspA familiy	-7,65	
1084473	1085188	[-->]	phoH	[1,084,215 -> 1,085,279]	ATP binding protein	-13,06	
1306593	1305240	<--	cls	[1,305,209 <- 1,306,669]	cardiolipin synthetase	-5,53	
1308061	1307048	<--	kch	[1,307,040 <- 1,308,293]	voltage-gated potassium channel	-7,84	
1393905	1392942	<--	ynaI	[1,392,915 <- 1,393,946]	conserved inner membrane protein	-8,68	
1575499	1573350	<--	yddB	[1,573,271 <- 1,575,643]	predicted porin protein	-4,36	
1653835	1654165	[-->]	ynfB	[1,653,832 -> 1,654,173]	predicted protein	-6,39	
1654212	1654691	[-->]	speG	[1,654,208 -> 1,654,768]	spermidine N1-acetyltransferase	-6,13	
1696047	1695331	<--	hdhA	[1,695,297 <- 1,696,064]	7-alpha-hydroxysteroid dehydrogenase	-4,26	
1717637	1717899	[-->]	"---"		anmK/slyB intergenic	-5,14	
1717898	1717640	<--	"---"		anmK/slyB intergenic	-4,28	
1717925	1718353	[-->]	slyB	[1,717,900 -> 1,718,367]	outer membrane lipoprotein	-6,75	
1864968	1866812	[-->]	yeaG	[1,864,932 -> 1,866,866]	protein kinase	-4,26	+
1994792	1994134	<--	sdiA	[1,994,134 <- 1,994,856]	DNA-binding transcriptional activator SdiA	-16,76	+
2006307	2007467	[-->]	yedE	[2,006,301 -> 2,007,506]	predicted inner membrane protein	-10,46	

LeuO targets							
Probe			Locus			Fold change	LeuO-bound
from	to	dir.	gene	gene position	function		
2023337	2023268	<--	dsrA	[2,023,251 <- 2,023,337]	ncRNA	-8,37	
2051799	2052899	[-->]	shiA	[2,051,667 -> 2,052,983]	shikimate transporter	-5,25	
2064049	2063940	<--	"---"		cubU/ IS5 intergenic	-5,79	
2095681	2095348	<--	cld	[2,095,345 <- 2,096,325]	regulator of length of O-antigen component	-7,17	+
2220620	2220682	[-->]	dld	[2,220,207 -> 2,221,922]	D-lactate dehydrogenase	-16,42	
2223844	2224330	[-->]	yohD	[2,223,823 -> 2,224,401]	conserved inner membrane protein	-4,97	
2301929	2302397	[-->]	eco	[2,301,927 -> 2,302,415]	ecotin, a serine protease inhibitor	-26,82	+
2481795	2482389	[-->]	evgA	[2,481,777 -> 2,482,391]	DNA-binding transcriptional activator EvgA	-10,84	
2482991	2485233	[-->]	evgS	[2,482,396 -> 2,485,989]	hybrid sensory histidine kinase in two-component regulatory system with EvgA	-4,53	
2787254	2787708	[-->]	csiD	[2,787,007 -> 2,787,984]	predicted protein	-5,09	
2807766	2808360	[-->]	ygaZ	[2,807,639 -> 2,808,376]	L-valine exporter complex	-8,32	
2808435	2808685	[-->]	ygaH	[2,808,366 -> 2,808,701]	L-valine exporter complex	-9,28	
2808794	2809236	[-->]	mprA	[2,808,792 -> 2,809,322]	multidrug resistance regulator	-4,90	
2969309	2969495	[-->]	ygdR	[2,969,293 -> 2,969,511]	predicted protein	-7,76	
3117091	3115353	<--	yghJ	[3,112,572 <- 3,117,134]	predicted inner membrane lipoprotein	-7,55	
3189960	3189804	<--	glgS	[3,189,761 <- 3,189,961]	predicted glycogen synthesis protein	-14,74	
3250327	3250665	[-->]	yhaH	[3,250,326 -> 3,250,691]	putative cytochrome	-12,50	+
3348602	3348704	[-->]	arcZ	[3,348,599 -> 3,348,719]	ncRNA	-4,02	
3436048	3436452	[-->]	mscL	[3,436,046 -> 3,436,456]	large-conductance mechanosensitive channel	-6,42	
3590333	3589039	<--	ugpB	[3,589,032 <- 3,590,348]	glycerol-3-phosphate transporter subunit	-4,09	
3624603	3623784	<--	yhhJ	[3,623,702 <- 3,624,826]	predicted transporter subunit	-7,71	
3627215	3624914	<--	rbbA	[3,624,826 <- 3,627,561]	ribosome-associated ATPase	-14,28	
3628624	3627582	<--	yhiI	[3,627,558 <- 3,628,625]	predicted HlyD family secretion protein	-18,20	
3628721	3628626	<--	"---"		yhiI/yhiJ intergenic	-23,19	
3628959	3628730	<--	"---"		yhiI/yhiJ intergenic	-21,76	
3638961	3640345	[-->]	dtpB	[3,638,885 -> 3,640,354]	dipeptide transporter	-12,15	
3654308	3653995	<--	hdeB	[3,653,989 <- 3,654,315]	acid-resistance protein	-5,91	+
3654740	3654491	<--	hdeA	[3,654,431 <- 3,654,763]	acid-resistance protein	-4,72	+
3655113	3655580	[-->]	hdeD	[3,655,018 -> 3,655,590]	acid-resistance membrane protein	-5,87	+
3655600	3656200	[-->]	"---"		hdeD/gadE intergenic	-5,80	+
3656419	3656911	[-->]	gadE	[3,656,389 -> 3,656,916]	DNA-binding transcriptional activator	-8,61	+
3662515	3661971	<--	gadW	[3,661,913 <- 3,662,641]	DNA-binding transcriptional activator	-7,44	+
3709926	3709041	<--	yhjX	[3,708,822 <- 3,710,030]	putative resistance protein	-7,29	
3789101	3788598	<--	tdh	[3,788,343 <- 3,789,368]	threonine 3-dehydrogenase	-6,12	
3790208	3789705	<--	kbl	[3,789,378 <- 3,790,574]	2-amino-3-ketobutyrate coenzyme A ligase	-8,72	
3816925	3817507	[-->]	yicG	[3,816,897 -> 3,817,514]	conserved inner membrane protein	-8,98	
3948346	3948443	[-->]	ilvL	[3,948,345 -> 3,948,443]	ilvG operon leader peptide	-4,95	
3956547	3957166	[-->]	ilvC	[3,955,993 -> 3,957,468]	acetohydroxy acid isomeroreductase	-4,83	
3978916	3979901	[-->]	yifK	[3,978,910 -> 3,980,295]	putative transport protein	-4,03	
4003176	4003589	[-->]	pldA	[4,002,885 -> 4,003,754]	phospholipase A	-4,82	
4356513	4354577	<--	cadA	[4,354,493 <- 4,356,640]	lysine decarboxylase 1	-19,78	
4358053	4356780	<--	cadB	[4,356,720 <- 4,358,054]	lysine/cadaverine antiporter	-23,77	
4440086	4439576	<--	msrA	[4,439,561 <- 4,440,199]	methionine sulfoxide reductase A	-16,43	
4549034	4548231	<--	gntP	[4,547,976 <- 4,549,319]	gluconate transporter	-9,07	
4609439	4609985	[-->]	osmY	[4,609,419 -> 4,610,024]	periplasmic protein	-4,16	

6. References

Ali, A. T., A. Iwata, A. Nishimura, S. Ueda & A. Ishihama, (1999) Growth phase-dependent variation in protein composition of the Escherichia coli nucleoid. *J. Bacteriol.* **181**: 6361-6370.

Alon, U., (2007) Network motifs: theory and experimental approaches. *Nat. Rev. Genet.* **8**: 450-461.

Arold, S. T., P. G. Leonard, G. N. Parkinson & J. E. Ladbury, (2010) H-NS forms a superhelical protein scaffold for DNA condensation. *Proc. Natl. Acad. Sci. U. S. A* **107**: 15728-15732.

Ausubel, F. M., R. Brent, R. E. Kingston, D. D. Moore, J. G. Seidman, J. A. Smith & K. Struhl, (2005) Current Protocols in Molecular Biology. In*.*: John Wiley & Sons, Inc.

Azam, T. A. & A. Ishihama, (1999) Twelve species of the nucleoid-associated protein from Escherichia coli. Sequence recognition specificity and DNA binding affinity. *J. Biol. Chem.* **274**: 33105-33113.

Barba, J., V. H. Bustamante, M. A. Flores-Valdez, W. Deng, B. B. Finlay & J. L. Puente, (2005) A positive regulatory loop controls expression of the locus of enterocyte effacement-encoded regulators Ler and GrlA. *J. Bacteriol.* **187**: 7918-7930.

Bertin, P., E. Terao, E. H. Lee, P. Lejeune, C. Colson, A. Danchin & E. Collatz, (1994) The H-NS protein is involved in the biogenesis of flagella in Escherichia coli. *J. Bacteriol.* **176**: 5537-5540.

Bi, W. & P. J. Stambrook, (1998) Site-directed mutagenesis by combined chain reaction. *Anal. Biochem.* **256**: 137-140.

Bouffartigues, E., M. Buckle, C. Badaut, A. Travers & S. Rimsky, (2007) H-NS cooperative binding to high-affinity sites in a regulatory element results in transcriptional silencing. *Nat. Struct. Mol. Biol.* **14**: 441-448.

Brouns, S. J., M. M. Jore, M. Lundgren, E. R. Westra, R. J. Slijkhuis, A. P. Snijders, M. J. Dickman, K. S. Makarova, E. V. Koonin & O. J. van der, (2008) Small CRISPR RNAs guide antiviral defense in prokaryotes. *Science* **321**: 960-964.

Caramel, A. & K. Schnetz, (2000) Antagonistic control of the Escherichia coli bgl promoter by FIS and CAP in vitro. *Mol. Microbiol.* **36**: 85-92.

Castanie-Cornet, M. P., K. Cam, B. Bastiat, A. Cros, P. Bordes & C. Gutierrez, (2010) Acid stress response in Escherichia coli: mechanism of regulation of gadA transcription by RcsB and GadE. *Nucleic Acids Res.* **38:** 1546-3554.

Chen, C. C., M. Y. Chou, C. H. Huang, A. Majumder & H. Y. Wu, (2005) A cis-spreading nucleoprotein filament is responsible for the gene silencing activity found in the promoter relay mechanism. *J. Biol. Chem.* **280**: 5101-5112.

Chen, C. C., M. Fang, A. Majumder & H. Y. Wu, (2001) A 72-base pair AT-rich DNA sequence element functions as a bacterial gene silencer. *J. Biol. Chem.* **276**: 9478-9485.

Chen, C. C., M. Ghole, A. Majumder, Z. Wang, S. Chandana & H. Y. Wu, (2003) LeuO-mediated transcriptional derepression. *J. Biol. Chem.* **278**: 38094-38103.

Chen, C. C. & H. Y. Wu, (2005) LeuO protein delimits the transcriptionally active and repressive domains on the bacterial chromosome. *J. Biol. Chem.* **280**: 15111-15121.

6. References

Chen, D., R. Bowater, C. J. Dorman & D. M. Lilley, (1992) Activity of a plasmid-borne leu-500 promoter depends on the transcription and translation of an adjacent gene. *Proc. Natl. Acad. Sci. U. S. A.* **89**: 8784-8788.

Chen, D., R. Bowater & D. M. Lilley, (1994) Topological promoter coupling in Escherichia coli: delta topA-dependent activation of the leu-500 promoter on a plasmid. *J. Bacteriol.* **176**: 3757-3764.

Cherepanov, P. P. & W. Wackernagel, (1995) Gene disruption in Escherichia coli: TcR and KmR cassettes with the option of Flp-catalyzed excision of the antibiotic-resistance determinant. *Gene* **158**: 9-14.

Chun, K. T., H. J. Edenberg, M. R. Kelley & M. G. Goebl, (1997) Rapid amplification of uncharacterized transposon-tagged DNA sequences from genomic DNA. *Yeast* **13**: 233-240.

Cordeiro, T. N., H. Schmidt, C. Madrid, A. Juarez, P. Bernado, C. Griesinger, J. Garcia & M. Pons, (2011) Indirect DNA Readout by an H-NS Related Protein: Structure of the DNA Complex of the C-Terminal Domain of Ler. *PLoS. Pathog.* **7**: e1002380.

D'Ari, L. & J. C. Rabinowitz, (1991) Purification, characterization, cloning, and amino acid sequence of the bifunctional enzyme 5,10-methylenetetrahydrofolate dehydrogenase/5,10-methenyltetrahydrofolate cyclohydrolase from Escherichia coli. *J. Biol. Chem.* **266**: 23953-23958.

Dame, R. T., (2005) The role of nucleoid-associated proteins in the organization and compaction of bacterial chromatin. *Mol. Microbiol.* **56**: 858-870.

Dame, R. T., M. C. Noom & G. J. Wuite, (2006) Bacterial chromatin organization by H-NS protein unravelled using dual DNA manipulation. *Nature* **444**: 387-390.

Dame, R. T., C. Wyman, R. Wurm, R. Wagner & N. Goosen, (2002) Structural basis for H-NS-mediated trapping of RNA polymerase in the open initiation complex at the rrnB P1. *J. Biol. Chem.* **277**: 2146-2150.

Datsenko, K. A. & B. L. Wanner, (2000) One-step inactivation of chromosomal genes in Escherichia coli K-12 using PCR products. *Proc. Natl. Acad. Sci. U. S. A.* **97**: 6640-6645.

De la Cruz, M. A., M. Fernandez-Mora, C. Guadarrama, M. A. Flores-Valdez, V. H. Bustamante, A. Vazquez & E. Calva, (2007) LeuO antagonizes H-NS and StpA-dependent repression in Salmonella enterica ompS1. *Mol. Microbiol.* **66**: 727-743.

Diederich, L., L. J. Rasmussen & W. Messer, (1992) New cloning vectors for integration in the lambda attachment site attB of the Escherichia coli chromosome. *Plasmid* **28**: 14-24.

Dillon, S. C. & C. J. Dorman, (2010) Bacterial nucleoid-associated proteins, nucleoid structure and gene expression. *Nat. Rev. Microbiol.* **8**: 185-195.

Dimri, G. P., G. F. Ames, L. D'Ari & J. C. Rabinowitz, (1991) Physical map location of the Escherichia coli gene encoding the bifunctional enzyme 5,10-methylene-tetrahydrofolate dehydrogenase/5,10-methenyl-tetrahydrofolate cyclohydrolase. *J. Bacteriol.* **173**: 5251.

Dole, S., S. Kuhn & K. Schnetz, (2002) Post-transcriptional enhancement of Escherichia coli bgl operon silencing by limitation of BglG-mediated antitermination at low transcription rates. *Mol. Microbiol.* **43**: 217-226.

Dorman, C. J., (2004) H-NS: a universal regulator for a dynamic genome. *Nat. Rev. Microbiol.* **2**: 391-400.

Dorman, C. J., (2007) H-NS, the genome sentinel. *Nat. Rev. Microbiol.* **5**: 157-161.

Doyle, M., M. Fookes, A. Ivens, M. W. Mangan, J. Wain & C. J. Dorman, (2007) An H-NS-like stealth protein aids horizontal DNA transmission in bacteria. *Science* **315**: 251-252.

Falconi, M., B. Colonna, G. Prosseda, G. Micheli & C. O. Gualerzi, (1998) Thermoregulation of Shigella and Escherichia coli EIEC pathogenicity. A temperature-dependent structural transition of DNA modulates accessibility of virF promoter to transcriptional repressor H-NS. *EMBO J.* **17**: 7033-7043.

Fang, M., A. Majumder, K. J. Tsai & H. Y. Wu, (2000) ppGpp-dependent *leuO* expression in bacteria under stress. *Biochem. Biophys. Res. Commun.* **276**: 64-70.

Fang, M. & H. Y. Wu, (1998a) A promoter relay mechanism for sequential gene activation. *J. Bacteriol.* **180**: 626-633.

Fang, M. & H. Y. Wu, (1998b) Suppression of leu-500 mutation in topA+ Salmonella typhimurium strains. The promoter relay at work. *J. Biol. Chem.* **273**: 29929-29934.

Farris, C., S. Sanowar, M. W. Bader, R. Pfuetzner & S. I. Miller, (2010) Antimicrobial peptides activate the Rcs regulon through the outer membrane lipoprotein RcsF. *J. Bacteriol.* **192**: 4894-4903.

Fass, E. & E. A. Groisman, (2009) Control of Salmonella pathogenicity island-2 gene expression. *Curr. Opin. Microbiol.* **12**: 199-204.

Fernandez-Mora, M., J. L. Puente & E. Calva, (2004) OmpR and LeuO Positively Regulate the Salmonella enterica Serovar Typhi ompS2 Porin Gene. *J. Bacteriol.* **186**: 2909-2920.

Flores-Valdez, M. A., J. L. Puente & E. Calva, (2003) Negative osmoregulation of the Salmonella ompS1 porin gene independently of OmpR in an hns background. *J. Bacteriol.* **185**: 6497-6506.

Francez-Charlot, A., B. Laugel, G. A. Van, N. Dubarry, F. Wiorowski, M. P. Castanie-Cornet, C. Gutierrez & K. Cam, (2003) RcsCDB His-Asp phosphorelay system negatively regulates the flhDC operon in Escherichia coli. *Mol. Microbiol.* **49**: 823-832.

Free, A., M. E. Porter, P. Deighan & C. J. Dorman, (2001) Requirement for the molecular adapter function of StpA at the Escherichia coli bgl promoter depends upon the level of truncated H-NS protein. *Mol. Microbiol.* **42**: 903-917.

Gao, R., T. R. Mack & A. M. Stock, (2007) Bacterial response regulators: versatile regulatory strategies from common domains. *Trends Biochem. Sci.* **32**: 225-234.

Giel, M., M. Desnoyer & J. Lopilato, (1996) A mutation in a new gene, *bglJ*, activates the bgl operon in Escherichia coli K-12. *Genetics* **143**: 627-635.

Gordon, B. R., Y. Li, A. Cote, M. T. Weirauch, P. Ding, T. R. Hughes, W. W. Navarre, B. Xia & J. Liu, (2011) Structural basis for recognition of AT-rich DNA by unrelated xenogeneic silencing proteins. *Proc. Natl. Acad. Sci. U. S. A.* **108**: 10690-10695.

Görke, B., (2003) Regulation of the Escherichia coli antiterminator protein BglG by phosphorylation at multiple sites and evidence for transfer of phosphoryl groups between monomers. *J. Biol. Chem.* **278**: 46219-46229.

Graf, L. H., Jr. & R. O. Burns, (1973) The supX-leu-500 mutations and expression of the leucine operon. *Mol. Gen. Genet.* **126**: 291-301.

Grainger, D. C., D. Hurd, M. D. Goldberg & S. J. Busby, (2006) Association of nucleoid proteins with coding and non-coding segments of the Escherichia coli genome. *Nucleic Acids Res.* **34**: 4642-4652.

Guyer, M. S., R. R. Reed, J. A. Steitz & K. B. Low, (1981) Identification of a sex-factor-affinity site in E. coli as gamma delta. *Cold Spring Harb. Symp. Quant. Biol.* **45 Pt 1**: 135-140.

6. References

Hames, C., S. Halbedel, O. Schilling & J. Stulke, (2005) Multiple-mutation reaction: a method for simultaneous introduction of multiple mutations into the glpK gene of Mycoplasma pneumoniae. *Appl. Environ. Microbiol.* **71**: 4097-4100.

Hamilton, C. M., M. Aldea, B. K. Washburn, P. Babitzke & S. R. Kushner, (1989) New method for generating deletions and gene replacements in Escherichia coli. *J. Bacteriol.* **171**: 4617-4622.

Haughn, G. W., S. R. Wessler, R. M. Gemmill & J. M. Calvo, (1986) High A + T content conserved in DNA sequences upstream of leuABCD in Escherichia coli and Salmonella typhimurium. *J. Bacteriol.* **166**: 1113-1117.

Henikoff, S., G. W. Haughn, J. M. Calvo & J. C. Wallace, (1988) A Large Family of Bacterial Activator Proteins. *Proc. Natl. Acad. Sci. U. S. A.* **85**: 6602-6606.

Henikoff, S., J. C. Wallace & J. P. Brown, (1990) Finding protein similarities with nucleotide sequence databases. *Methods Enzymol.* **183**: 111-132.

Hernandez-Lucas, I., A. L. Gallego-Hernandez, S. Encarnacion, M. Fernandez-Mora, A. G. Martinez-Batallar, H. Salgado, R. Oropeza & E. Calva, (2008) The LysR-type transcriptional regulator LeuO controls expression of several genes in Salmonella enterica serovar Typhi. *J. Bacteriol.* **190**: 1658-1670.

Hirakawa, H., A. Takumi-Kobayashi, U. Theisen, T. Hirata, K. Nishino & A. Yamaguchi, (2008) AcrS/EnvR represses expression of the acrAB multidrug efflux genes in Escherichia coli. *J. Bacteriol.* **190**: 6276-6279.

Hommais, F., E. Krin, C. Laurent-Winter, O. Soutourina, A. Malpertuy, J. P. Le Caer, A. Danchin & P. Bertin, (2001) Large-scale monitoring of pleiotropic regulation of gene expression by the prokaryotic nucleoid-associated protein, H-NS. *Mol. Microbiol.* **40**: 20-36.

Huang, Y. H., L. Ferrieres & D. J. Clarke, (2006) The role of the Rcs phosphorelay in Enterobacteriaceae. *Res. Microbiol.* **157**: 206-212.

Klauck, E., J. Bohringer & R. Hengge-Aronis, (1997) The LysR-like regulator LeuO in Escherichia coli is involved in the translational regulation of rpoS by affecting the expression of the small regulatory DsrA-RNA. *Mol. Microbiol.* **25**: 559-569.

Ko, M. & C. Park, (2000) H-NS-Dependent regulation of flagellar synthesis is mediated by a LysR family protein. *J. Bacteriol.* **182**: 4670-4672.

Krin, E., A. Danchin & O. Soutourina, (2010) Decrypting the H-NS-dependent regulatory cascade of acid stress resistance in Escherichia coli. *BMC. Microbiol.* **10**: 273.

Laaberki, M. H., N. Janabi, E. Oswald & F. Repoila, (2006) Concert of regulators to switch on LEE expression in enterohemorrhagic Escherichia coli O157:H7: interplay between Ler, GrlA, HNS and RpoS. *Int. J. Med. Microbiol.* **296**: 197-210.

Laishram, R. S. & J. Gowrishankar, (2007) Environmental regulation operating at the promoter clearance step of bacterial transcription. *Genes Dev.* **21**: 1258-1272.

Lamblin, A. F. & J. A. Fuchs, (1994) Functional analysis of the Escherichia coli K-12 cyn operon transcriptional regulation. *J. Bacteriol.* **176**: 6613-6622.

Lang, B., N. Blot, E. Bouffartigues, M. Buckle, M. Geertz, C. O. Gualerzi, R. Mavathur, G. Muskhelishvili, C. L. Pon, S. Rimsky, S. Stella, M. M. Babu & A. Travers, (2007) High-affinity DNA binding sites for H-NS provide a molecular basis for selective silencing within proteobacterial genomes. *Nucleic Acids Res.* **35**: 6330-6337.

Laubacher, M. E. & S. E. Ades, (2008) The Rcs phosphorelay is a cell envelope stress response activated by peptidoglycan stress and contributes to intrinsic antibiotic resistance. *J. Bacteriol.* **190**: 2065-2074.

Lawrenz, M. B. & V. L. Miller, (2007) Comparative analysis of the regulation of rovA from the pathogenic yersiniae. *J. Bacteriol.* **189**: 5963-5975.

Li, G., C. Ewers, C. Laturnus, I. Diehl, J. Dai, E.-M. Antao, K. Schnetz & L. H. Wieler, (2008) Characterization of a *yjjQ* mutant of avian pathogenic *E. coli* (APEC). *Microbiol.* **154**: 1082-1093.

Lilley, D. M. & C. F. Higgins, (1991) Local DNA topology and gene expression: the case of the leu-500 promoter. *Mol. Microbiol.* **5**: 779-783.

Lim, C. J., Y. R. Whang, L. J. Kenney & J. Yan, (2011) Gene silencing H-NS paralogue StpA forms a rigid protein filament along DNA that blocks DNA accessibility. *Nucleic Acids Res*. (epub ahead of print)*.*

Liu, Y., H. Chen, L. J. Kenney & J. Yan, (2010) A divalent switch drives H-NS/DNA-binding conformations between stiffening and bridging modes. *Genes Dev.* **24**: 339-344.

Lucchini, S., G. Rowley, M. D. Goldberg, D. Hurd, M. Harrison & J. C. Hinton, (2006) H-NS mediates the silencing of laterally acquired genes in bacteria. *PLoS. Pathog.* **2**: e81.

Lucht, J. M., P. Dersch, B. Kempf & E. Bremer, (1994) Interactions of the nucleoid-associated DNA-binding protein H-NS with the regulatory region of the osmotically controlled proU operon of Escherichia coli. *J. Biol. Chem.* **269**: 6578-6578.

Maddocks, S. E. & P. C. F. Oyston, (2008) Structure and function of the LysR-type transcriptional regulator (LTTR) family proteins. *Microbiology* **154**: 3609-3623.

Madhusudan, S., A. Paukner, Y. Klingen & K. Schnetz, (2005) Independent regulation of H-NS-mediated silencing of the bgl operon at two levels: upstream by BglJ and LeuO and downstream by DnaKJ. *Microbiology* **151**: 3349-3359.

Majdalani, N. & S. Gottesman, (2005) The Rcs phosphorelay: a complex signal transduction system. *Annu. Rev. Microbiol.* **59**: 379-405.

Majdalani, N., M. Heck, V. Stout & S. Gottesman, (2005) Role of RcsF in signaling to the Rcs phosphorelay pathway in Escherichia coli. *J. Bacteriol.* **187**: 6770-6778.

Majumder, A., M. Fang, K. J. Tsai, C. Ueguchi, T. Mizuno & H. Y. Wu, (2001) LeuO expression in response to starvation for branched-chain amino acids. *J. Biol. Chem.* **276**: 19046-19051.

Margolin, P., L. Zumstein, R. Sternglanz & J. C. Wang, (1985) The Escherichia coli supX locus is topA, the structural gene for DNA topoisomerase I. *Proc. Natl. Acad. Sci. U. S. A.* **82**: 5437-5441.

Medina-Aparicio, L., J. E. Rebollar-Flores, A. L. Gallego-Hernandez, A. Vazquez, L. Olvera, R. M. Gutierrez-Rios, E. Calva & I. Hernandez-Lucas, (2011) The CRISPR/Cas immune system is an operon regulated by LeuO, H-NS, and leucine-responsive regulatory protein in Salmonella enterica serovar Typhi. *J. Bacteriol.* **193**: 2396-2407.

Miller, J. H., (1992) *A short course in bacterial genetics. A laboratory manual and handbook for Escherichia coli and related bacteria*. Cold Spring Harbor Laboratory Press.

Momany, C. & E. L. Neidle, (2012) Defying stereotypes: the elusive search for a universal model of LysR-type regulation. *Mol. Microbiol.* **83**: 453-456.

Moorthy, S. & P. I. Watnick, (2005) Identification of novel stage-specific genetic requirements through whole genome transcription profiling of Vibrio cholerae biofilm development. *Mol. Microbiol.* **57**: 1623-1635.

Muller, C. M., U. Dobrindt, G. Nagy, L. Emody, B. E. Uhlin & J. Hacker, (2006) Role of histone-like proteins H-NS and StpA in expression of virulence determinants of uropathogenic Escherichia coli. *J. Bacteriol.* **188**: 5428-5438.

6. References

Muller, C. M., G. Schneider, U. Dobrindt, L. Emody, J. Hacker & B. E. Uhlin, (2010) Differential effects and interactions of endogenous and horizontally acquired H-NS-like proteins in pathogenic Escherichia coli. *Mol. Microbiol.* **75**: 280-293.

Nagarajavel, V., S. Madhusudan, S. Dole, A. R. Rahmouni & K. Schnetz, (2007) Repression by binding of H-NS within the transcription unit. *J. Biol. Chem.* **282**: 23622-23630.

Navarre, W. W., M. McClelland, S. J. Libby & F. C. Fang, (2007) Silencing of xenogeneic DNA by H-NS-facilitation of lateral gene transfer in bacteria by a defense system that recognizes foreign DNA. *Genes Dev.* **21**: 1456-1471.

Navarre, W. W., S. Porwollik, Y. Wang, M. McClelland, H. Rosen, S. J. Libby & F. C. Fang, (2006) Selective silencing of foreign DNA with low GC content by the H-NS protein in Salmonella. *Science* **313**: 236-238.

Noom, M. C., W. W. Navarre, T. Oshima, G. J. Wuite & R. T. Dame, (2007) H-NS promotes looped domain formation in the bacterial chromosome. *Curr. Biol.* **17**: R913-R914.

Oshima, T., S. Ishikawa, K. Kurokawa, H. Aiba & N. Ogasawara, (2006) Escherichia coli histone-like protein H-NS preferentially binds to horizontally acquired DNA in association with RNA polymerase. *DNA Res.* **13**: 141-153.

Owen-Hughes, T. A., G. D. Pavitt, D. S. Santos, J. M. Sidebotham, C. S. Hulton, J. C. Hinton & C. F. Higgins, (1992) The chromatin-associated protein H-NS interacts with curved DNA to influence DNA topology and gene expression. *Cell* **71**: 255-265.

Parker, C. T., A. W. Kloser, C. A. Schnaitman, M. A. Stein, S. Gottesman & B. W. Gibson, (1992) Role of the rfaG and rfaP genes in determining the lipopolysaccharide core structure and cell surface properties of Escherichia coli K-12. *J. Bacteriol.* **174**: 2525-2538.

Pruss, G. J. & K. Drlica, (1985) DNA supercoiling and suppression of the leu-500 promoter mutation. *J. Bacteriol.* **164**: 947-949.

Pul, U., R. Wurm, Z. Arslan, R. Geissen, N. Hofmann & R. Wagner, (2010) Identification and characterization of E. coli CRISPR-cas promoters and their silencing by H-NS. *Mol. Microbiol.* **75:** 1495-1512.

Pul, U., R. Wurm & R. Wagner, (2007) The role of LRP and H-NS in transcription regulation: involvement of synergism, allostery and macromolecular crowding. *J. Mol. Biol.* **366**: 900-915.

Radde, N., J. Gebert, U. Faigle, R. Schrader & K. Schnetz, (2008) Modeling feedback loops in the H-NS-mediated regulation of the Escherichia coli bgl operon. *J. Theor. Biol.* **250**: 298-306.

Repoila, F. & S. Gottesman, (2001) Signal transduction cascade for regulation of RpoS: temperature regulation of DsrA. *J. Bacteriol.* **183**: 4012-4023.

Reynolds, A. E., S. Mahadevan, S. F. LeGrice & A. Wright, (1986) Enhancement of bacterial gene expression by insertion elements or by mutation in a CAP-cAMP binding site. *J. Mol. Biol.* **191**: 85-95.

Richardson, S. M., C. F. Higgins & D. M. Lilley, (1988) DNA supercoiling and the leu-500 promoter mutation of Salmonella typhimurium. *EMBO J.* **7**: 1863-1869.

Rimsky, S., (2004) Structure of the histone-like protein H-NS and its role in regulation and genome superstructure. *Curr. Opin. Microbiol.* **7**: 109-114.

Rodriguez-Morales, O., M. Fernandez-Mora, I. Hernandez-Lucas, A. Vazquez, J. L. Puente & E. Calva, (2006) Salmonella enterica serovar Typhimurium ompS1 and ompS2 mutants are attenuated for virulence in mice. *Infect. Immun.* **74**: 1398-1402.

Salmon, K. A., C.-R. Yang & G. W. Hatfield, (2006) Chapter 3.6.1.5, Biosynthesis and regulation of the branched-chain amino acids. In: EcoSal—Escherichia coli and Salmonella: Cellular and Molecular Biology. A. Böck, R.

Curtiss III, J. B. Kaper, P. D. Karp, F. C. Neidhardt, T. Nyström, J. M. Slauch, C. L. Squires & D. Ussery (eds). Washigton, D.C.: ASM Press.

Sayed, A. K. & J. W. Foster, (2009) A 750 bp sensory integration region directs global control of the Escherichia coli GadE acid resistance regulator. *Mol. Microbiol.* **71**: 1435-1450.

Scharf, B. E., (2010) Summary of useful methods for two-component system research. *Curr. Opin. Microbiol.* **13**: 246-252.

Schell, M. A., (1993) Molecular biology of the LysR family of transcriptional regulators. *Annu. Rev. Microbiol.* **47**: 597-626.

Schneider, D. A., W. Ross & R. L. Gourse, (2003) Control of rRNA expression in Escherichia coli. *Curr. Opin. Microbiol.* **6**: 151-156.

Schnetz, K. & J. C. Wang, (1996) Silencing of the Escherichia coli bgl promoter: effects of template supercoiling and cell extracts on promoter activity in vitro. *Nucleic Acids Res.* **24**: 2422-2428.

Shi, X. & G. N. Bennett, (1995) Effects of multicopy LeuO on the expression of the acid-inducible lysine decarboxylase gene in Escherichia coli. *J. Bacteriol.* **177**: 810-814.

Shimada, T., A. Bridier, R. Briandet & A. Ishihama, (2011) Novel roles of LeuO in transcription regulation of E. coli genome: antagonistic interplay with the universal silencer H-NS. *Mol. Microbiol.* **82**: 378-397.

Shimada, T., K. Yamamoto & A. Ishihama, (2009) Involvement of the leucine response transcription factor LeuO in regulation of the genes for sulfa drug efflux. *J. Bacteriol.* **191**: 4562-4571.

Shin, M., M. Song, J. H. Rhee, Y. Hong, Y. J. Kim, Y. J. Seok, K. S. Ha, S. H. Jung & H. E. Choy, (2005) DNA looping-mediated repression by histone-like protein H-NS: specific requirement of Esigma70 as a cofactor for looping. *Genes Dev.* **19**: 2388-2398.

Shoval, O. & U. Alon, (2010) SnapShot: network motifs. *Cell* **143**: 326-e321.

Sonden, B. & B. E. Uhlin, (1996) Coordinated and differential expression of histone-like proteins in Escherichia coli: regulation and function of the H-NS analog StpA. *EMBO J.* **15**: 4970-4980.

Stella, S., R. Spurio, M. Falconi, C. L. Pon & C. O. Gualerzi, (2005) Nature and mechanism of the in vivo oligomerization of nucleoid protein H-NS. *EMBO J.* **24**: 2896-2905.

Stoebel, D. M., A. Free & C. J. Dorman, (2008) Anti-silencing: overcoming H-NS-mediated repression of transcription in Gram-negative enteric bacteria. *Microbiology* **154**: 2533-2545.

Stratmann, T., S. Madhusudan & K. Schnetz, (2008) Regulation of the yjjQ-*bglJ* operon, encoding LuxR-type transcription factors, and the divergent yjjP gene by H-NS and LeuO. *J. Bacteriol.* **190**: 926-935.

Stratmann, T., U. Pul, R. Wurm, R. Wagner & K. Schnetz, (2012) RcsB-BglJ activates the Escherichia coli *leuO* gene, encoding an H-NS antagonist and pleiotropic regulator of virulence determinants. *Mol. Microbiol.* (epub ahead of print).

Sung, Y. C. & J. A. Fuchs, (1988) Characterization of the cyn operon in Escherichia coli K12. *J. Biol. Chem.* **263**: 14769-14775.

Sung, Y. C. & J. A. Fuchs, (1992) The Escherichia coli K-12 cyn operon is positively regulated by a member of the lysR family. *J. Bacteriol.* **174**: 3645-3650.

Tan, J., L. Shu & H. Y. Wu, (1994) Activation of the leu-500 promoter by adjacent transcription. *J. Bacteriol.* **176**: 1077-1086.

6. References

Ueguchi, C., T. Ohta, C. Seto, T. Suzuki & T. Mizuno, (1998) The *leuO* gene product has a latent ability to relieve bgl silencing in Escherichia coli. *J. Bacteriol.* **180**: 190-193.

Uyar, E., K. Kurokawa, M. Yoshimura, S. Ishikawa, N. Ogasawara & T. Oshima, (2009) Differential binding profiles of StpA in wild-type and h-ns mutant cells: a comparative analysis of cooperative partners by chromatin immunoprecipitation-microarray analysis. *J. Bacteriol.* **191**: 2388-2391.

Venkatesh, G. R., F. C. Kembou Koungni, A. Paukner, T. Stratmann, B. Blissenbach & K. Schnetz, (2010) BglJ-RcsB heterodimers relieve repression of the Escherichia coli bgl operon by H-NS. *J. Bacteriol.* **192**: 6456-6464.

Vieira, J. & J. Messing, (1987) Production of single-stranded Plasmid DNA. *Methods Enzymol.* **153**: 3-11.

Volpon, L., C. Lievre, M. J. Osborne, S. Gandhi, P. Iannuzzi, R. Larocque, M. Cygler, K. Gehring & I. Ekiel, (2003) The solution structure of YbcJ from Escherichia coli reveals a recently discovered alphaL motif involved in RNA binding. *J. Bacteriol.* **185**: 4204-4210.

Wagner, E. G. H. & J. Vogel, (2005) Approaches to identify novel non-messenger RNAs in bacteria and to investigate their biological functions: functional analysis of identified non-mRNAs. . In: Handbook of RNA Biochemistry. R. K. Hartmann, A. Bindereif, A. Schön & E. Westhof (eds). Weinheim: WILEY-VCH, pp. 632-642.

Wang, W., G. W. Li, C. Chen, X. S. Xie & X. Zhuang, (2011) Chromosome organization by a nucleoid-associated protein in live bacteria. *Science* **333**: 1445-1449.

Watson, N., D. S. Dunyak, E. L. Rosey, J. L. Slonczewski & E. R. Olson, (1992) Identification of elements involved in transcriptional regulation of the Escherichia coli cad operon by external pH. *J. Bacteriol.* **174**: 530-540.

Wehland, M. & F. Bernhard, (2000) The RcsAB Box. Characterization of a new operator essential for the regulation of exopolysaccharide biosynthesi in enteric bacteria. *J. Biol. Chem.* **275**: 7013-7020.

Wessler, S. R. & J. M. Calvo, (1981) Control of leu operon expression in Escherichia coli by a transcription attenuation mechanism. *J. Mol. Biol.* **149**: 579-597.

Westra, E. R., U. Pul, N. Heidrich, M. M. Jore, M. Lundgren, T. Stratmann, R. Wurm, A. Raine, M. Mescher, H. L. Van, M. Mastop, E. G. Wagner, K. Schnetz, O. J. van der, R. Wagner & S. J. Brouns, (2010) H-NS-mediated repression of CRISPR-based immunity in Escherichia coli K12 can be relieved by the transcription activator LeuO. *Mol. Microbiol.* **77**: 1380-1393.

Wilson, G. G., K. Y. Young, G. J. Edlin & W. Konigsberg, (1979) High-frequency generalised transduction by bacteriophage T4. *Nature* **280**: 80-82.

Winter, S. E., M. G. Winter, P. Thiennimitr, V. A. Gerriets, S. P. Nuccio, H. Russmann & A. J. Baumler, (2009) The TviA auxiliary protein renders the Salmonella enterica serotype Typhi RcsB regulon responsive to changes in osmolarity. *Mol. Microbiol.* **74**: 175-193.

Wolf, T., W. Janzen, C. Blum & K. Schnetz, (2006) Differential dependence of StpA on H-NS in autoregulation of stpA and in regulation of bgl. *J. Bacteriol.* **188**: 6728-6738.

Wu, H. Y. & M. Fang, (2003) DNA supercoiling and transcription control: a model from the study of suppression of the leu-500 mutation in Salmonella typhimurium topA- strains. *Prog. Nucleic Acid Res. Mol. Biol.* **73**: 43-68.

Wu, H. Y., J. Tan & M. Fang, (1995) Long-range interaction between two promoters: activation of the leu-500 promoter by a distant upstream promoter. *Cell* **82**: 445-451.

Zhang, A., S. Rimsky, M. E. Reaban, H. Buc & M. Belfort, (1996) Escherichia coli protein analogs StpA and H-NS: regulatory loops, similar and disparate effects on nucleic acid dynamics. *EMBO J.* **15**: 1340-1349.

Abbreviations

5'RACE	rapid amplification of cDNA 5´ ends
amp	ampicillin
bp	base pairs
BTB	bromothymol blue
cam	chloramphenicol
CCR	combined chain reaction
DMSO	dimethyl sulfoxide
dNTP	deoxynucleoside triphosphate
EDTA	ethylenediaminetetraacetic acid
EMSA	electrophoretic mobility shift assay
FRT (FRT site)	Flp recombinase target site
HTH	helix-turn-helix (motif)
IPTG	isopropyl-β-D-thiogalactopyranosid
kan	kanamycin
KIC	α-ketoisocaproic acid (4-methyl-oxovaleric acid) sodium salt
KIL	α-ketoisoleucine (3-methyl-2-oxovaleric acid) sodium salt
KIV	α-ketoisovaleric acid (3-methyl-2-oxobutyrate) sodium salt
NAP	nucleoid-associated protein
nt	nucleotide
NTP	nucleoside triphosphate
OD_X	optical density at X nm wavelength
ONPG	o-nitrophenyl-β, D-galactopyranoside
PAGE	polyacrylamide gel electrophoresis
PCR	polymerase chain reaction
PT	phenotype
rpm	revolutions per minute
spec	spectinomycin
sRNA	small regulatory RNA
TAP	tobacco acid pyrophosphatase
tet	tetracycline
URE	upstream regulatory element
v/v	volume per volume
w/v	weight per volume
wHTH	winged helix-turn-helix (motif)
wt	wild-type
X-gal	5-bromo-4-chloro-3-indolyl-β-D-galactopyranoside

Figure Index

Table Index

Erklärung

Ich versichere, dass ich die von mir abgegebene Dissertation selbstständig angefertigt habe, die benutzten Quellen und Hilfsmittel vollständig angegeben und die Stellen der Arbeit - einschließlich Tabellen, Karten und Abbildungen -, die anderen Werken im Wortlaut oder dem Sinn nach entnommen sind, in jedem Einzelfall als Entlehnung kenntlich gemacht habe; dass diese Dissertation noch keiner anderen Fakultät oder Universität zur Prüfung vorgelegen hat; dass sie - abgesehen von unten angegebenen Teilpublikationen - noch nicht veröffentlicht worden ist sowie, dass ich eine solche Veröffentlichung vor Abschluss des Promotionsverfahrens nicht vornehmen werde.

Die Bestimmungen der Promotionsordnung sind mir bekannt. Die von mir vorgelegte Dissertation ist von Prof. Dr. Karin Schnetz, Institut für Genetik, betreut worden.

Nachfolgend genannte Teilpublikationen liegen vor:

Stratmann, T., S. Madhusudan & K. Schnetz (2008) Regulation of the *yjjQ-bglJ* operon, encoding LuxR-type transcription factors, and the divergent *yjjP* gene by H-NS and LeuO. *J. Bacteriol.* 190: 926-935.

Venkatesh, G. R., F. C. Kembou Koungni, A. Paukner, T. Stratmann, B. Blissenbach & K. Schnetz (2010) RcsB-BglJ heterodimers relieve repression of the *Escherichia coli bgl* operon by H-NS. *J. Bacteriol.* 192: 6456-6464.

Westra, E. R., U. Pul, N. Heidrich, M. M. Jore, M. Lundgren, T. Stratmann, R. Wurm, A. Raine, M. Mescher, H. L. Van, M. Mastop, E. G. Wagner, K. Schnetz, O. J. van der, R. Wagner & S. J. Brouns (2010) H-NS-mediated repression of CRISPR-based immunity in *Escherichia coli* K12 can be relieved by the transcription activator LeuO. *Mol. Microbiol.* 77: 1380-1393.

Stratmann, T., Pul, U., Wurm, R., Wagner, R., & Schnetz, K. (2012) RcsB-BglJ activates *leuO*, encoding an H-NS antagonist and pleiotropic regulator of virulence determinants. (accepted for publication in *Mol. Microbiol.*)

Ich versichere, dass ich alle Angaben wahrheitsgemäß nach bestem Wissen und Gewissen gemacht habe und verpflichte mich, jedmögliche, die obigen Angaben betreffenden Veränderungen, dem Dekanat unverzüglich mitzuteilen.

Köln, den 23. Februar 2012 _____

Thomas Stratmann